THE
PHYSICAL REVIEW
A Journal of Experimental and Theoretical Physics Established by E. L. Nichols in 1893
VOL. 53, NO. 3 FEBRUARY 1, 1938 SECOND SERIES

New Evidence as to the Nature of the Incoming Cosmic Rays, Their Absorbability in the Atmosphere, and the Secondary Character of the Penetrating Rays Found in Such Abundance at Sea Level and Below

I. S. BOWEN, R. A. MILLIKAN AND H. VICTOR NEHER
California Institute of Technology, Pasadena, California
(Received November 29, 1937)

The intensity of latitude-sensitive cosmic rays as would be measured by an electroscope placed just outside the atmosphere has been calculated. The ionization due to incoming electrons of 10 billion electron volts energy in this same electroscope placed 1/20th of an atmosphere beneath the top is found to be 13 times that outside. Electrons do not become penetrating by virtue of high energies even up to 17 billion electron volts. Neither protons nor other penetrating particles of any sort enter the atmosphere in significant numbers from outside the atmosphere. The observed penetrating particles and all other cosmic-ray effects, latitude-sensitive and non-latitude-sensitive, found in the lower atmosphere are practically all secondary effects—splashes from the absorption of electrons, or photons, or both taking place in the outer layers of the atmosphere.

I. EVIDENCE AS TO THE CHARACTER OF THE COSMIC RAYS AS THEY ENTER THE ATMOSPHERE

HAVING obtained[1] the nearly complete "depth-ionization" curve due to the band of charged particle rays of energy between 6.7×10^9 ev and 17×10^9 ev (weighted mean value 10×10^9 ev) which can break through the blocking effect of the earth's magnetic field between the magnetic equator and the magnetic latitude of San Antonio, Texas (mag. lat. 38° 30′) we are in position, by following the technique which we have already used[2] and which was also used still earlier by Millikan and Cameron[3] to compute the precise number of charged-particle-rays that enter the earth's atmosphere within this energy range. This is done as follows.

The total number of ions produced in a column of air 1 sq. cm in section and extending from the top of the atmosphere down to the lowest depth to which the ionizing influence of these rays extends, is obtained simply by a graphical integration of the area underneath the lower curve of Fig. 4, p. 83 of reference 1 and reproduced here as curve *A* of Fig. 1. This number comes out 2.80×10^7 ions.[4] This number represents the total effect in the production of ions of all the energy contained in these particular rays which enter each square cm of the earth's surface per sec. The number of ions which each of these 10×10^9 ev rays can produce, and must produce, since the whole energy is expended in

[1] Bowen, Millikan and Neher, Phys. Rev. **52**, 83 (1937).
[2] Bowen, Millikan and Neher, Phys. Rev. **44**, 252 (1933).
[3] Millikan and Cameron, Phys. Rev. **31**, 929 (1928).

[4] In the article in question we stated that in order to make the results comparable with those found in airplane flights with the use of thicker walled electroscopes we had added 10 percent to all the values obtained with the very thin walled (0.5 mm of steel) electroscopes used in our sounding balloon flights at San Antonio and Madras. The figures used above are those actually obtained in these thin-walled electroscopes rather than those corresponding to the graph given in Fig. 4, p. 83 of that paper, for the reason that for the purposes of the computation herein contained the extreme thinness of the electroscope wall is of vital importance.

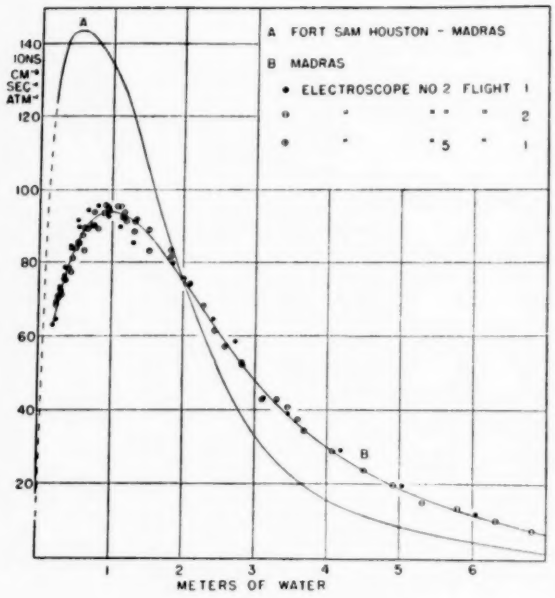

FIG. 1.

the production of ions, is $10\times10^9/32$ since each ion in air requires on the average 32 ev for its production; so that the number of these charged particle rays which fall per sec. on each square cm of the earth's surface is $2.80\times10^7\times32/10\times10^9 = 0.09$. Let us call this number N.

The problem which we then set ourselves is to find how much ionization these rays will produce in one of our thin-walled electroscopes when it is placed just outside the earth's atmosphere where it is exposed to all the rays coming in from all directions from the hemisphere above it but is screened off by the earth from the entrance of rays from the hemisphere below it.

Since N is the number of rays of the given energy passing through each sq. cm of surface, the total number passing through the electroscope of radius r is $2\pi r^2N$. These rays traverse every possible chord of the sphere of radius r, and the average length of these chords is $4r/3$. If now we make the assumption that, in view of the extreme thinness of the electroscope wall, the only ionizing effect produced in the air at atmospheric pressure within the electroscope (for all the readings obtained with our argon-filled electroscopes have been reduced to air at $p=76$ cm Hg, $t=23$°C) is found in the ions produced in the gas within the electroscope along the ion track, here taken as 60 per cm of length, then the expression for the number of ions per cc per sec. produced in the electroscope by the rays in question is

$$\frac{2\pi r^2N\times(4r/3)\times60}{4\pi r^3/3}=120N=11 \text{ ions per cc per sec.}$$

If the foregoing assumpton is a correct one, this value of 11 ions per cc/sec. should give us the intercept of the above curve on the ionization axis. We have in the figure extended a dotted line from the last observed point to that intercept, and thus obtained the complete curve to the top of the atmosphere of the ionization produced by all the incoming charged particles of energies between 6.7×10^9 and 17×10^9 electron volts.

Since the number of ions produced by these rays is seen from A, Fig. 1 to reach a maximum of 144 ion cc/sec. the multiplication of ions in penetrating 0.5 m of water is about 13-fold. This is not far from the multiplication computed by Carlson and Oppenheimer from the Bethe-Heitler theory of the absorption of the atmosphere for electrons of this energy. Their computed number for 10 billion volt electrons is 12.6. *This result constitutes a bit of new evidence that practically all the incoming latitude-sensitive rays are electrons, and that no appreciable number of protons or other penetrating particles are mixed with them.*

The only uncertainty that can inhere in the foregoing analysis lies in the assumption of the negligible effect of the thin wall on the ionization produced within the electroscope and in the choice of 60 as the most probable value of the ionization along the ion track of a 10×10^9 ev electron ray. As to this last it is larger than the mean of the direct counts of most of the observers who have directly attempted to count ions in high energy electron tracks, but it represents as fair a mean as we can find when the ions produced by the delta-rays are included. Even if it is in error, the foregoing reasoning is not seriously affected.

So far as the first assumption is concerned, if we rely upon Carlson and Oppenheimer's analysis as to how rapidly, according to the Bethe-Heitler theory, ionizing rays are multiplied by walls of given thickness and given materials as depicted in the curve which they give[5] walls of iron 0.5 mm thick, such as our electroscopes are made of, can contribute no appreciable new ionization.

[5] Carlson and Oppenheimer, Phys. Rev. **51**, 230 (1937).

The foregoing evidence as to very rapid absorbability obtained from a comparison of the ionizing power of the rays outside of the atmosphere and that found one-twentieth of the way through it, is merely confirmation of the evidence which we have already derived[6] from the ionization found as the rays penetrate below the first twentieth, for between this point and one-half the way through (5 meters of water) the ionizing power fell to 1/16th its maximum value (144 ions per cc/sec.), while at sea level it had dropped to 1/500th its highest value.

This demonstration of the very high absorbability of the incoming charged particles by the nuclei of the atoms of the atmosphere up to the huge value of 17 billion electron volts is in general accord with the requirements of the Bethe-Heitler theory, but it is completely irreconcilable with the absorbability of protons or any other particles too heavy to make radiative collisions, i.e., to produce "impulse radiation" or "*bremsstrahlung*." For the theory makes the rate of absorption vary inversely as the square of the mass, and the mass of a proton is two thousand times that of an electron. These experiments, therefore, force us to reaffirm the following conclusions: (1) *The latitude-sensitive rays contain no appreciable number of incoming protons or other penetrating particles* of any sort, since we find it impossible to build up the observed curve out of an appreciable mixture of incoming penetrating particles with highly absorbable particles (electrons). (2) *Electrons do not become penetrating by virtue of high energies*, at least up to 17 billion ev, as we ourselves and also Bethe-Heitler have heretofore assumed. Otherwise stated, these experiments remove what have been heretofore regarded as insuperable objections to the validity of the Bethe-Heitler theory *for electrons of very high energies*. They force the conclusion that the high energy penetrating particles definitely revealed in great numbers both by cloud-chamber photographs and by ion-counter experiments near the earth's surface are not ordinary electrons at all, though they carry the electronic charge and produce tracks thus far undifferentiable from electron tracks (+ and −). For they prove that, clear up to an energy of 17 billion ev, electrons *do* make radiative collisions, or at any rate are very rapidly absorbed. Certainly, then, observed penetrating particles of energies under 17 billion ev cannot be electrons. They must be either protons or else particles of mass intermediate between protons and electrons. If they are protons, since according to all observers they are nearly equally divided in sign between positive and negative, *the negative proton has been discovered*. In any case a new particle has come to light as Neddermeyer and Anderson have already announced[7] for another reason, namely, that they have actually observed a very considerable number of apparent electron tracks of the same curvature in a magnetic field but of entirely different penetrability and of too small ionizing power to be protons.

[6] Bowen, Millikan and Neher, Nature **140**, 23 (1937).

II. The Probable Origin of the Penetrating Particles Observed in the Lower Part of the Atmosphere

In the previous article we have shown that the top part of the latitude-sensitive curve (see Fig. 5,

[7] Neddermeyer and Anderson, Phys. Rev. **51**, 884 (1937). The history of this discovery is as follows: In 1934 it was pointed out by Anderson and Neddermeyer (Report of London Int. Conf. on Physics, Vol. I, Section on Nature of Cosmic-Ray Particles and footnote, page 182 (1934)) that there are serious difficulties in identifying the penetrating cosmic-ray particles at sea level with either electrons or protons. Further evidence of a new kind indicating the existence of particles of a new type was reported by them in the Phys. Rev. **50**, 270 (1936), captions under Figs. 12 and 13. In a colloquium on November 12, 1936 new evidence showing a difference in penetrability of single particles and shower particles was presented, in which the conclusion was reached that these data could be understood only in terms of a new type of particle. A brief report of this colloquium was published in Science, November 20, 1936, page 9 of the supplement. Further publication was withheld until a long series of careful measurements had been completed on 55 particles which showed that shower particles of a given curvature have an entirely different penetrability from nonshower particles of the same curvature. Further, practically all of these particles had much too small ionizing power to be protons. These results were reported in the Phys. Rev. **51**, 884 (1937). At practically the same time as this last publication Street and Stevenson, Abstract No. 40, Phys. Rev. **51**, 1005 (1937) presented data showing the existence of particles less ionizing than protons and more penetrating than electrons could be *on the assumption that the Bethe-Heitler law holds for high enough energies*. They thus confirmed the conclusion reached by Anderson and Neddermeyer in 1934 based on measurements reported to the London Conference at that time. That the Bethe-Heitler law does not break down at very high energies, as it had been assumed to do by Millikan, Bethe, Heitler, Oppenheimer and many others, was first shown in the San Antonio-Madras experiments published in Nature **140**, 23 (1937) and the Phys. Rev. **52**, 80 (1937).

p. 86 of reference 1) reveals if anything an even more rapid rate of absorption, or a lower penetrating power, than the Bethe-Heitler theory demands of incoming electrons, while the lower part of the curve corresponds, on the contrary, to a very considerably *higher* penetrating power than is predicted by this theory.

We conclude, therefore, that the incoming electrons, while mostly absorbed by the mechanisms assumed in the Bethe-Heitler theory, are yet able by some additional absorptive process to *produce* enough penetrating *secondaries* to give to the curve the increased absorption that it needs at the top and the more penetrating character which its lower half reveals.

The simplest assumption to account for these penetrating secondaries is merely that *a photon has the power not only of producing electron pairs, as Bethe-Heitler theory requires, but also, at much rarer intervals, of transferring its energy through a nuclear collision to a penetrating particle, which particle merely acts as an agent, or link, for carrying the energy downward*, but which may, through another collision, retransform its energy into electron-photon showers of the usual type.[8] It is assumed that it is through this mechanism that the incoming electrons of 6 billion electron-volts of energy are able to throw their influences down as far as to sea level, and thus produce there the cosmic-ray shelf, or diminution in sea-level intensity, which is found to set in at magnetic latitude 41°N, in spite of the fact that as already stated pure Bethe-Heitler theory does not permit even ten-billion volt electrons to produce one-thirtieth of the observed sea-level effect. It is also with the aid of these penetrating secondary links that we can explain the fact that showers some times representing a total energy of as much as several billion electron volts are found at sea level and below, as well as the observed fact that at least in the lower part of the atmosphere there is a strong Z component of absorption in substances of different atomic number Z, in spite of the fact that the Bethe-Heitler theory requires a Z^2 law, and that such a law actually appears in most shower experiments.

[8] We discussed this suggestion at length with the group at the Norman Bridge Laboratory as soon as, in February and March 1936, we had analyzed the results of the Madras flights made in October, 1935. Oppenheimer and Serber of this group have already published a brief note embodying this suggestion. (Phys. Rev. **51**, 1113 (1937).)

III. The Non-Field-Sensitive Cosmic Rays

The Madras curve reproduced in curve B represents all of the ionization produced by the non-field-sensitive cosmic rays. It is the background, present the world over, on which the ionizing effect of the latitude-sensitive rays is imposed. Its shape and its area give us at least some knowledge about the nature of these non-field-sensitive rays.

Its similarity of shape to curve A, particularly the fact that the maximum of ionization is reached so near the top of the atmosphere, namely, at 1/10th of the way through, instead of 1/20th as in the case of curve A, tells us at once that it is predominantly composed of highly absorbable rays (i.e., of electrons, photons, or both, for according to Bethe-Heitler these differ but little in absorbability), not of *penetrating* rays of any sort. This is our first bit of knowledge as to its composition.

Secondly, let us raise the following query: Can we admit in its constitution any significant ingredient of such incoming penetrating charged particles as the well-nigh universally accepted mode of treatment of the so-called "penetrating component" of the cosmic rays requires? Our own answer to that question is in the negative, but to show why we draw this conclusion we must compare the total areas of curves A and B. The latter's area, extended down to the lowest depths at which appreciable ionization can be observed at all, is a little larger than that of curve A, but when we add the latitude-sensitive rays found north of San Antonio, recently determined by us and soon to be published in detail, we find that the total energy represented by all latitude-sensitive rays is only a little larger than the energy represented in the area of curve A. For our present purposes we shall then treat curves A and B as of approximately equal area and as representing the respective energies of the latitude-sensitive and the non-latitude-sensitive components of the incoming cosmic radiation.

We have seen in §I that the average energy of the incoming rays responsible for curve A is 10 billion electron volts, since it is composed of the whole of the band of incoming charged particle rays (in this case electrons,—see §II) of energies between 6.7 billion electron volts and 17 billion electron volts. Even if the extreme and as yet

wholly gratuitous assumption be made that curve B is due *entirely* to incoming charged particles—no photons at all—the average energy of these particles, no matter whether they are protons, electrons, or something of intermediate mass, must be above 17 billion electron volts, let us say *at the least* 20 billion, in order to enable the particles to get through the blocking effect of the earth's field and become a part of the non-field-sensitive component. It follows, then, from the mere equality in the areas of A and B that the number of *particle* rays responsible for B cannot at the most be more than half that responsible for A, since the same total energy combined with twice the individual energy means half the number. This tells us, then, something quite sharp and definite about the *distribution of energies* among the incoming charged particles. We may formulate it thus: *The great bulk of the incoming particle rays are in any case in the latitude-sensitive range of energies, i.e., in the band of energies between 6 and 17 billion electron volts.* Under the most extreme possible of assumptions there cannot be 1/10th that number of incoming particle rays of energies as high as 10^{11} electron volts, and probably not one-hundredth that number.

The third bit of knowledge about the non-field-sensitive component of the incoming cosmic rays is derived from the fact that 88 percent of the cosmic-ray ionization found at sea level is due to the background of non-latitude-sensitive incoming rays. This is evident from the fact that the maximum value of the equatorial dip—that found at Singapore—is 12 percent. Further, the cloud-chamber experiments at sea level show that by far the larger part of the tracks found there are those of *penetrating particles.*

The question to which we are now seeking an answer is "do these penetrating particles come in from outside or are they secondaries formed in our atmosphere?"[9] The most direct answer to that question is found in the original finding of Anderson,[10] confirmed by Kunze,[11] Anderson,[12] Anderson and Neddermeyer,[13] Blackett and Brode;[14] and recently notably extended by LePrince Ringuet and Jean Crussard,[15] that the penetrating particles actually found in cloud-chamber work at sea level are divided nearly equally between positives and negatives. In view of the fact that we know from the east-west effect that the *incoming* charged particles are predominantly positives, the near equality in the number of positives and negatives observed at sea level apparently means that these observed penetrating particles are not *the incoming particles at all*, at least to any significant degree, *but are secondaries produced in the atmosphere by incoming rays which have practically the same chance of transferring their energy directly or indirectly, in whole or in part, to a penetrating positive as to a penetrating negative.*

There is, however, a second mode of approach to the question as to whether the penetrating particles actually found near the earth's surface and below it are secondaries formed in the atmosphere or primaries coming in from outside. Remembering that only 12 percent of the sea-level ionization is due directly or indirectly to incoming latitude-sensitive rays and 88 percent to the non-latitude-sensitive component, we ask ourselves whether we can build up the observed curve B out of an appreciable mixture of incoming protons, or other penetrating rays, such as we actually find in cloud chambers, with highly absorbable rays which follow the Bethe-Heitler theory, as both electrons and photons are assumed to do. This is, in fact, the picture that is most in vogue among European physicists today, the penetrating particles being in general thought of simply as protons, the highly absorbable rays as electrons.

Here again the shapes and the areas of curves A and B seem to us to negate this assumption. For no matter whether these incoming particles are protons or electrons, in order to get through the blocking effect of the earth's field and become

[9] The suggestion that all the observed cosmic-ray effects found in the lower atmosphere might be secondary effects arising from the absorption of electrons in the outer layers of the atmosphere was made as early as 1928. See Nature **121**, 20 (1927), also **140**, 23 (1937). The secondary character of the great bulk of cosmic-ray effects was also strongly emphasized in December, 1932. See Phys. Rev. **43**, 664 (1933).

[10] Anderson, Phys. Rev. **41**, 405 (1932).
[11] Kunze, Zeits. f. Physik **80**, 559 (1933).
[12] Anderson, Phys. Rev. **44**, 406 (1933).
[13] Anderson and Neddermeyer, International Conference on Physics **1**, 171 (1934).
[14] Blackett and Brode, Proc. Roy. Soc. **154**, 573 (1936).
[15] LePrince Ringuet et Jean Crussard, Comptes rendus **204**, 112 (1937); also J. de phys. **8**, 213 (1937).

a part of the non-field-sensitive component they must have energies of around 20 billion electron-volts at the least, and, as already shown, their number must therefore be at the most half the number of latitude-sensitive electrons of mean energy 10 billion electron volts which are responsible for curve *A*. This small number, though they are practically all needed to explain the very large ionization in the upper portion of the atmosphere (for the area of curve *B* down to 5 meters of water is practically as large as that of curve *A*) must, according to our present hypothesis, be divided between penetrating particles and electrons in such a way as to enable the penetrating particles to produce all the ionization found in the lower atmosphere, for pure Bethe-Heitler electrons cannot throw any appreciable ionizing influences down anywhere near that far. Indeed, the idea of the admixture of penetrating particles was introduced just to "explain" the great preponderance of penetrating particles found below 6 meters of water in cloud chambers and in counter experiments. With this assumption of an admixture of incoming electrons and penetrating particles it is the latter that are just able to get through the atmosphere at an energy of 6 billion volts and thus cause the equatorial dip to set in at magnetic latitude 41°N, but because they are *penetrating* particles and do not make radiative collisions they cannot ionize appreciably more strongly in the upper air or anywhere on the way down than they do at sea level, so that there is no way whatever in which to account for the large increase in ionization actually found between sea level and say 5 meters below the top. This argument may be stated a little more quantitatively as follows:

Just how penetrating particles coming in from all directions do actually ionize as a function of depth was first pointed out by Bowen and later by Langer and Epstein, all of whom showed that the ionization produced by such rays of a given energy ionizing approximately uniformly along their paths produce within a constant pressure electroscope an ionization which varies linearly with the distance of the electroscope above the end of the range of the particles. Furthermore, since each of the hypothetical incoming penetrating particles with which we are here concerned must have an energy of at least 20 billion electron volts in order to get through the blocking effect of the earth's field, and must lose 5.7 billion electron volts in penetrating vertically through the atmosphere, this "range" is $20/5.7=3.5$ atmospheres, and the ionization at a depth of one atmosphere below sea level should be $1.5/2.5$ or 0.6 of the sea-level ionization, while the ionization at the top of the atmosphere should be $3.5/2.5=1.4$ times the sea-level ionization. But in fact the direct measurement of the ionization one atmosphere below sea level shows it to be but 0.35 of its sea-level value.[16] And the quantitative argument applied to a point a few meters of water *above* sea level is still more striking. Thus at say 6 meters (curve *B*)—a depth to which 20 billion volt Bethe-Heitler electrons cannot penetrate so as to produce, even if the incoming equatorial rays were all electrons more than 2.5 ions/cc sec. the observed ionization is some five times its value at sea level namely about 12 ions/cc sec. (see *B*), while that due to incoming penetrating particles alone should be $2.9/2.5$ or 1.15 that at sea level, so that the observed ionization is here more than twice at the least what the foregoing assumptions permit.

Another closely allied argument is as follows: As already stated, a mere mixture of penetrating particles with absorbable rays which follow the Bethe-Heitler theory requires all the ionization found in the lower part of the atmosphere to be due to the penetrating component. On the other hand, the non-field-sensitive rays in order to get through the blocking effect of the earth's magnetic field must have an entering energy of about 20 billion electron volts at least, and of this they will have retained about 14 billion electron volts even after they have penetrated to sea level. None of these 14 billion electron volt penetrating rays could be stopped by 10 cm of lead, which is equivalent to but one-ninth of an atmosphere. Therefore an electroscope shielded by 10 cm of lead at sea level should show practically as large an ionization as an unshielded electroscope, and if any secondaries at all are formed in the lead the shielded electroscope should show the larger discharge rate. In fact, however, the shielded electroscope shows about 67 percent of the ionization found in an unshielded one. This is inexplicable in terms of the foregoing picture.

[16] Millikan and Cameron, Phys. Rev. **37**, 244 (1931).

We conclude, therefore, (1) from reading of shielded and unshielded electroscopes in the lower atmosphere, (2) from the shape and area of curve *B*, and (3) from the near equality in the number of the high energy positives and negatives, *that incoming penetrating particles are not a significant factor in the near sea-level ionization*, that instead the observed penetrating particles are secondaries produced in the atmosphere.

In a word, they are the same "penetrating links" which we have already introduced to obtain a consistent interpretation of curve *A*.

The net result of all the considerations advanced thus far in this paper is contained in the statement that *practically all of the cosmic ray effects observed in the lower part of the atmosphere are secondary effects—splashes of various kinds—produced in the upper layers of the atmosphere by the inflow from outside of electrons* (+ *or* −) *or of electrons and photons combined, which no matter what their energy, cannot themselves penetrate through the upper layers because of the powerful barrier set by the laws of nuclear absorption.*

Our experiments thus far yield no crucial evidence as to the relative roles played by electrons and photons in producing the ionization due to the non-field-sensitive half, as measured by energies, of the incoming cosmic rays. A minor part of the incoming non-field-sensitive rays must in any case be electrons to account for the equatorial east-west effect. If they are all electrons, then in accordance with the reasoning in §I we may expect the intercept of curve *B* on the vertical axis to be at 5.5 (half of 11) or less; since the lower limit to the average energy of these hypothetical electrons cannot be placed at less than about 20 billion electron volts. If curve *B* should actually be found to cross the axis outside this range then something other than electrons or protons or penetrating charged particles of any sort must be a constituent of the incoming rays. We can probably follow the actual course of curve *B* farther to the left than we have yet done, though this is not a promising prospect for differentiating between incoming electrons and photons. With suitable *ad hoc* and as yet *unverifiable* assumptions, either hypothesis—electrons alone or a mixture of photons and electrons—can be made to work. The answer to this question, if found at all, will probably be found from more fundamental considerations as to the mode of origin of the rays rather than from a further study of curves *A* and *B*.

FEBRUARY 1, 1938 PHYSICAL REVIEW VOLUME 53

Neutrons from Lithium Plus Deuterons

W. E. STEPHENS
W. K. Kellogg Radiation Laboratory, California Institute of Technology, Pasadena, California
(Received December 13, 1937)

The energy distribution of the neutrons from the disintegration of lithium by deuterons has been measured by the method of α-recoils in a helium-filled high pressure cloud chamber. The stopping power was calibrated with thorium C′ α-particles in the chamber. Two distinct groups of neutrons were found with disintegration energies of 15.05±0.2 Mev and 11.8±0.4 Mev. The 15.05 Mev group is attributed to the formation of Be^8 in a normal state and the 11.8 Mev group to the formation of Be^8 in an excited state of about 3.3 Mev with a width at half-maximum of about 1.5 Mev. A more or less continuous distribution was observed from 9 Mev to 3 Mev (the limit of observation). These neutrons may come from higher wider states of Be^8.

INTRODUCTION

THE neutrons resulting from bombardment of lithium with deuterons were first observed by Crane, Lauritsen and Soltan.[1] The neutron energy distribution was measured by Bonner and Brubaker[2,3] by the method of proton recoils in a methane filled high pressure cloud chamber[4] with a mica sheet to further

[1] Crane, Lauritsen and Soltan, Phys. Rev. **44**, 693 (1933).

[2] Bonner and Brubaker, Phys. Rev. **47**, 973 (1935).
[3] Bonner and Brubaker, Phys. Rev. **48**, 742 (1935).
[4] Brubaker and Bonner, Rev. Sci. Inst. **6**, 143 (1935).

a part of the non-field-sensitive component they must have energies of around 20 billion electron-volts at the least, and, as already shown, their number must therefore be at the most half the number of latitude-sensitive electrons of mean energy 10 billion electron volts which are responsible for curve *A*. This small number, though they are practically all needed to explain the very large ionization in the upper portion of the atmosphere (for the area of curve *B* down to 5 meters of water is practically as large as that of curve *A*) must, according to our present hypothesis, be divided between penetrating particles and electrons in such a way as to enable the penetrating particles to produce all the ionization found in the lower atmosphere, for pure Bethe-Heitler electrons cannot throw any appreciable ionizing influences down anywhere near that far. Indeed, the idea of the admixture of penetrating particles was introduced just to "explain" the great preponderance of penetrating particles found below 6 meters of water in cloud chambers and in counter experiments. With this assumption of an admixture of incoming electrons and penetrating particles it is the latter that are just able to get through the atmosphere at an energy of 6 billion volts and thus cause the equatorial dip to set in at magnetic latitude 41°N, but because they are *penetrating* particles and do not make radiative collisions they cannot ionize appreciably more strongly in the upper air or anywhere on the way down than they do at sea level, so that there is no way whatever in which to account for the large increase in ionization actually found between sea level and say 5 meters below the top. This argument may be stated a little more quantitatively as follows:

Just how penetrating particles coming in from all directions do actually ionize as a function of depth was first pointed out by Bowen and later by Langer and Epstein, all of whom showed that the ionization produced by such rays of a given energy ionizing approximately uniformly along their paths produce within a constant pressure electroscope an ionization which varies linearly with the distance of the electroscope above the end of the range of the particles. Furthermore, since each of the hypothetical incoming penetrating particles with which we are here concerned must have an energy of at least 20 billion electron volts in order to get through the blocking effect of the earth's field, and must lose 5.7 billion electron volts in penetrating vertically through the atmosphere, this "range" is $20/5.7=3.5$ atmospheres, and the ionization at a depth of one atmosphere below sea level should be $1.5/2.5$ or 0.6 of the sea-level ionization, while the ionization at the top of the atmosphere should be $3.5/2.5=1.4$ times the sea-level ionization. But in fact the direct measurement of the ionization one atmosphere below sea level shows it to be but 0.35 of its sea-level value.[16] And the quantitative argument applied to a point a few meters of water *above* sea level is still more striking. Thus at say 6 meters (curve *B*)—a depth to which 20 billion volt Bethe-Heitler electrons cannot penetrate so as to produce, even if the incoming equatorial rays were all electrons more than 2.5 ions/cc sec. the observed ionization is some five times its value at sea level namely about 12 ions/cc sec. (see *B*), while that due to incoming penetrating particles alone should be $2.9/2.5$ or 1.15 that at sea level, so that the observed ionization is here more than twice at the least what the foregoing assumptions permit.

Another closely allied argument is as follows: As already stated, a mere mixture of penetrating particles with absorbable rays which follow the Bethe-Heitler theory requires all the ionization found in the lower part of the atmosphere to be due to the penetrating component. On the other hand, the non-field-sensitive rays in order to get through the blocking effect of the earth's magnetic field must have an entering energy of about 20 billion electron volts at least, and of this they will have retained about 14 billion electron volts even after they have penetrated to sea level. None of these 14 billion electron volt penetrating rays could be stopped by 10 cm of lead, which is equivalent to but one-ninth of an atmosphere. Therefore an electroscope shielded by 10 cm of lead at sea level should show practically as large an ionization as an unshielded electroscope, and if any secondaries at all are formed in the lead the shielded electroscope should show the larger discharge rate. In fact, however, the shielded electroscope shows about 67 percent of the ionization found in an unshielded one. This is inexplicable in terms of the foregoing picture.

[16] Millikan and Cameron, Phys. Rev. **37**, 244 (1931).

We conclude, therefore, (1) from reading of shielded and unshielded electroscopes in the lower atmosphere, (2) from the shape and area of curve *B*, and (3) from the near equality in the number of the high energy positives and negatives, *that incoming penetrating particles are not a significant factor in the near sea-level ionization*, that instead the observed penetrating particles are secondaries produced in the atmosphere.

In a word, they are the same "penetrating links" which we have already introduced to obtain a consistent interpretation of curve *A*.

The net result of all the considerations advanced thus far in this paper is contained in the statement that *practically all of the cosmic ray effects observed in the lower part of the atmosphere are secondary effects—splashes of various kinds—produced in the upper layers of the atmosphere by the inflow from outside of electrons* (+ *or* −) *or of electrons and photons combined, which no matter what their energy, cannot themselves penetrate through the upper layers because of the powerful barrier set by the laws of nuclear absorption.*

Our experiments thus far yield no crucial evidence as to the relative roles played by electrons and photons in producing the ionization due to the non-field-sensitive half, as measured by energies, of the incoming cosmic rays. A minor part of the incoming non-field-sensitive rays must in any case be electrons to account for the equatorial east-west effect. If they are all electrons, then in accordance with the reasoning in §I we may expect the intercept of curve *B* on the vertical axis to be at 5.5 (half of 11) or less; since the lower limit to the average energy of these hypothetical electrons cannot be placed at less than about 20 billion electron volts. If curve *B* should actually be found to cross the axis outside this range then something other than electrons or protons or penetrating charged particles of any sort must be a constituent of the incoming rays. We can probably follow the actual course of curve *B* farther to the left than we have yet done, though this is not a promising prospect for differentiating between incoming electrons and photons. With suitable *ad hoc* and as yet *unverifiable* assumptions, either hypothesis—electrons alone or a mixture of photons and electrons—can be made to work. The answer to this question, if found at all, will probably be found from more fundamental considerations as to the mode of origin of the rays rather than from a further study of curves *A* and *B*.

FEBRUARY 1, 1938 PHYSICAL REVIEW VOLUME 53

Neutrons from Lithium Plus Deuterons

W. E. STEPHENS
W. K. Kellogg Radiation Laboratory, California Institute of Technology, Pasadena, California
(Received December 13, 1937)

The energy distribution of the neutrons from the disintegration of lithium by deuterons has been measured by the method of α-recoils in a helium-filled high pressure cloud chamber. The stopping power was calibrated with thorium C′ α-particles in the chamber. Two distinct groups of neutrons were found with disintegration energies of 15.05±0.2 Mev and 11.8±0.4 Mev. The 15.05 Mev group is attributed to the formation of Be^8 in a normal state and the 11.8 Mev group to the formation of Be^8 in an excited state of about 3.3 Mev with a width at half-maximum of about 1.5 Mev. A more or less continuous distribution was observed from 9 Mev to 3 Mev (the limit of observation). These neutrons may come from higher wider states of Be^8.

INTRODUCTION

THE neutrons resulting from bombardment of lithium with deuterons were first observed by Crane, Lauritsen and Soltan.[1] The neutron energy distribution was measured by Bonner and Brubaker[2, 3] by the method of proton recoils in a methane filled high pressure cloud chamber[4] with a mica sheet to further

[1] Crane, Lauritsen and Soltan, Phys. Rev. **44**, 693 (1933).

[2] Bonner and Brubaker, Phys. Rev. **47**, 973 (1935).
[3] Bonner and Brubaker, Phys. Rev. **48**, 742 (1935).
[4] Brubaker and Bonner, Rev. Sci. Inst. **6**, 143 (1935).

increase the stopping power. The stopping power of the gas and mica were calculated and hence somewhat uncertain. In order to obtain a more accurate value of the maximum energy of the neutrons, this experiment was repeated

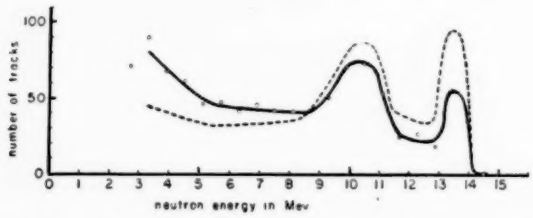

FIG. 1. Energy distribution of neutrons emitted at 90° from lithium bombarded with 0.93 Mev deuterons as inferred from recoils in helium. The points are the observed number of tracks. The dashed curve is the distribution after being corrected for $n-\alpha$ cross section and geometrical conditions.

by the method of α-recoils[5] in a helium filled high pressure cloud chamber with the stopping power of the chamber calibrated with thorium C′ α-particles.

EXPERIMENTAL PROCEDURE

A lithium metal target[6] was bombarded with deuterons accelerated by a peak voltage of 0.93 Mev[7] in a short ion path a.c. tube. The cloud chamber was filled with a mixture of 95 percent helium and 5 percent air to a pressure of 11.9 atmospheres. The stopping power of this gas was determined by finding the mean range of the thorium C′ α-particles given off into the chamber from a pin with a deposit of thorium B on the end. After the thorium B had decayed sufficiently, α-recoils from the neutrons were similarly photographed, reprojected and measured. The stopping power was corrected for change in amount of alcohol vapor with temperature and for a slight leakage of the gas during the course of the experiment. The chamber was refilled and recalibrated for the last 1000 pictures to check the calibration.

In a total of 9000 stereoscopic pictures, 1034 α-recoil tracks, which had directions within 8° of a line to the center of the target, were measured. Recoils from neutrons with energies less than 3 or 4 Mev were short enough to be easily missed. Even in the range from 3 Mev to about 6 Mev, the recoils are so short that the resolving power is poor. The distribution in energy of the neutrons inferred from the measured α-recoils is shown in Fig. 1. The dashed curve is the distribution after being corrected for the $n-\alpha$ collision cross section and the probability of observing a track of a given length. The $n-\alpha$ collision cross section used was that given by Bonner.[8] Values above 5 Mev were obtained by extrapolating Bonner's curve to a value of $0.44 \cdot 10^{-24}$ at 14 Mev. In using these values we must assume that the angular distribution of the scattering does not change with energy. No measurements have been reported on the angular distribution of the $n-\alpha$-scattering. Indeed, above 2 Mev energy of the neutron the deBroglie wavelength of the neutron is no longer large compared to the radius of interaction between neutron and α-particle and the scattering is no longer expected to be spherically symmetrical in the center of gravity coordinates. Nevertheless, measurements on the energy distribution of neutrons from $B-d-n$ which have been made both with helium recoils and proton recoils[5, 9] give quite similar relative intensities of the groups. Hence for our purposes between 6 Mev and 12 Mev the $n-\alpha$ forward scattering seems to be similar to that for $n-p$, which should not depart appreciably from spherical symmetry in the center of gravity coordinates in this region. The relative probability of measuring tracks of different lengths depends on the area of the chamber in which they can start and still not hit the wall. To correct for this, the observed number of tracks of a length R was multiplied by the graphically determined and approximate factor $7.5/(7.5-R)$.

To determine the maximum energy of the neutrons, the measured tracks were plotted in an integral number range curve as shown in Fig. 2. It is easier to fit a smooth curve to the integral points and extrapolate, and also Livingston and Bethe's[10] corrections are for integral or semi-

[5] Bonner and Brubaker, Phys. Rev. **50**, 308 (1936).
[6] The lithium targets turn black in air, probably due to the formation of a thin layer of Li_3N on the surface, as suggested by Sheperd, Haxby and Hill, Phys. Rev. **52**, 675 (1937).
[7] The voltage on the tube has been calibrated against the sparkless sphere gap voltmeter of Sorenson, Hobson and Ramo, A. I. E. E. **54**, 651 (1935).
[8] T. W. Bonner, Phys. Rev. **45**, 601 (1934).
[9] Stephens and Bonner, Phys. Rev. **52**, 527 (1937).
[10] Livingston and Bethe, Rev. Mod. Phys. **9**, 389 (1937).

integral curves. No correction for "area" error[11] need be applied to the integral curve. In addition to the corrections given by Livingston and Bethe for natural straggling, thick target, obliquity, and angle between neutron and α-recoil,[10] we have included in the total straggling term (called S'' by Livingston and Bethe) a term for the straggling due to error in measuring the tracks. No correction was made for the fact that a.c. was used to accelerate the deuterons.[12] The angle χ_0 in the correction for angle between neutron and α-recoil was taken as 10° since due to the wide target it was possible to measure a few recoils which had angles of 8° to 16° with the neutron direction but still only 8° with a line to the center of the target. Bethe's revised 1937 range energy curve[13] was used. After making these corrections, the observed neutron energy at 90° to 0.93 Mev deuterons is 14.01 Mev. The disintegration energy calculated from the observed neutron energy is then $Q_{10}=15.05\pm0.2$ Mev.

If we treat the second peak in the same way, allowing for the spread due to the natural width of the group by adding 1 Mev to the straggling correction, we find the energy of the neutrons to be 11.1 Mev and the disintegration energy $Q_{11}=11.8\pm0.4$ Mev. This is quite uncertain, because it is not known how such a level width changes the extrapolation. We can fit the high energy group approximately with a Gaussian error curve with its center at about 13.5 and a straggling of about 0.5 Mev. If we assume this to be the experimental neutron distribution from a narrow level then we can spread a dispersion curve out by such a Gaussian error curve and by fitting this to the second group we can get an idea of the real width. The width at half-maximum by this method is $\gamma=1.5$ Mev. We get another value for the energy of the level by taking the difference between the peaks. This comes out 3.5 Mev, slightly larger than the value 3.3 Mev obtained from the extrapolations. The 11.8 Mev group is about twice as intense as the 15.05 Mev group.

Discussion

The high energy peak was found by Bonner and Brubaker and attributed by them, to the reaction

$$Li^7+H^2\rightarrow Be^8+n^1+Q_1,$$

where Be^8 is left in its normal state. The present value of $Q_{10}=15.05$ Mev is somewhat higher than that of Bonner and Brubaker. From the known masses of Li^7, H^2 and n^1, the mass of Be^8 is calculated to be just stable with respect to two α-particles. However, the accuracy of the experiment is not enough to rule out the value of 0.1 Mev unstable which Livingston and Bethe[14] calculate from the corrected energies of the reactions[15, 16]

$$B^{11}+H^1\rightarrow Be^8+He^4+8.60\pm0.11 \text{ Mev}$$

and

$$B^{11}+H^1\rightarrow {}^*Be^8+He^4$$
$$\rightarrow He^4+2He^4+8.70\pm0.2 \text{ Mev}.$$

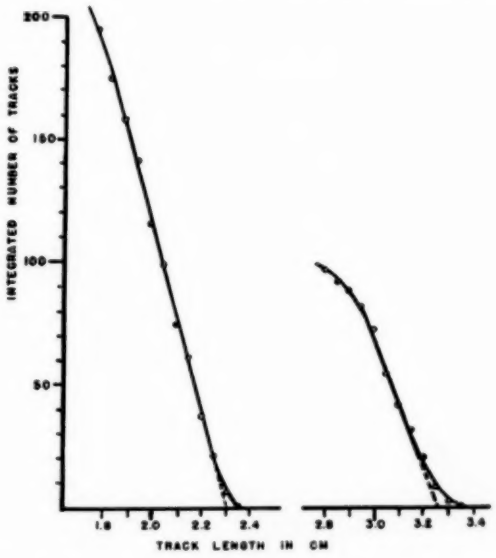

FIG. 2. Integrated number of tracks plotted against track length for the two groups of neutrons. The track length scale should be shifted 0.025 cm to the right.

[11] King and Rayton, Phys. Rev. **51**, 826 (1937).

[12] The effect of using a.c. voltage to accelerate the deuterons has been investigated by Dr. H. Staub. He has calculated graphically the theoretical curve for the range distribution of measured tracks for a.c. incident energy of the deuteron and finds no appreciable difference between the extrapolated value in this case and the case of d.c. incident energy as treated by Livingston and Bethe, Rev. Mod. Phys. **9**, 385 (1937).

[13] Private communication. In this region the new curve does not differ appreciably from the one given in Livingston and Bethe, Rev. Mod. Phys. **9**, 266 (1937).

[14] Livingston and Bethe, Rev. Mod. Phys. **9**, 310 (1937).

[15] Kirchner and Neuert, Physik. Zeits. **35**, 292 (1934); Oliphant, Kempton and Rutherford, Proc. Roy. Soc. **150**, 241 (1935).

[16] Dee and Gilbert, Proc. Roy. Soc. **154**, 279 (1936).

The fact that Bonner and Brubaker's curve does not show the second group of neutrons may possibly be due to uncertainty in their corrections for the probability of measuring a track of a given length which went through the mica. The correction they applied varies from about +150 percent at 8.4 Mev to 0 percent at 9.9 Mev to +150 percent at 11.2 Mev, and might well have obscured a peak here. It should be pointed out, however, that if there were a strong homogeneous group of neutrons at 1.7 Mev, then recoil protons from the alcohol vapor in the chamber, might, if treated as α-recoils, give the 11.8 Mev peak observed in helium. The low energy part of Bonner and Brubaker's curve gives no evidence of such a group. This second group then probably represents a 3.3 Mev level in Be^8 with a width at half-maximum of about 1.5 Mev. This is presumably the $^1D_2$ level which theoretical calculations[17] place at 1.9 Mev. There is quite a lot of evidence for such a level. A 2.8 Mev level with a width of 0.77 Mev has been observed in the $B^{11}-p-\alpha$ reaction[16] and a similar 3 Mev level was found in the $B^{10}-d-\alpha$ reaction.[18, 19] Also the radioactive α-particles from Li^8 indicate such a level with an energy between 4.7 and 2.6 Mev and a width of 1.4 to 1.0 Mev.[20, 21]

The neutrons between 5 and 9 Mev may come from a wide excited state around 6 Mev. Evidence for such a level has been found in the $B^{11}-d-\alpha$ reaction[18, 19] and also perhaps in the $Li^8-e^-\alpha$ reaction[20, 21] and in theoretical calculations of the ^1G level.[17] The ^1P level has been calculated[17] to come at about 12 Mev and would give neutrons around 3 Mev in some agreement with Bonner and Brubaker's corrected low energy maximum. Further evidence for this 12 Mev level is found in Fowler and Lauritsen's[21] radioactive $Li^8-e^-\alpha$ energy distribution. When they correct their observed energy distribution for the fact that the probability of the beta-transition should increase at least as $(E_{\beta\,\max})^5$, then a very wide level seems to be present around 10 to 12 Mev.

If these considerations are correct, then it may be possible to account for the disintegration of Li^7 by deuterons by the two primary reactions[22]

$$Li^7+H^2\rightarrow Be^8+n^1+Q_1,$$
$$Li^7+H^2\rightarrow He^5+He^4+Q_2$$

and then

$$Be^8\rightarrow He^4+He^4+Q_3,$$
$$He^5\rightarrow He^4+n^1+Q_4,$$

where Be^8 and possibly He^5 are also formed in excited states. It also seems possible that these higher levels of Be^8 are quite wide and merge into a sort of continuum in accord with the idea of Kempton, Browne and Maasdorp.[23]

I wish to thank Dr. T. W. Bonner for valuable suggestions; Dr. H. Staub for calculating the a.c. correction; and Dr. C. C. Lauritsen for continued encouragement. I also wish to express appreciation to the Seeley W. Mudd Fund for financial support.

[17] Feenberg and Phillips, Phys. Rev. **51**, 597 (1937).
[18] Cockcroft and Lewis, Proc. Roy. Soc. **154**, 246 (1936).
[19] Wheeler (mentioned in Livingston and Bethe, Rev. Mod. Phys. **9**, 320 (1937)).
[20] Lewis, Burcham and Chang, Nature **139**, 24 (1937).
[21] Fowler and Lauritsen, Phys. Rev. **51**, 1103 (1937).
[22] Evidence for the He^5 reaction has been found by Williams, Shepherd and Haxby, Phys. Rev. **51**, 888 and **52**, 390 (1937).
[23] Kempton, Browne and Maasdorp, Proc. Roy. Soc. **146**, 922 (1934).

Slow Neutron Disintegration of B^{10} and Li^6

M. STANLEY LIVINGSTON AND J. G. HOFFMAN
Cornell University, Ithaca, New York

(Received December 10, 1937)

The disintegration of B^{10} by slow neutrons is found to result in two groups of alpha-particles, of ranges 0.80 ± 0.03 and 0.66 ± 0.05 cm and with relative intensities 1 : 3, corresponding to disintegration into the ground state of the Li^7 product nucleus and the 0.44 Mev excited state, respectively. The reaction energies obtained from these ranges with the best available range energy relation check well with those computed from atomic masses if a mass of B^{10} is used which is consistent with other nuclear disintegrations. The slow neutron disintegration of Li^6 results in H^3 particles of 5.90 ± 0.06 cm range, indicating a reaction energy of 4.86 Mev. This is in disagreement with the value obtained from atomic masses and suggests errors in the mass values or the proton range energy relation. Techniques for the measurement of very short particle ranges are described, including methods for the determination of the depth of penetration into the recording ionization chamber.

INTRODUCTION

THE strong absorption of slow neutrons by boron and lithium has been of great value to slow neutron experimenters. The reactions assumed to result in these strong absorptions are:

$$B^{10}+n^1\rightarrow Li^7+He^4+Q_a, \quad \text{(a)}$$

$$Li^6+n^1\rightarrow He^4+H^3+Q_b. \quad \text{(b)}$$

Neutron absorption coefficients have been measured and used for the determination of neutron resonance energies. The reactions are utilized in instruments for the detection and measurement of slow neutrons, and as slow neutron shields. The probability of the reactions is thought to be inversely proportional to neutron velocity and to have no resonance maxima.

Measurements of particle ranges and reaction energies, necessary for the theoretical interpretation of these high neutron absorptions, have resulted in large discrepancies. Chadwick and Goldhaber[1] first observed the alpha-particles from boron to have ranges of 5 to 10 mm. Taylor and Dabholkar[2] found the over-all Li^7+He^4 range to be 1.14 cm air equivalent using a photographic emulsion technique. Rotblat[3] has reported a range of 0.818 cm for the alphas using a variable pressure method. Haxel[4] interprets his results to indicate two groups of alphas, of 0.64 and 0.94 cm range, and suggests an excitation level in the Li^7 nucleus at about 0.9 Mev. Fünfer[5] has more recently reported the Li^7 and He^4 ranges to be 0.40 and 0.86 cm, respectively, using a proportional counter and a pressure variation method. In the lithium reaction the first observation was by Chadwick and Goldhaber;[1] a singly charged group (H^3 particles) of 5.5 cm range and a doubly charged group (He^4) of 1.5 cm were observed. Rotblat[3] has remeasured these to be 5.36 and 1.08 cm. In a preliminary report of these experiments the present authors[6] found a considerably longer range for the H^3 particles.

A property of reactions among such light elements is that the reaction energy depends sensitively upon the energy of the incident particle. However, the processes to be investigated are exoergic and probably occur with slow neutrons only so there can be no ambiguity with regard to the energy of the incident particle. It was the purpose of this investigation to obtain accurate values of the particle ranges, using appropriate corrections for thickness of the target and for the depth of penetration of the disintegration particles into the recording ionization chamber.

PART I: RANGE MEASUREMENTS

Experimental

The slow neutron source used in these experiments was the usual Rn-Be "bomb," of approximately 500 mC Rn strength, located in a slow neutron "howitzer." The howitzer is found to give from 3 to 5 times the intensity of slow

[1] Chadwick and Goldhaber, Proc. Camb. Phil. Soc. **31**, 612 (1935).
[2] Taylor and Dabholkar, Proc. Phys. Soc. London **48**, 285 (1936).
[3] Rotblat, Nature **138**, 202 (1936).
[4] Haxel, Zeits. f. Physik **104**, 540 (1937).
[5] Fünfer, Ann. d. Physik **29**, 1 (1937).
[6] Livingston and Hoffman, Phys. Rev. **50**, 401 (1936).

neutrons as from a paraffin sphere, depending upon the distance from the source. The targets were placed inside the muzzle of the howitzer to obtain the maximum intensity (see Fig. 1).

The targets were thin layers of B_4C and Li_2CO_3 deposited on aluminum plates of 10.3 cm diameter. They were thin relative to the slow neutron absorption (about 0.01 g/cm²) but thick relative to the ranges of the particle products. This requires a thick target analysis of the experimental data to obtain the true range.

A shallow ionization chamber (5.1 cm diameter and 0.4 cm deep) was mounted parallel to the plane of the target. A scale and vernier attached to the supporting aluminum tubing was used to record the relative positions of the target and chamber. A linear pulse amplifier, thyratron scale-of-eight counter and electrical impulse counter were used to record the number of particles entering the chamber. A suitable bias voltage impressed on the grid of the first thyratron was used to eliminate the background noise level of the amplifier, and served to determine a limit to the minimum size of pulse in the chamber required to produce a count. The background, with neutron source removed, was of the order of 0.2 counts/minute. The maximum counting rates obtained (1500 counts/minute) were low enough to make corrections for resolving time of the counting circuits unnecessary.

Results

With the experimental arrangement described above motion of the ionization chamber relative to the target resulted in number distance curves showing a gradual increase with decreasing distance, starting at about 0.8 cm for boron and 6.1 cm for lithium. The particle groups were superimposed on a background due to nitrogen disintegrations and fast neutron recoils in the air of the chamber. Thin aluminum disks, for which the neutron absorption is small, were placed between the target and chamber to obtain a measure of this background. Counts were taken for 10 minutes or more for each setting of the scale.

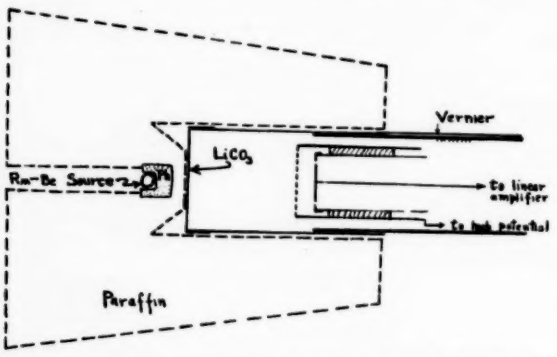

FIG. 1. Slow neutron source, target and recording ionization chamber assembly for observing slow neutron disintegration products. The ionization chamber is moved relative to the target.

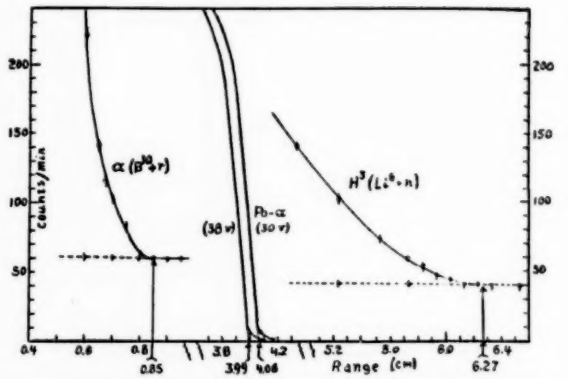

FIG. 2. Number distance curves under operating conditions for the alpha-particles from $B^{10}+n$, Po alphas using two thyratron bias voltages and the H^3 particles from Li^6+n.

In order to obtain a more accurate calibration of the distance between the target and ionization chamber than possible from physical measurements, this distance (including the depth of penetration of alphas into the chamber) was calibrated with Po alpha-particles. A thin layer of Po on a duplicate Al target plate was placed behind a collimating screen formed from a brass disk drilled with many holes of small diameter, so that the maximum angle to the normal was restricted to 8°. This resulted in a well-defined straggling curve from which the extrapolated range of the alphas could be read to ±0.005 cm. Po alphas have an extrapolated range at 15°C and 760 mm pressure of 3.848 cm,[7] which becomes 4.062 cm under operating conditions of 24°C and 742 mm for example. The readings of the arbitrary scale of the vernier are then shifted to allow the observed extrapolated range of the alphas to intersect the axis at this calculated point.

In Fig. 2 one set of experimental data obtained for the alphas from a boron target, the alpha-particle group from Po, and the H^3 group from a lithium target are plotted on the scale men-

[7] Rutherford, Wynn-Williams, Lewis and Bowden, Proc. Roy. Soc. **139**, 617 (1933).

tioned above to illustrate the results. The H^3 particles have a different specific ionization than the calibrating alphas and hence penetrate further into the chamber. This additional penetration was estimated by varying the bias voltage.

The thyratron tube to which the amplifier output was connected was operated with a grid bias of 30 volts. The "flash-point" of the thyratron was at 22 volts, so that pulses which operated the counter were proportional in size to 8 volts bias of the thyratron. When the bias was increased from 30 to 38 volts the Po alpha-range was decreased by 0.07 cm (Fig. 2), indicating that alphas producing twice the ionization in the chamber penetrated 0.07 cm further. The energy of an alpha-particle of residual range z, sufficient to produce a count through the 30 volt bias, must then be equal to half the energy of a particle of residual range $(z+0.07)$ cm. Using the Cornell range energy curve of 1937[8] (revised according to the recent data of Blewett and Blewett[9]), we find that the residual range z, which is the penetration of the alphas to produce a count, is 0.10_5 cm. This has an energy equivalent of 0.14 Mev. The range of an H^3 particle of this energy is about 0.13_5 cm, or 0.03 cm greater than the alpha range. This correction must be added to the observed range of the H^3 particles under the operating conditions.

The difference in shape of the disintegration particle curves from that of the calibrating alpha-group is due to two features, the thick target and the lack of angular collimation necessitated by the low intensities. This shape can be interpreted in the following way: If the range of the particles is R, the distance between target and chamber is x, and the layer dy from which the particles originate is y equivalent centimeters below the surface, only those particles falling within the solid angle measured by the linear angle θ will be observed, where $\cos\theta=(x+y)/R$. If N_0 is the number emitted per unit solid angle per cm² per second in the direction of the normal, the number observed will be:

$$N=2\pi N_0\int_0^{\arccos\,(x+y)/R}\sin\theta\,d\theta$$
$$=2\pi N_0(R-(x+y))/R,$$

and since N_t, the total number emitted from the layer dy in all directions is $2\pi N_0$, we have:

$$N=N_t(R-(x+y))/R.$$

To get the effect of the thick target we must integrate between the limits of $y=0$ and $y=R-x$:

$$N_{0b}=N_t\int_0^{R-x}R-(x+y)/R\,dy=\tfrac{1}{2}N_t(R-x)^2/R.$$

In the range in which the data are taken ($R-x$ small) this equation will be valid, and represents a parabola with an axis at $R=x$. If we plot the square root of the observed intensities (after subtracting the background) as a function of x the curve should be linear and should extrapolate to the true range, $R=x$, for $N^{\frac{1}{2}}=0$.

In Fig. 3 the data of Fig. 2 are plotted in this manner, resulting in an alpha-particle mean range of 0.85 ± 0.04 cm and a H^3 range of 6.27 ±0.10 cm. Adding the penetration correction to the H^3 range and reducing to standard conditions of 15°C and 760 mm from the experimental conditions prevailing during the observations we find: range He^4 from $B^{10}+n=0.81\pm0.04$ cm, and range H^3 from $Li^6+n=5.91\pm0.10$ cm.

In the range of observation the data fall on well-defined straight lines in the square root plot, justifying the analysis and the mean ranges indicated by the intercepts. The probable error of each point is indicated by the extent of a vertical line through the point, obtained from the square root of the total number of counts. The errors for the range intercepts are estimated

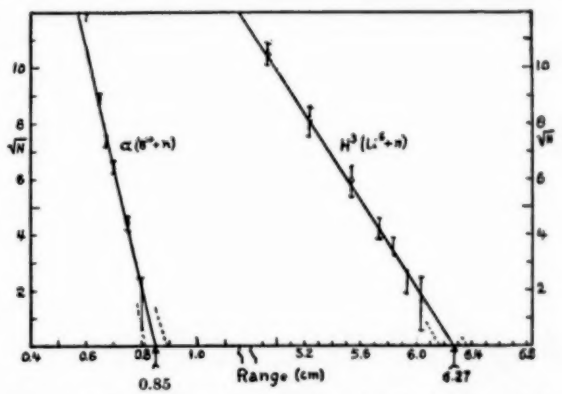

FIG. 3. Plot of $N^{\frac{1}{2}}$ *vs.* distance for the B alphas and the Li H^3 particles to determine the mean range by extrapolation.

[8] Livingston and Bethe, Rev. Mod. Phys. **9**, 266 (1937).
[9] Private communication, soon to be published in Proc. Roy. Soc.

TABLE I.

	RANGE He^4 FROM $B^{10}+n$	RANGE H^3 FROM Li^7+n
I	0.81±0.04 cm	5.91±0.10 cm
II	0.80±0.05	5.79±0.10
III	0.78±0.06	6.01±0.10
	Av. 0.80±0.03 cm	5.90±0.06 cm

TABLE II.

REACTION	Q (calc.)	Q (obs.)	DIFF.
B^{10}–d–p	9.30	9.14±0.06	0.16±0.06
B^{10}–d–α	17.90	17.76±0.08	0.14±0.08
B^{10}–d–n	6.34	6.08±0.20	0.26±0.20
(Aston)	(B^{10} = 10.0161±.0003)		0.20±0.30
	Weighted average diff.		0.17 Mev

from the limiting straight lines that could be drawn through the points.

Three complete determinations were made for the Li and the B targets, including Po alpha-calibration curves in each case. The geometry was varied by choosing different chamber depths and collimation screens and different thyratron bias settings were used. The result of each determination was computed in the manner described above and a value obtained for the range under standard conditions. These values and the final averages are given in Table I.

Discussion

In attempting to evaluate the energy equivalents of these observed particle ranges we encounter serious difficulties. The alpha-particle range of 0.80 cm falls in the region of the range energy relation in which the experimental determinations are poor and where the capture and loss of charge invalidates the theoretical calculations which seem to be satisfactory for higher energies. The Cornell curves of 1937[8] were based upon the data of Briggs and of Mano (corrected for known errors of calibration) and upon Neuert's measurement of the short He^3 and He^4 ranges in the Li^6–p–α disintegration. This suggests an energy equivalent of 1.51 Mev for the B alphas. Recent data by Blewett and Blewett[9] diverge widely from the Cornell curve in this low energy region. An extrapolation of the curve from their data to somewhat lower energies gives an energy equivalent of 1.75±0.05 Mev for 0.80 cm alphas. The error indicated is just the experimental error and does not include the inaccuracies of the range-energy relation. From momentum considerations we find that 11/7 of the alpha-particle energy represents the reaction energy. The two values above result in reaction energies Q_a=2.38 and 2.75±0.08 Mev. That predicted by the atomic masses[10] is 2.99 Mev, showing discrepancies of 0.61 and 0.24 Mev for the two relations used, and far outside the experimental probable error in either case.

In searching for an explanation of this discrepancy it was found that all nuclear reactions involving B^{10} show similar discrepancies between observed and calculated reaction energies. This suggests strongly that the B^{10} mass used in the calculations is in error. The accepted value,[10] 10.01631, is obtained from the mass-spectroscopic measurements of the $B^{10}H_2-C^{12}$ doublet by Bainbridge and Jordan. If we list the nuclear reactions involving B^{10} which are of sufficient accuracy,[11] and obtain a weighted average of the discrepancies, this proves to be about 0.17 Mev (see Table II). The B^{10}–α–p reaction shows an even larger discrepancy in the same direction (0.85 Mev), but the possibility of constant errors in the measurement of ranges of particles produced in alpha-particle disintegrations makes it impossible to state an error. This reaction should be re-investigated with artificially accelerated alphas. The Be^9–d–n–B^{10} reaction cannot be considered since the Be^9 mass is based upon that of B^{10}, and will also be in error. The result of this summary is to indicate that the B^{10} mass should be reduced by 0.17 Mev (to 10.01613), giving a better check with disintegration results and predicting a reaction energy for the B^{10}–n–α reaction of 2.82 Mev, in much better agreement with the observed value of 2.75±0.08 Mev. This also suggests that the Blewett and Blewett range energy relation for alphas is essentially correct.

The H^3 range of 5.90 cm from the Li^6–n–α reaction may be evaluated from the proton range energy relation. Assuming that the range of particles of the same charge but different mass is proportional to their mass for the same velocity we find: the range of a H^3 particle is three times the range of a proton of $\frac{1}{3}$ the energy

[10] Livingston and Bethe, reference 8, p. 373.

[11] Livingston and Bethe, reference 8, p. 371–372.

of the H^3. This forces us to evaluate the H^3 range from a proton range of 1.96_7 cm. This, again, is in the low energy region which was inaccurately known until recently. The Cornell curves were based on the data of Blackett and Lees at low energy and included an empirical factor of 0.2 cm representing the difference between proton and alpha range due to the difference in capture and loss of charge. Recently Parkinson, Herb, Bellamy and Hudson[12] have reported on the ranges of protons accelerated in their pressure electrostatic generator discharge tube. Their data check the Cornell curves above 2.5 cm range, but show somewhat larger energies in the region between 0 and 2.5 cm. According to these data the protons of 1.97 cm range have an energy equivalent of 0.925 Mev. The H^3 energy is three times this value and the reaction energy 7/4 of the H^3 energy, or $Q_b = 4.86 \pm 0.04$ Mev. The low probable error again includes only the experimental fluctuations. This value is to be compared with that of 4.56 Mev expected from the atomic mass values, a discrepancy of 0.30 Mev.

The discrepancy in the observed and calculated reaction energies for Li^6–n–α is much greater than expected from the possible experimental errors in the range measurements. This statement has more meaning when it is noted that the values obtained for the B target are smaller than those predicted by masses, while from the Li target they are larger. If the 4.56 Mev calculated Q is assumed correct the range of H^3 particles expected would be 5.6 cm under the conditions of Figs. 2 and 3. Exactly similar techniques and calibrations were used for the two targets. Furthermore, the low intensities observed should be expected to lead to ranges shorter than the true range rather than larger.

It seems probable that in the Li case also there are errors much greater than in the range measurements either in the mass values or in the proton range energy relation at these low energies. The Li^6 mass is determined from the mass spectrograph values of Li^7 and He^4 through two disintegration reactions, Li^6–d–p and Li^6–d–α. There are discrepancies in these reactions and in other reactions involving Li^7 which seem to be larger than experimental errors, but they cannot be analyzed to show an error in any single mass value and are probably due to simultaneous errors in the mass values of many of the light atoms.

[12] Parkinson, Herb, Bellamy and Hudson, Phys. Rev. **52**, 75 (1937).

Part II. Evidence for the Excited State of Li^7 from the B^{10}–n–α Reaction

In the analysis of the distance variation data of Part I it was found that there was an excess number of counts due to short range alpha-particles from the boron target. This was indicated by the observation that the counts below 0.6 cm distance rose above the straight line used for extrapolation in the square root plot. This effect was not observed with the Li target. Accordingly a different technique was used to study the short range region.

The distance between the target and the face of the ionization chamber was kept constant (1.00 cm) and the depth of the ionization chamber fixed at 0.40 cm. The region between target and chamber and the chamber itself was sealed so that the pressure could be varied (see Fig. 4). With decreasing pressures the alpha-particle ranges extended into the chamber where they were observed; the number of counts was found to increase with decreasing pressure to a maximum value and then fall off to zero with the decreasing efficiency of the ionization chamber at very low pressures. The background counting rate, observed by inserting a thin aluminum disk between target and chamber, decreased regularly with decreasing pressure.

When a screen faced chamber (no collimation) was used the data plotted in Fig. 5 were observed. This showed the boron counts appearing above the background at about 500 mm, rising very rapidly below 400 mm and reaching a maximum at about 200 mm pressure. The data can be analyzed in a manner entirely similar to

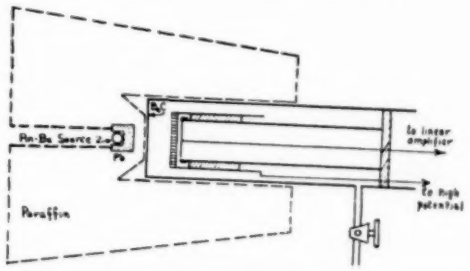

FIG. 4. Pressure variation apparatus for observing the short range alpha-particles from $B^{10}+n$.

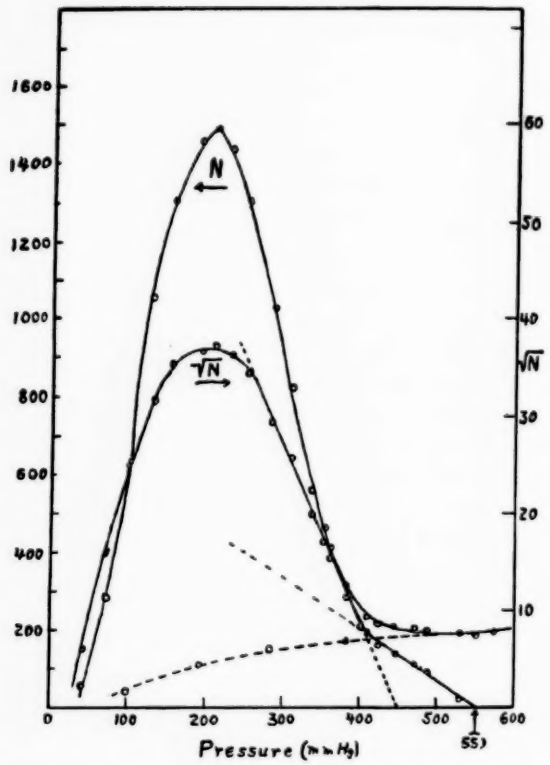

FIG. 5. Number *vs.* pressure curve of alpha-particles from $B^{10}+n$; $N^{\frac{1}{2}}$ *vs.* pressure curve to determine pressure extrapolation.

that used for the distance variation method by plotting the square root of the number of counts (less background) and extrapolating to obtain a pressure representing the range of the alpha-particles. On another scale of Fig. 5 the data are plotted in this manner. It is seen that there are two roughly linear portions of the high pressure side of the curve, one extrapolating to about 550 mm and one to 450 mm. As will be shown later these seem to indicate respectively an alpha-particle group of about 0.81 cm range and another of about 0.66 cm range.

Before range values can be obtained from the pressure intercepts it is necessary to determine the depth of penetration of the particles into the chamber to produce a count, a quantity which is in this case an inverse function of the pressure. This can be determined by an analysis of the shape of the pressure variation curve.

In order to produce a count a particle must release an amount of ionization I (in Mev units) in the chamber. At high pressures a particle stopping in the chamber will result in a count when the residual energy of the particle at the face of the chamber is equal to or greater than I. At low pressures many of the particles will cross the chamber; the limiting condition will be the pressure at which an alpha-particle having the maximum specific ionization (peak of the Bragg curve) will just produce the ionization I in the full chamber depth d. With no angular collimation the high pressure side of the curve will be parabolic, and can be extrapolated by plotting the square root of the number of counts. The low pressure intercept will be significant only if the particles are collimated, so that the depth d represents the length of the particle path in the chamber. From this intercept the ionization I can be determined and so the penetration at the high pressure intercept.

Accordingly, a collimation grid limiting the alphas to within 20° of the normal was substituted for the screen face of the chamber. A pressure variation run with this arrangement resulted in the data plotted in Fig. 6. The boron alpha-counts were much smaller than in the

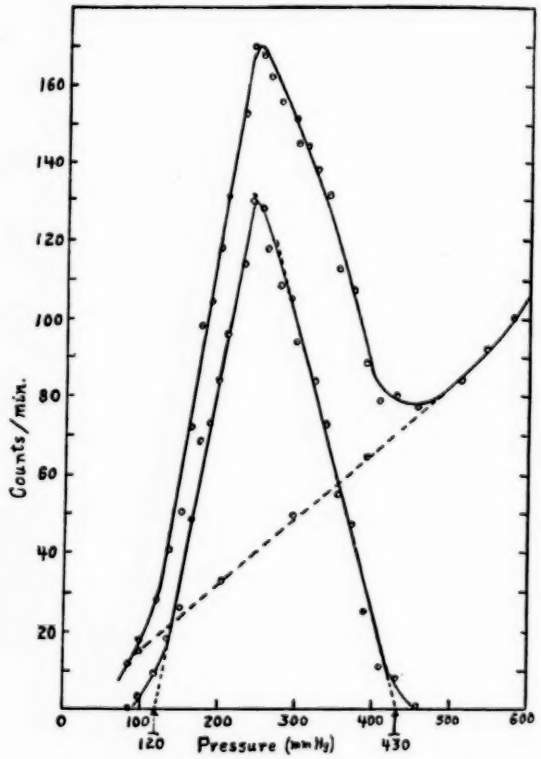

FIG. 6. Number *vs.* pressure curve of alpha-particles from $B^{10}+n$ under 20° collimation, showing pressure intercept for the short range alpha-group.

uncollimated arrangement, but when the background is subtracted they give a sharply peaked curve extrapolating to 120 mm on the low pressure side and 430 mm on the high pressure side. A linear extrapolation of the data is used in this instance (rather than the square root) because with the angular collimation the only disturbing factor is the thickness of the target. It may be noted that the counts due to the longer range alphas (0.81 cm) are now so small that they are not observable above the background, and so the 430 mm extrapolated value should give the range of the short range alpha-group with good accuracy.

The 120 mm low pressure intercept (at 24°C) indicates an air equivalent of the 0.40 cm chamber at standard conditions of 0.061 cm, which when multiplied by the specific ionization at the peak of the Bragg curve (2.36 Mev/cm) gives an energy equivalent of the ionization I of 0.145 Mev. A particle of this energy has a range of $0.10_7 \pm 0.03$ cm, the penetration at standard conditions required to produce a count. This figure is in excellent agreement with that of 0.10_5 cm obtained in Part I for the penetration under essentially standard conditions, and for the same thyratron bias. Since this latter figure was obtained from the revised Cornell range energy curve the check is a confirmation of the correctness of this relation.

The 550 mm intercept of Fig. 5 results in a range to the face of the chamber of 0.702 cm under standard conditions. Adding the 0.107 cm penetration distance we obtain a range for the long range alphas of 0.81 ± 0.05 cm, in good agreement with the value obtained in Part I.

When the straight line extrapolating to 550 mm in Fig. 5 is extended and these values subtracted from the total N^1 curve we find a second extrapolation of 420 mm, indicating a group of shorter range alphas. A better value is obtained from the linear extrapolation of Fig. 6, of 430 mm. This may be used to obtain the range equivalent of the 1.00 cm distance to the face of the chamber of 0.550 ± 0.04 cm. Again adding the penetration distance we find the short range group of alphas to have a range of 0.66 ± 0.05 cm.

Discussion

The interpretation of the experimental results of Part II to indicate two groups of alpha-particles, although experimentally justified, is largely due to the knowledge that the residual Li^7 nucleus has an excited state at about 0.44 Mev above the ground state. This has been observed in the Li^6–d–p reaction as two proton groups,[13] and by the measurement of a 0.4 Mev gamma-ray.[14] In fact, before the evidence discussed in Part I leading to the lower B^{10} mass was analyzed, it seemed probable that the B^{10}–n–α reaction led always to this excited state. We see now that the longer range alphas (0.80 cm) indicate a disintegration into the ground state. Although the range energy relation for alpha-particles is very poorly known in the region about 0.66 cm we can use the best relation available (Cornell—1937—revised according to Blewett and Blewett) to determine a reaction energy for the reaction producing these short range particles. This proves to be 2.27 Mev. The difference between this value and that obtained for the 0.8 cm alphas is 0.48 Mev, in very good agreement with that expected for the 0.44 Mev excitation state of Li^7.

The relative intensities of the two alternate reactions can be obtained from the experimental data of Fig. 5 by extrapolating the two straight line portions of the N^1 curve to zero pressure and comparing the respective ordinates. We find that the excited state transition is 3 times as probable as that leading to the ground state.

The results make it possible to understand the contradictory nature of previous measurements, due to the existence of the two groups of alpha-particles. The good checks with the reaction energies obtained from the new B^{10} mass give a strong confirmation of the essential correctness of the alpha-particle range energy relation used for these low energies. The analysis of the data also shows the necessity of correcting for the distance of penetration of such short range particles into the recording ionization chamber.

The authors wish to express their appreciation for financial assistance in these investigations by the Committee on Radiation of the National Research Council, and to Professor H. A. Bethe and Dr. E. J. Konopinski for valuable suggestions concerning the analysis of the data.

[13] Rumbaugh and Hafstad, Phys. Rev. **50**, 681 (1936).
[14] Shepherd, Haxby and Williams, Phys. Rev. **52**, 247 (1937).

The Photodisintegration of the Deuteron by the Gamma-Radiation from Na^{24}

J. Reginald Richardson* and Lorenzo Emo
Radiation Laboratory, Department of Physics, University of California, Berkeley, California

(Received December 14, 1937)

The photodisintegration of the deuteron by the gamma-radiation from radioactive sodium Na^{24} has been observed in a cloud chamber filled with deuterium at a pressure of one atmosphere. A sample of NaF was activated by deuteron bombardment in the cyclotron to a gamma-ray strength equivalent to about 12 mg of radium, and was then brought close to the cloud chamber. Pictures were taken with a stereoscopic camera. Of the 100 proton tracks observed on 5000 pictures, only 42 were deemed suitable for range measurement, although the angular orientation of 61 could be determined. The range distribution of these tracks indicates a mean air equivalent range of 4.4 mm, corresponding to a mean energy of 410 kv for the photoprotons. This indicates that the difference between the energy of the Na^{24} gamma-ray and the binding energy of the deuteron is 820 ± 35 kv. Since the new range energy relation for slow protons has thrown doubt upon the binding energy of the deuteron, we can use the value of 3.00 ± 0.05 Mev obtained by the Compton recoil method for the energy of the gamma-radiation from Na^{24}, and obtain 2.18 ± 0.07 Mev for the binding energy of the deuteron. The angular distribution of the tracks indicates that the disintegration is predominantly photoelectric, although a small contribution from the photomagnetic effect is not ruled out. A rough calculation from the yield of tracks indicates a cross section for the disintegration of 1×10^{-27} cm². The possibilities of the method for the determination of the energy of strong gamma-radiation is discussed.

1. Introduction

A DIRECT interaction between gamma-radiation and the nucleus was discovered by Chadwick and Goldhaber[1] in 1934. At that time they found evidence indicating that the deuteron was disintegrated into a neutron and a proton when it was irradiated with the hard gamma-rays of Th C″. This corresponds to the reaction

$$_1H^2+Q_\gamma\rightarrow{}_1H^1+{}_0n^1.$$

Later,[2] they reported the measurement (with a linear amplifier) of the energy of the protons produced in the reaction. From the energy of the gamma-rays (2.62 Mev) it was then possible to calculate $Q_\gamma=\epsilon$ the binding energy of the deuteron, for which they obtained the value 2.1 Mev. A calculation of the cross section for the process yielded a value of 6×10^{-28} cm², with a possible error of a factor of two.

The photoneutrons produced in the reaction were also observed and their angular distribution was roughly found to have a maximum at right angles to the direction of propagation of the gamma-ray. On the other hand, the neutrons produced by the photodisintegration of beryllium (first reported by Szilard and Chalmers[3]) were found to have a more or less isotropic angular distribution.

A more exact method of measuring the energy of the photoprotons is to measure their range in a cloud chamber. This has been done by Chadwick, Feather and Bretscher,[4] although no details have been published as yet. A value of the range was found which leads Bethe and Bacher to evaluate the binding energy of the deuteron at 2.22 Mev.

It seemed that one could perhaps exploit this phenomenon to measure accurately the energy of the gamma-radiation from strong sources. This could be done by measuring the range of the photoprotons ejected in a deuterium filled cloud chamber. From the energy of the proton and assuming the binding energy of the deuteron one can determine the energy of the gamma-ray which caused the disintegration. Radio sodium, Na^{24}, offers a convenient source of high energy gamma-radiation to use in testing the method.

2. Theoretical Considerations

The photoelectric effect is a transition of the deuteron from the ground state ^3S to that ^3P state in the continuum which has no angular momentum around the direction of polarization

* Now National Research Fellow at the University of Michigan.

[1] Chadwick and Goldhaber, Nature **134**, 237 (1934).

[2] Chadwick and Goldhaber, Proc. Roy. Soc. **151**, 479 (1935).

[3] Szilard and Chalmers, Nature **134**, 494 (1934).

[4] Chadwick, Feather and Bretscher, *An Introduction to Nuclear Physics*, N. Feather (1936).

of the gamma-ray. This means that the relative probability of ejecting a photoproton at an angle θ with the direction of polarization of a quantum is proportional to $\cos^2\theta$. If one averages this over all directions of polarization for an unpolarized beam, one obtains that the number of photoprotons will be proportional to $\sin^2\psi$ per unit solid angle, where ψ is the angle between the direction of the incident gamma-ray and the velocity of the proton.

There is another transition, however, which could effect the disintegration of the deuteron by gamma-rays, and that is from the ^3S to an hypothetical ^1S state. This transition is forbidden, of course, for the electric dipole, but it can be accomplished by the magnetic dipole moment if there is an admixture of some spin dependent Heisenberg force in the neutron proton interaction. This assumption was originally introduced to explain the scattering of slow neutrons by protons. Evaluating the matrix elements of the magnetic dipole moment, Bethe and Bacher[5] have calculated its contribution to the cross section, assuming zero interaction range. They find for the total cross section for the photodisintegration

$$\sigma=\frac{4}{3}\frac{e^2}{c}\frac{h}{M}\left\{\frac{\epsilon^{\frac{1}{2}}E^{\frac{3}{2}}}{(E+\epsilon)^3}+\frac{(\mu_p-\mu_n)^2}{4}\frac{E^{\frac{1}{2}}\epsilon^{\frac{1}{2}}(\epsilon^{\frac{1}{2}}\pm\epsilon'^{\frac{1}{2}})^2}{(E+\epsilon)(E+\epsilon')Mc^2}\right\},$$

where ϵ' is the binding energy of the ^1S level—either real or virtual; μ_p, μ_n are the magnetic moments of the proton and neutron, and $E=h\nu-\epsilon$. The minus or plus sign stands according to whether the singlet state of the deuteron is stable or virtual. For a finite range of interaction the electric contribution is increased by 60 percent, the magnetic contribution by 15 percent. (If $\epsilon'\sim 120$ kv.)

Since the photomagnetic effect corresponds to a transition $^3S\rightarrow{}^1S$, the angular distribution of the ejected protons (or neutrons) will be isotropic per unit solid angle. Thus if τ represents the ratio of the magnetic to the electric contributions, the total distribution per unit solid angle will be $\sigma_\omega d\omega\sim(\sin^2\psi+2\tau/3)d\omega$.

[5] Bethe and Bacher, Rev. Mod. Phys. **8**, 83 (1936).

In an investigation of the amount of energy which a proton will receive in the disintegration, it is found that the contribution of the momentum of the gamma-ray cannot be completely ignored. Thus if ψ is the angle between the direction of propagation of the gamma-ray and the velocity of the proton, the conservation of momentum and energy indicates the energy of the proton will be:

$$E_H=\tfrac{1}{2}[h\nu(1-h\nu/2Mc^2)+h\nu\cdot(V/c)\cos\psi-\epsilon],$$

where M and V are the mass and velocity of the proton. Thus it is seen that the energy of the proton will vary with ψ in a symmetrical manner around the mean at $\psi=\pi/2$. If one takes into account the number of protons ejected per unit solid angle, neglecting the term $h\nu/2Mc^2$, the distribution of protons with energy can be obtained. This distribution for the photoelectric effect turns out to be a parabola as shown in Fig. 1. The width of the curve at half-maximum ordinate is seen to be 0.7δ where $\delta=h\nu\cdot(v/c)$ and in particular, for $h\nu=3.0$ Mev, $\delta=85$ kv. The bearing of this result on the measurement of gamma-ray energies will be discussed further in Section 5.

3. Apparatus

The cloud chamber used in these experiments was of the Blackett type, with an aluminum piston mounted in a rubber diaphragm. A source

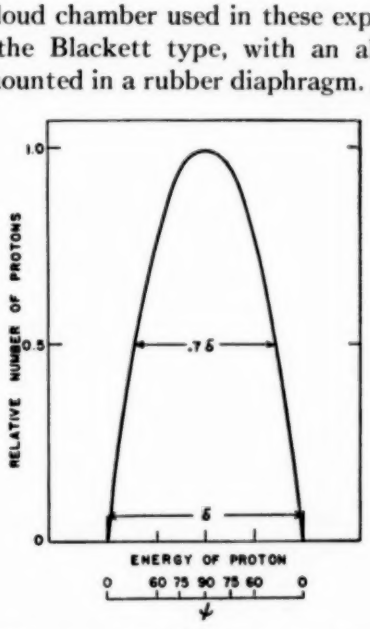

FIG. 1. The energy distribution of the photoprotons ejected by a gamma-ray of energy $h\nu\cdot\psi$ is the angle between the velocity of the proton V and the direction of propagation of the gamma-ray. $\delta=h\nu\cdot v/c$.

of alpha-particles was provided by an active deposit of polonium on the end of a copper wire. The particles were allowed to enter the cloud chamber through a copper foil equivalent in stopping power to 1.1 cm of air. A shutter, mounted on the piston, allowed only fresh tracks to enter the chamber during the expansion. The homogeneity and range of the source was also investigated by means of a linear amplifier.

Since the expected range of the photoprotons was around half a centimeter air equivalent, it was obvious that as much of the stopping power as possible should be due to atoms of deuterium which contribute to the probability of a disintegration. For this reason the chamber was filled with deuterium instead of heavy methane, although the technical difficulties in getting good tracks are somewhat greater with the former. Considerable difficulty was encountered at first in obtaining good heavy particle tracks in the presence of the high electron ionization produced by the strong gamma-ray sources used. As is the usual practice, the clearing field of the chamber was shorted out just preceding each expansion (in order to produce sharp heavy particle tracks). When the clearing field was strong enough to sweep out the general ionization, it was found that a quantity of charge collected on the glass roof of the chamber and so the field could not be taken off. This resulted in an undesirable diffusion of the heavy particle tracks. The most convenient remedy for this condition was found to be a screen of fine wire suspended across the top of the chamber.

The gamma-ray source was a target of NaF which had been bombarded in the deuteron beam of the cyclotron until it had a gamma-ray strength usually equivalent to about 12 mg of radium. The strength of the source was estimated roughly by comparing the gamma-ray ionization it produced in an electroscope with that produced by a known mesothorium source. The NaF was placed in the plane of the cloud chamber at a distance from the walls that was usually about 8 cm.

A stereoscopic camera designed by F. N. D. Kurie[6] was employed in the experiments. This camera uses an f: 4.5 lens and it was found that the light supplied by overloading eight 150-watt 110-volt lamps across 220 volts was quite sufficient for the photography of heavy particle tracks. The tracks were measured by reprojecting the images on the film through the original optical system of the camera. The reprojection image is formed on a table which may be oriented in such a way as to find the angle which a proton track makes with the incident gamma-ray. The length of the image is measured with a pair of dividers and scale. In order to test the reliability of the development and reprojection process, some glass fibers were placed in the chamber, photographed, and then their reprojected images were measured. The distribution of values obtained indicated a probable error of about two percent for the measurement of a clear track.

[6] F. N. D. Kurie, Rev. Sci. Inst. 3, 655 (1932).

4. Results

In a total of about 5000 cloud chamber photographs there appeared sixty-one tracks for which the angle made with the direction of propagation of the gamma-ray could be measured. Forty-two of these tracks were deemed of suitable clearness for range measurement.

The tracks were classified into grades according to their clearness in the photographs, their apparent newness in the cloud chamber, and facility with which they could be recombined for measurement. The number of tracks in each class will give an idea of the subjective criteria employed:

Class	1	2	3	4	5
Number	13	29	19	18	20

Class 1 and class 2 included the tracks which were sufficiently clear so that their length could be measured, while in class 3 the ends of the tracks were not quite distinct enough for range measurement but the angular orientation ψ could be determined.

All the experiments were performed after midnight when the cyclotron had been turned off. It was also ascertained that there was no other source of neutrons in the effective neighborhood at the times concerned.

In order to obtain the energy of a proton from the length of its track in a cloud chamber, it is necessary to obtain the stopping power of the gas in the chamber. If this stopping power S_a is the ratio of the range of alpha-particles in air to the range in the gas, one obtains the reduced air

range by multiplying the length of the proton by S_α. Then it is necessary to find the air equivalent[7] range by multiplying the reduced air range by the appropriate factor in order to take care of the fact that the relative stopping power of hydrogen for slow protons is much larger than for alpha-particles.[8] This factor for the case under consideration is 1.23. The value of S_α was found by measuring the extrapolated range of the alpha-particles in the cloud chamber at the time of the experiment, and performing the corresponding measurement in air (reduced to S.T.P.) with a linear amplifier or cloud chamber. The values for S_α were checked by computation, knowing the composition of the gas in the cloud chamber.

The lengths of the tracks of class 1 and class 2 were multiplied by the appropriate values of S_α to give their reduced air range. These ranges were then segregated into groups of $\frac{1}{4}$ mm width and the number in each group was counted, giving each class 1 track a weight of three class 2 tracks. Normalizing the numbers again to the actual forty-two tracks, one obtains the data plotted in histogram form in Fig. 2. The asymmetry of the curve is at first sight surprising but it is easily explained as follows: In a cloud chamber investigation in which the yield is so small, there are bound to be some old tracks which are included unwittingly with the new. These old tracks will have traversed the chamber before the completion of the expansion so that their length will be somewhat shorter than the majority of the tracks. This could very easily produce the larger tail observed on the short range side.

It is interesting to observe the individual reduced air ranges of the four class 1 tracks which make an angle greater than 80° with the direction of propagation of the gamma-ray. They are: 0.345, 0.349, 0.357, 0.372 cm, giving a mean of 0.356 ± 0.004 cm. This value, together with an inspection of Fig. 2, leads to a choice for the mean reduced air range of the photoprotons of 0.36 cm. Multiplying this by the factor 1.23 mentioned previously, we obtain the value 0.44 cm for the mean air equivalent range of the photoprotons.

Since this work was first reported,[9] an improved determination of the range energy relationship for slow protons has been published by Parkinson, Herb, Bellamy and Hudson.[10] They have measured the extrapolated range in air of protons accelerated in their two million volt generator. Their results indicate an energy for a given range (around 0.5 cm) which is about 30 percent higher than the old value based on the measurements of Blackett and Lees. This probably means that Feather's determination of the binding energy of the deuteron should now yield a lower value close to 2.1 Mev.

Application of the new range energy relationship to our data indicates that the difference between the energy of the sodium gamma-radiation and the binding energy of the deuteron is 820 ± 35 kv. This is the best that can be said toward obtaining the energy of the gamma-radiation until the value for the binding energy of the deuteron is cleared up. Recently,[11] an improved energy determination of the high energy gamma-ray line of Na^{24} has been made using Compton recoil electrons, and yielding the value 3.00 ± 0.05 Mev. We can use this value, together with the difference given above, to make an estimate of the binding energy of the deuteron. It turns out to be 2.18 ± 0.07 Mev.

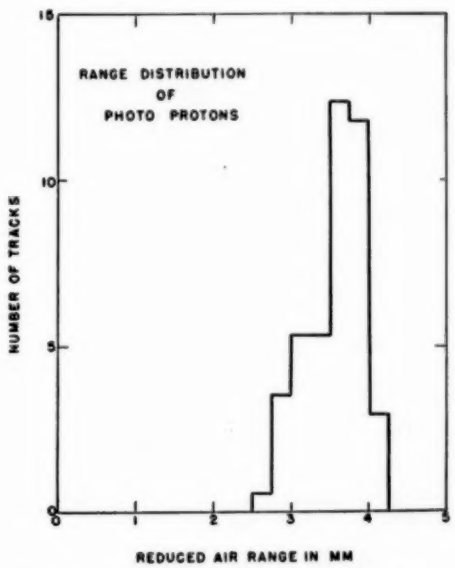

FIG. 2. The range distribution of the photoprotons ejected from deuterium by the gamma-radiation of Na^{24}. The total number of tracks is forty-two.

[7] Blackett and Lees, Proc. Roy. Soc. **134**, 658 (1932).
[8] Blackett, Proc. Roy. Soc. **135**, 132 (1932).
[9] J. R. Richardson and L. Emo, Phys. Rev. **51**, 1014 (1937).
[10] Parkinson, Herb, Bellamy and Hudson, Phys. Rev. **52**, 75 (1937).
[11] J. R. Richardson, Phys. Rev. **53**, 124 (1938).

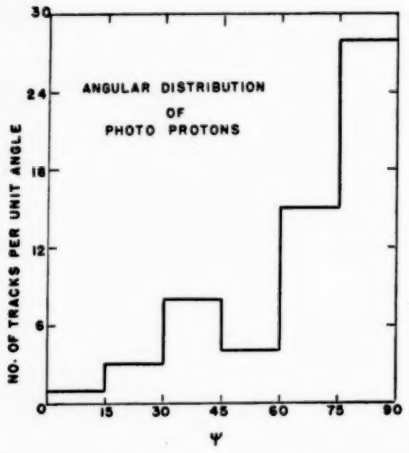

FIG. 3. The experimental distribution of the photoprotons per unit angle. Total number of tracks is sixty-one.

The angular distribution of the photoprotons was also observed. The number of tracks in each fifteen degree interval was counted and the histogram shown in Fig. 3 was drawn. In order to facilitate comparison with theory, the numbers were divided by sin ψ and renormalized, thus obtaining the number of tracks per unit solid angle. The resulting histogram is plotted in Fig. 4. The smooth curve represents the theoretical distribution to be expected from a purely photoelectric effect and has the form $\sin^2\psi$. Experiments on the scattering of slow neutrons by protons, however, indicate the presence of a probably virtual singlet state of the deuteron at about 120 kv. By substituting this value of ϵ' into the formula of Section 2, the contribution to the cross section of the so-called photomagnetic effect can be determined. Since this effect leads to a ^1S state in the continuous spectrum of the deuteron, the angular distribution of the protons due to it will be isotropic in solid angle. The dotted curves represent the theoretical prediction for a 3.0 Mev gamma-ray and a virtual singlet state of the deuteron at 120 kv. They have been normalized to the area of the experimental histogram. Unfortunately, from the data one cannot say whether the photomagnetic effect exists or not. All that can be said is that the photoelectric effect is predominant at this gamma-ray energy.

One can make a rough estimate of the cross section for the disintegration from the yield of tracks if one knows the sensitive time of the cloud chamber, the gamma-ray strength of the Na^{24} source, the fraction of the strength in the 3.0 Mev line, etc. σ turns out to be 1.1×10^{-27} cm^2. This result is probably uncertain by a factor two. The theoretical prediction for the combined photoelectric and photomagnetic effects at $h\nu=3.0$ Mev, if one takes into account the finite range of the neutron proton interaction, is $\sigma=1.8\times10^{-27}$ cm^2.

5. The Measurement of Gamma-Ray Energies

There are two obvious disadvantages to this method of measuring the energy of gamma-radiation. The first is the condition that there must be very few fast neutrons in the neighborhood, because they will knock forward some of the deuterons in the cloud chamber which will leave tracks indistinguishable from those of the photoprotons. Taking into account the relative cross sections for the two processes one sees that it is necessary that there be less than one neutron per thousand gamma-rays in order to get a reliable distribution of tracks. This precludes any work being done on the transmutation gamma-rays from bombardment by deuterons, neutrons, or alpha-particles. However, it should be possible to investigate the gamma-radiation emitted when various substances are bombarded by low energy protons.

The second disadvantage is the small cross section for the disintegration. In practice this

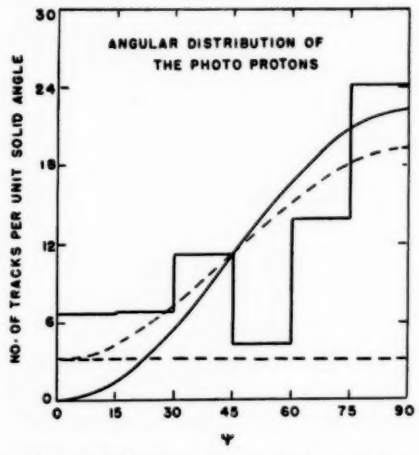

FIG. 4. The distribution of the photoprotons per unit solid angle. Formed by dividing the histogram of Fig. 3 by sin ψ and renormalizing to sixty-one tracks. The solid curve is the distribution to be expected if the disintegration is purely photoelectric. The broken curve is to be expected if there is a singlet virtual state of the deuteron at 120 kv.

TABLE I. *Information relative to the power of the method to resolve gamma-ray lines.*

Energy of gamma-ray $=h\nu$ in Mev	3.0	5.0	10	16
Energy of photoproton $=E_H$ in Mev	0.4	1.4	4	7
h.w. of E_H due to straggling in percent of E_H	7	5	4	3.5
h.w. of E_H in kv due to energy spread for all ψ	60	190	650	1370
h.w. of $h\nu$ in percent of $h\nu$	5	8	14	19
h.w. of $h\nu$ in kv taking $75° < \psi < 105°$	60	150	400	800

means that the source must have a strength of at least two millicuries in the gamma-ray line being investigated.

Whether or not two gamma-ray lines can be resolved by the method, can be determined from the width of the probable energy values of the photoprotons to be expected from a single line. Table I contains the essential information (neglecting instrumental error, which can be made small). The width at half-maximum ordinate (designated in the table by h.w.) is a convenient measure of the difference in the energy of two lines which can be just resolved.

Thus one sees that by using an angular restriction (Fig. 1) it would be possible to resolve lines differing in energy by 60 kv at 3 Mev or 800 kv at 16 Mev. This is probably the best that can be done by any method at present, particularly for the lower energies. There is also a distinct advantage in having the gamma-ray energy depend upon the mean of a distribution rather than its end point (as in the case of the Compton recoils[12] because it makes unnecessary an estimate of the instrumental probable error. Another advantage is the comparatively small dependence on angular variation, so that good results can be obtained under very difficult geometrical conditions. Obviously, the method is only applicable to gamma-radiation of energy greater than 2.2 Mev.

We are very grateful to Professor E. O. Lawrence and to Professor J. R. Oppenheimer for many discussions of this work. Thanks are due to Dr. F. N. D. Kurie for helpful criticism. The experimental work was supported by the Josiah Macy, Jr., Foundation and the Research Corporation and the Chemical Foundation.

[12] J. R. Richardson and F. N. D. Kurie, Phys. Rev. **50**, 999 (1936).

FEBRUARY 1, 1938 PHYSICAL REVIEW VOLUME 53

The Scattering of Protons by Protons

L. R. HAFSTAD, N. P. HEYDENBURG AND M. A. TUVE
Department of Terrestrial Magnetism, Carnegie Institution of Washington, Washington, D. C.

(Received December 13, 1937)

Our measurements of proton-proton scattering during 1936 established the existence of large *nuclear forces* between protons at close distances, in addition to the usual Coulomb forces. These nuclear forces give rise to scattering in excess of the Coulomb prediction, appreciable at 700 kilovolts and very marked at 900 kv. In the energy region between 200 kv and 600 kv the amount of scattering to be expected on the basis of *attractive* nuclear forces is radically different from that to be expected on the hypothesis of *repulsive* nuclear forces since in the first case a decrease and in the second an increase, with respect to the classical scattering, is predicted. We have accordingly extended our measurements to include this energy region, and have obtained results which can only be explained by the assumption of a strong *attractive* force of short range acting in addition to the repulsive Coulomb forces between the particles. The magnitude of the nuclear force required is in approximate quantitative agreement with that deduced from our results of 1936, experimental difficulties due to the low residual energies of the scattered particles, and the very small numbers of counts in some regions of voltage and angle (as low as three percent of the Coulomb prediction) preventing a high precision in these results below 600 kv.

INTRODUCTION

MEASUREMENTS on the scattering of protons by protons made in this laboratory last year[1] showed a considerable excess in the scattering at angles around 45° over that which would be expected for ordinary Coulomb interaction between the particles as assumed by Mott.[2] By a careful mathematical analysis,

[1] Tuve, Heydenburg and Hafstad, Phys. Rev. **50**, 806–825 (1936).

[2] Mott, Proc. Roy. Soc. **A126**, 259–267 (1930).

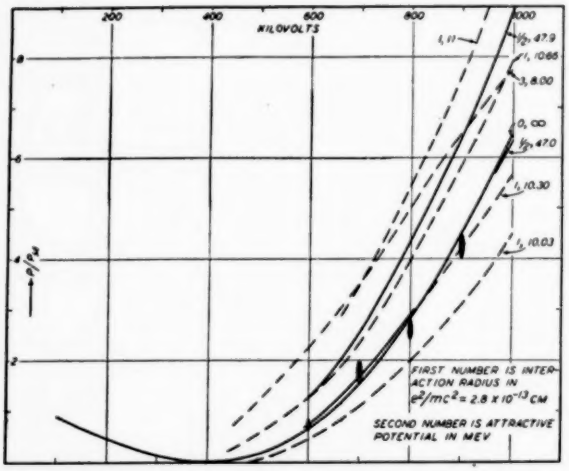

FIG. 1. Theoretical variation of P/P_M, with energy at scattering angle of 45° (ovals obtained from second set of data of T.H.H. using theoretical angular distribution curves fitted to experiment at higher scattering angles) [after Breit, Condon, and Present].

Breit, Condon and Present[3] were able to show that, while either strong repulsive or strong attractive forces in addition to the ordinary Coulomb force could account for the observed excess scattering at 45° at the various voltages, agreement with the experimental results as a function of angle (15° to 50°) at the various voltages was obtained only on the assumption of an *attractive* force of short range (under 10^{-12} cm). If such an attractive force exists between two protons, then one may expect that for some specific combination of the impact parameters the effect of the repulsive Coulomb force should be approximately canceled by the short range attractive force, and at this point a decrease in the number of scattered particles should be observed. This expectation is, of course, largely independent of any specific type of theoretical analysis of the problem. The results of the analysis of Breit, Condon and Present are summarized in Fig. 12 of their paper which is reproduced here as Fig. 1. The ordinates P/P_M are the ratios of the number of scattered protons actually observed or expected on the assumption of attractive forces to the number which would be expected on the basis of repulsive Coulomb forces alone as assumed by Mott. It is seen that the experimental points agree satisfactorily with the theoretical curves in the region above 600 kv, but that no data were available in the neighborhood of the predicted minimum at 400 kv which might serve to verify the deduction made from the higher voltage observations that the "new" force encountered in very close collisions, and superposed on the Coulomb repulsion, is an attractive force and not a suddenly increased repulsion (as for elastic spheres).

The observations of last year were made with the use of an ionization chamber attached to a linear amplifier. This combination was chosen because it permits particles of different kinds, or different energies, to be readily distinguished, and thus reduces the danger of misleading results due to spurious counts. However, this apparatus suffers from the disadvantage that it responds only to particles which are able to produce several thousand ions within the collecting chamber, and therefore fails to detect, with certainty, protons with a residual range, after energy-losses on scattering and on penetrating the ionization-chamber window, of less than about three millimeters. In the case of protons scattered at 45°, which retain only half of the incident energy, the limit for safe detection was reached at 600 kv, and consequently no observa-

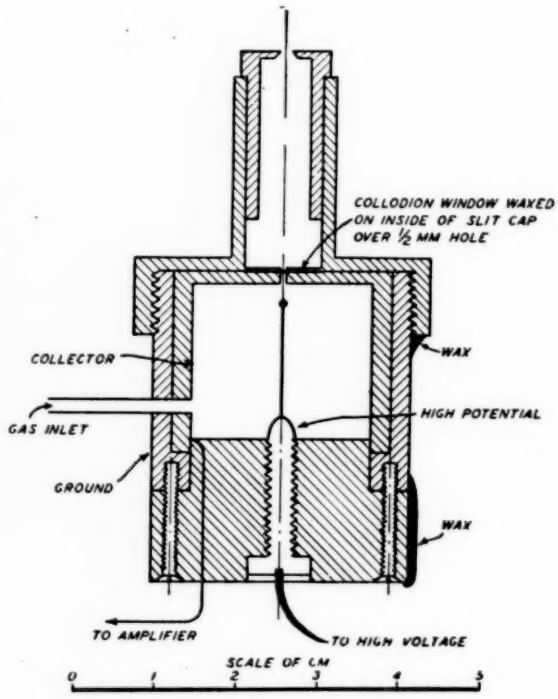

FIG. 2. Geiger point-counter.

[3] Breit, Condon and Present, Phys. Rev. **50**, 825–845 (1936). See also, Sexl, Naturwiss. **50**, 795–796 (1936).

tions by this method were attempted at lower voltages.

Since it was especially desirable to establish definitely the existence or nonexistence of the minimum required by the assumption of an attractive force, measurements on proton scattering have now been extended down to 220 kv by the use of the less reliable, but highly sensitive, Geiger point-counter for the detection of the scattered particles.

As will be found below, the results obtained with the Geiger counter detection technique are as yet not satisfactory from a quantitative standpoint. However, since the qualitative fact of the existence of the "scattering minimum" required by the assumption of attractive forces is so directly and strikingly demonstrated by the observations so far obtained, and since it will not be possible to repeat these observations for some time, it seems desirable to report our results in their present form.

Apparatus and Technique

A new scattering apparatus was built following the observations made last year. This was done to improve the alignment of the detector with respect to the incident beam, to provide a less troublesome ground joint for rotating the detecting chamber, and to provide a more accurate angular scale with a vernier for measuring the position of the detector. The dimensions of the new slit-systems, for the incident beam and for the detector, were not changed significantly from those of last year.[1]

The detector for the scattered protons consisted of a Geiger point-counter, with a 3-stage amplifier of the type by Johnson and Street,[4] which was available in the laboratory. The output of the amplifier was connected to a scale-of-eight thyratron recorder of a design due to Giarratana.[5] A cross section of the Geiger counter is shown in Fig. 2.* A platinum wire 0.002 inch in diameter, with a bead about three times this diameter, formed on the end of the wire in an oxygen gas flame, was used in the

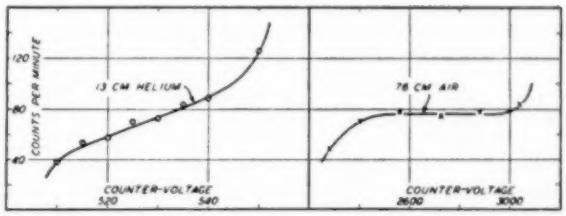

FIG. 3. Characteristics for Geiger point-counter.

counter. The chamber was operated at a helium pressure of 13 cm of mercury. A collodion[6] window of about 1 mm stopping power was placed over the aperture of the counter to close the chamber from the scattering volume. It was found difficult to make a bead on the platinum wire which had satisfactory operating characteristics. Various techniques for making points were tried[7] without consistent results. It is possible that the use of other circuits[8] would have been more successful.

In general, while a good voltage "plateau" was relatively easily obtainable at high operating pressures, as shown in Fig. 3, it was practically impossible to obtain a satisfactory plateau at the low pressures we were constrained to use because of our thin windows. This fact in itself was sufficient to prevent us from obtaining a measure of the scattering on an absolute scale. However, it is probable that no large error is introduced by this difficulty for though, as shown in Fig. 3, there was usually no definite plateau at the low pressure, a setting nevertheless could be made on the point of inflection which could be reproduced from day to day with an accuracy of perhaps 25 percent. Relative values, taken during a single run, were of course much more accurate, since, with a stabilized counter voltage, no appreciable variation in the counting rate for any given voltage setting was observed. The data were always taken as *ratios*, the 25° value usually being adopted as the standard for each day's comparisons.

A more subtle difficulty was encountered in the fact that, for most Pt points, when the output

[4] Johnson and Street, J. Frank. Inst. **215**, 239–246 (1933).
[5] Giarratana, Rev. Sci. Inst. **8**, 390–393 (1937).
* The cross hatching should have been omitted in Fig. 2 between the inner face marked "collector" and the outer brass case. The collector was a thin-walled brass cup spaced from the outer case by a groove in the hard rubber end-plug at the bottom.

[6] We have found ordinary pharmacist's "New Skin" highly satisfactory for windows.
[7] J. R. Dunning and S. M. Skinner, Rev. Sci. Inst. **6**, 243–246 (1935); H. Geiger, *Handbuch der Physik*, Vol. 22, part 2, p. 155.
[8] H. V. Neher and W. W. Harper, Phys. Rev. **49**, 940–943 (1936); N. S. Gingrich, R. D. Evans and H. E. Edgerton, Rev. Sci. Inst. **7**, 450–456 (1936); and G. Brubaker and E. Pollard, Rev. Sci. Inst. **8**, 254–258 (1937).

from the Geiger counter was carefully observed with cathode-ray monitor at low counting rates, a single isolated "count" would often appear as a ragged group of four or more peaks usually partly unresolved. Such a peak would register as an indefinite number of counts on our "fast" thyratron recorder, thus leading to false results. This difficulty was particularly marked when air was used in the Geiger counter. The effect would probably not be observed when using electrometers or other slower methods of detection. The point which was finally used (in helium) showed sharp, clean kicks and not more than one "residual" count in five minutes.

When the Geiger point-counter was tested in the scattering chamber, it was found that there were too many background counts, these being of the same order as the scattered protons at 45°. Most of these counts were due to stray x-rays from the high voltage accelerating tube, and were eliminated by building a lead shielding box $2\frac{1}{2}$ cm thick around the scattering chamber. There still remained from 2 to 5 counts per minute which varied linearly as the number of protons entering the scattering chamber. These counts could be observed independently of the scattered protons by setting the detector at 90° to the incident beam. Counts at 90° might be due to protons scattered from heavy atoms present as a contaminating vapor or gas in the chamber. This possibility was eliminated by closing off the chamber from the pumps and, without introducing hydrogen, observing the scattering at some smaller angle. No increase in the residual counts was observed at 20° even after the chamber had remained sealed off for 30 minutes or more. The observed counts might also be due to "delta-rays" from the incident beam. Since these electrons should have small energies, a magnetic field at the counter slit-system should deflect them out before they entered the counter. The number of counts remained the same, however, with the magnetic field present. It was finally found that these counts could be eliminated by placing a thin opaque foil over the counter aperture. This indicated that the counts were due to ultraviolet light being produced by the proton beam passing through the hydrogen in the scattering chamber, this ultraviolet light producing photoelectrons in the sensitive region of the counter. We then evaporated a thin aluminum coating onto the collodion window of the counter; this increased the stopping power of the window by less than one mm while the background counts were reduced to less than one count in five minutes.

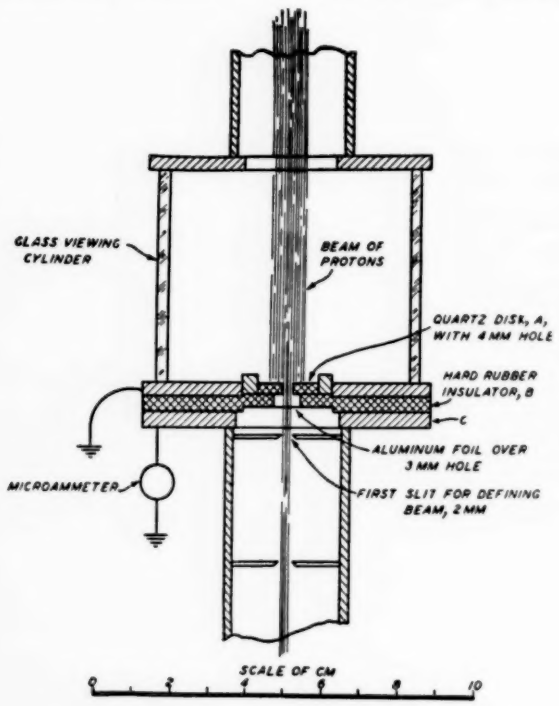

FIG. 4. Proton current monitor.

The operating conditions in the scattering chamber were similar to those of last year. Hydrogen at 12-mm pressure purified by passing through a palladium tube (at a few hundred degrees centigrade) was used in the scattering chamber. The zero angular position of the detecting chamber was determined by running a scattering curve on either side of the zero, the angle about which the two curves are symmetrical being adopted as the zero angle and the vernier being then set to read zero at this position. The mechanical zero of the instrument agreed with this position within the limits of measurement.

In an effort to overcome the difficulty of not being able to record the scattering and to monitor the beam-current into the scattering chamber simultaneously throughout a run, an arrangement shown in Fig. 4 was installed. The scattering chamber was insulated by the

TABLE I. *Experimental results on scattering of protons by protons.*

VOLTAGE (kv)	ITEM	ANGLE AND RELATIVE MOTT VALUE									REMARKS
		20° 362	25° 107	30° 44.0	35° 20.2	40° 11.3	45° 8.18	50° 7.91	55° 9.95	60° 13.4	
220	Counts per min.	...	106	42	18	9.1	4.1	2.4	1.0	...	Current about 8×10^{-10} ampere
	Total counts	...	860	417	381	182	83	48	10	...	
	$(P/P_M)_{25}=1.00$	...	1.00	0.95	0.90	0.81	0.51	0.30	0.10	...	
	$(P/P_M)_{25}=0.87$	...	0.87	0.83	0.78	0.70	0.44	0.26	0.09	...	
335	Counts per min.	...	135	47.5	16.5	6.4	3.4	4.0	4.3	...	Current reading not satisfactory
	Total counts	...	2426	523	330	128	68	40	43	...	
	$(P/P_M)_{25}=1.00$	...	1.00	0.86	0.65	0.45	0.33	0.40	0.34	...	
	$(P/P_M)_{25}=0.75$	...	0.75	0.64	0.49	0.34	0.25	0.30	0.26	...	
450	Counts per min.	...	123	38.4	11.1	3.0	0.55	2.1	5.0	...	Current about 4.3×10^{-9} ampere
	Total counts	...	2458	384	221	59	10	21	50	...	
	$(P/P_M)_{25}=1.00$	...	1.00	0.76	0.48	0.23	0.058	0.23	0.44	...	
	$(P/P_M)_{25}=0.61$	...	0.61	0.46	0.29	0.14	0.03	0.14	0.27	...	
550	Counts per min.	...	125	44.3	17.3	7.0	4.2	...	...	...	Current about 6.2×10^{-9} ampere
	Total counts	...	1756	421	173	140	84	...	...	...	
	$(P/P_M)=1.00$	...	1.00	0.86	0.73	0.53	0.44	...	...	...	
	$(P/P_M)=0.58$	...	0.58	0.50	0.42	0.31	0.25	...	...	...	
640	Counts per min.	154	45.2	17.3	8.1	6.0	5.9	3.2	...	5.5	Current about 3.9×10^{-9} ampere
	Total counts	3085	362	346	161	126	123	13	...	55	
	$(P/P_M)_{25}=1.00$	1.01	1.00	0.95	0.95	1.26	1.71	0.96	...	0.97	
	$(P/P_M)_{25}=0.56$	0.57	0.56	0.53	0.53	0.71	0.96	0.54	...	0.54	

hard rubber disk B and was connected through a microammeter to ground. The proton beam was partially defined by the hole in the quartz disk A, then passed through the thin aluminum window in the plate C and through the slit system of the scattering chamber. The true total current into the scattering chamber cannot be measured in this way because of secondary electrons from the aluminum window (and because the hole in our quartz window was slightly larger than the hole into the scattering chamber). However, it was found that the current into the chamber was proportional to this current so long as the current density remained reasonably uniform throughout the cross section of the beam. The arrangement accordingly served as a fairly satisfactory monitor on the beam current during a run.

RESULTS

A summary of the data obtained is given in Table I. Since for reasons given above it appears unwise to attempt to get absolute magnitudes from these results, only *relative* values are given. In order to show the degree of statistical validity of the results, the total number of counts, as well as the counting rate per minute is recorded. Current measurements, when satisfactory, are given in the supplementary column. Relative Mott values, giving the expected variation of counts with angle for Coulomb forces, are shown at the top of the table.

Two alternative possibilities arise in attempting to compare the observed data with theory. Since for small angles the scattering depends chiefly on Coulomb forces, the Mott ratio for small angles will be unity, and relative values such as the above might be correctly normalized by assuming a Mott ratio of unity for some angle sufficiently small. Observations below 25° not being available, the data may be *arbitrarily* normalized at this angle and, the results, though in error by an appreciable amount, will give the correct trend with voltage. Mott ratios normalized in this way are given in Table I labeled $(P/P_M)_{25}=1$ and are plotted in Fig. 5.

The alternative possibility arises in recog-

TABLE II. *Proton-scattering data, 45° value against energy of proton.*

OBSERVED RATIO	VOLTAGE (kv)							
	220	335	450	550	640	725	820	910
$S_{45°}/S_{25°}$	0.039	0.025	0.0045	0.034	0.038	...	...	...
$S_{45°}/S_{20°}$	...	...	...	...	...	0.067	0.113	0.167

nizing the error involved in the above normalization and using the estimate of the nuclear force obtained by Breit, Condon and Present[3] to calculate a more nearly correct value for the Mott ratio at 25°. This is done in the table and labeled $(P/P_M)_{25}=0.87$ to 0.56, respectively, but is not plotted since it leads to a confusing overlapping of curves. It is perhaps of interest to note that with this closer approximation, the Mott ratio for 45° drops to the very low value of 0.03 at 450 kv.

The first scattering curves were taken before the photoelectrons discussed above were eliminated by coating the counter window with an opaque layer of aluminum. The curve for 220 kv in Fig. 5 was taken under these conditions. At this energy a small proton beam current could be used because of the larger scattering at lower energies. Therefore the photoelectric effect, which varied linearly as the current, was sufficiently small to be neglected. At 335 kv the photoelectric correction was already appreciable. Hence the curves at this voltage and for all higher voltages were taken with the evaporated aluminum window giving a background count of less than one in five minutes.

The 220-kv curve breaks off rather rapidly beyond 40°, for beyond this angle most of the protons do not have sufficient range after passing through the counter-window to actuate the point-counter. The curve at 335 kv was carried beyond 45° to show that at this angle all protons were counted. The symmetry about 45° of the ratio to Mott is clearly shown by the 450-kv curve.

The ratios of counts at 45° to those at 20° (or 25°) at voltages from 220 kv to 900 kv are given in Table II. The values for 220, 335, 450, 550, and 640 kv were taken from Table I. Higher voltage ratios were separately determined this year for this curve. In Fig. 6 these data have been plotted giving ratios to Mott, the value of R at 20° (or 25°) being taken as 0.75 which was the average value found last year for the region 15° to 25°. The points for last year using the linear amplifier for detecting the scattered protons are also given in Fig. 6. It may be noted that these old points are displaced slightly from the values given last year. This is due to a correction which has been applied, based on new information on the stopping power of aluminum

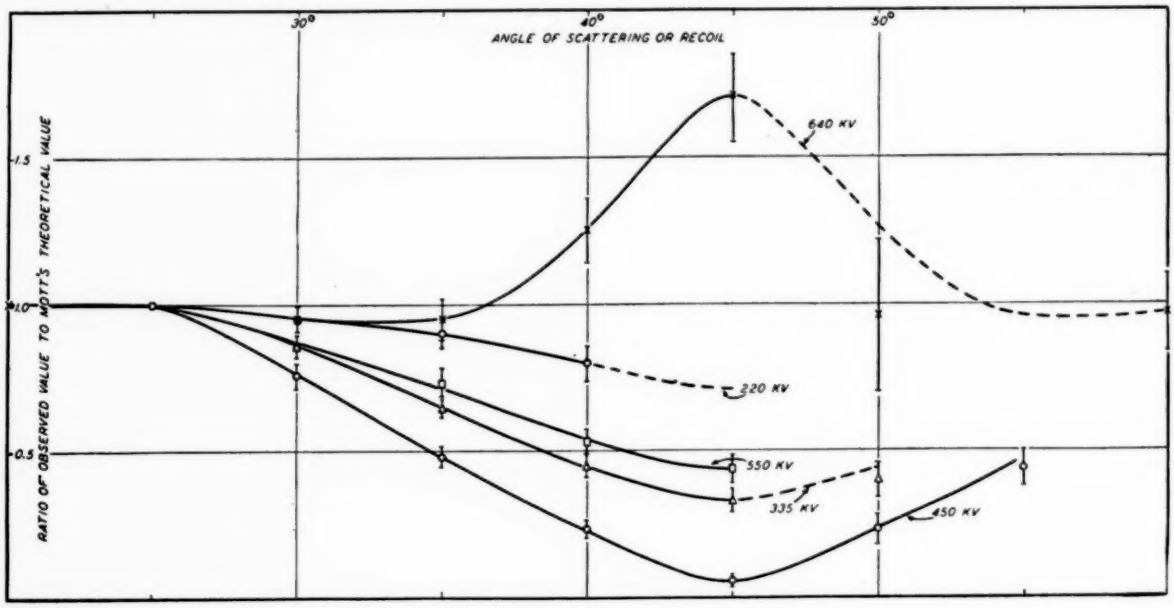

FIG. 5. Proton-proton scattering (ratios adjusted to unity at 25°).

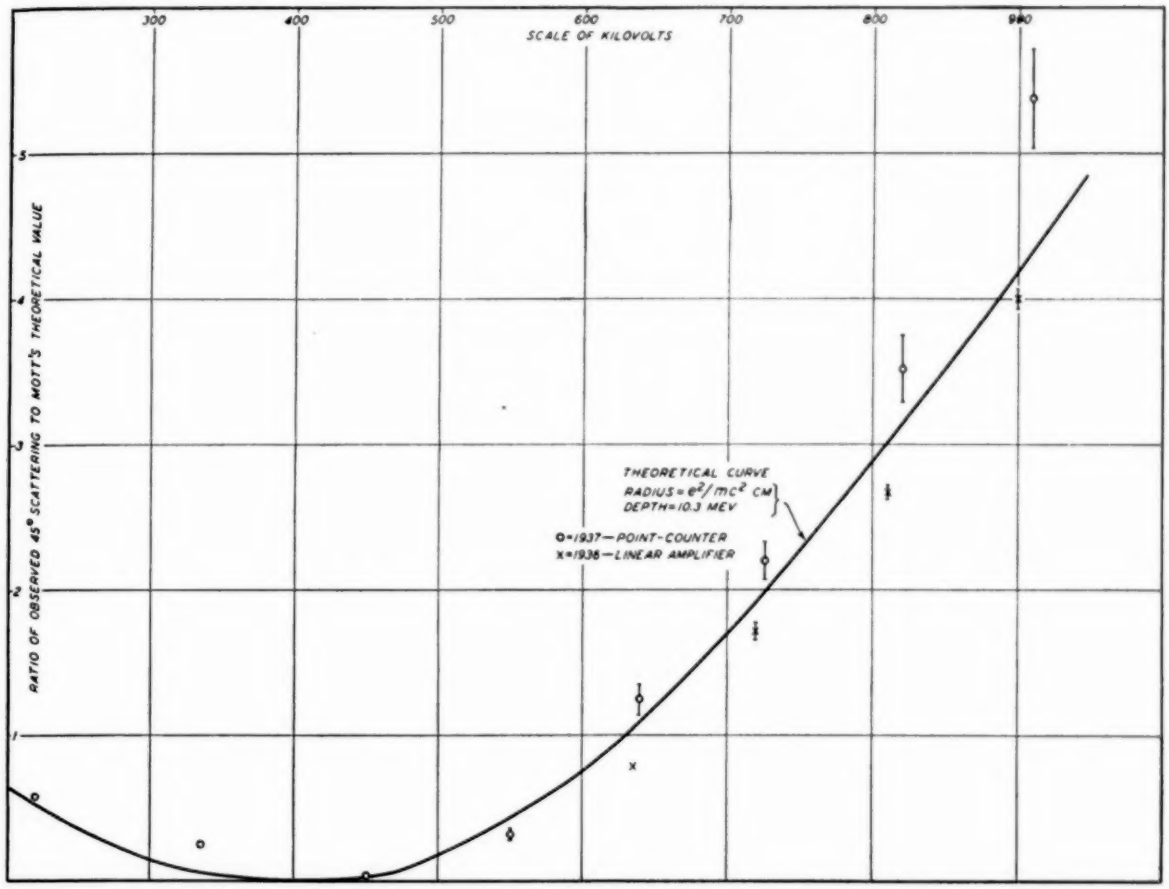

FIG. 6. Variation of scattering with voltage at 45°.

for protons.[9] The values found this year are slightly higher, one conceivable explanation for this being that with the linear amplifier as used last year some of the scattered protons were missed at 45° due to their short range at this angle. However, we feel that the point-counter technique is inherently less quantitative than the linear amplifier, and accordingly we do not consider that these point-counter observations invalidate our last year's curve in any way.

We are now engaged in repeating the curves of last year with a new technique to investigate this difference and to determine the absolute values more accurately.

DISCUSSION

Breit, Condon and Present[3] have shown that our results of last year on proton scattering could be interpreted theoretically by assuming a strongly attractive force between protons at very close distances of approach. The shapes of the curves for angular distribution of scattered protons and the variation of the scattering anomaly with proton energy was reasonably well accounted for by phase shifts in the partial wave having $L=0$ and assuming an interaction potential independent of the proton energy.

In Fig. 1, due to Breit, Condon and Present, several curves have been plotted for the theoretical variation with energy of P/P_M, where P is the scattering probability from the S wave interaction and P_M is Mott's value at 45°. Each curve is for a definite value of the parameters r_0, the radius of the potential well in units of e^2/mc^2, and E_0 is the interaction potential in Mev. The observed values of last year gave $r_0=1$, $E_0=10.30$ as the best values. From the

[9] Parkinson, Herb, Bellamy and Hudson, Phys. Rev. **52**, 75–79 (1937).

values found this year it would appear that an E_0 slightly larger than this may be necessary, but not as large as $E_0=10.66$ for $r_0=1$.

The observed values at 45° in Fig. 5 and Table I clearly show the minimum required by Breit, Condon and Present at approximately the value of energy predicted on the basis of our higher voltage data. The observed value at 45°, 450 kv, goes almost to zero. This offers a striking confirmation of the existence of a short range *attractive* interaction between protons.

It is seen from the curves in Fig. 5 that the scattering is nearly classical at 220 kv. The effect of the attractive force becomes quite appreciable at 335 kv in the region of 45°. At 450 kv and 45° scattering the effect of the attractive force almost completely neutralizes the Coulomb force. With increasing energy of the incident proton the attractive force becomes predominant, giving rise to an increase in the scattering until at roughly 650 kv it exceeds the Mott value.

FEBRUARY 1, 1938 PHYSICAL REVIEW VOLUME 53

The 4.3μ Fundamental Band in the Spectrum of CO_2

DONALD M. CAMERON AND HARALD H. NIELSEN
Mendenhall Laboratory of Physics, Ohio State University, Columbus, Ohio

(Received December 14, 1937)

The fundamental absorption band due to the oscillation ν_3 in the CO_2 molecule has been remeasured and almost completely resolved into its rotational fine structure. The lines are found to fit the formula $\nu=2350.1+0.780N-0.0031N^2$. The convergence factor -0.0031 seems to fit our data a little better than the value -0.0035 given by Martin and Barker, and is in agreement with the theoretically determined value given by Adel and Dennison.

THE spectrum of carbon dioxide has been very carefully investigated in the infrared by several investigators[1] who have succeeded in resolving the majority of the most interesting bands into rotational structure. One band, however, which has been only very imperfectly resolved is that occurring near 4.3μ in the spectrum of CO_2 and due to the fundamental oscillation ν_3 of the molecule. The frequency ν_3 may be thought of as arising when the carbon atom oscillates unsymmetrically along the figure axis of the molecule relative to the center of mass of the oxygen atoms and it is accompanied by an intense change in the electric moment. The intensity of this band is in fact so intense that

[1] P. E. Martin and E. F. Barker, Phys. Rev. **41**, 291 (1932); E. Barker and A. Adel, Phys. Rev. **44**, 185 (1933); E. F. Barker and T. Y. Wu, Phys. Rev. **45**, 1 (1934).

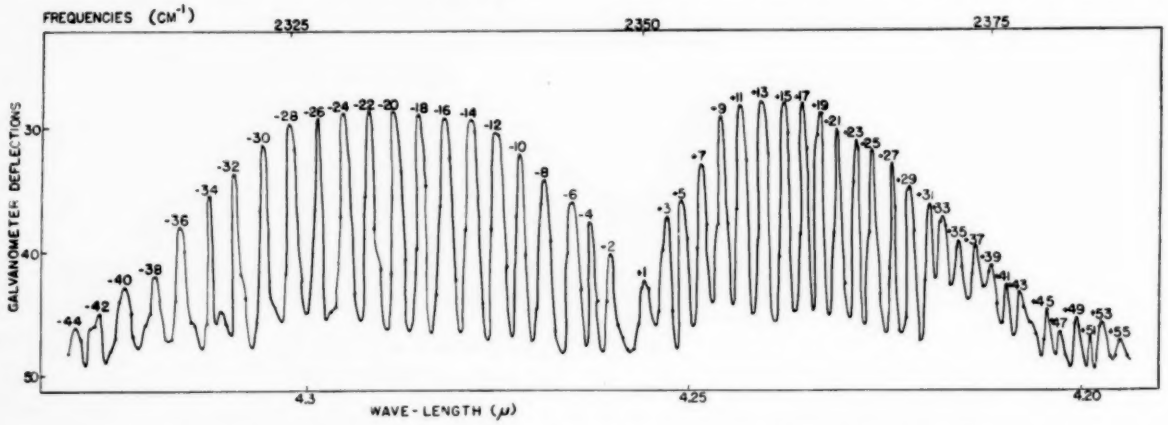

FIG. 1. Galvanometer deflections taken of the fundamental absorption band in CO_2.

the usual amount of CO_2 in the atmosphere will suffice to absorb out completely all the radiant energy of this wave-length coming from the light source. In order, therefore, to make measurements on the absorption by other molecules which have bands in this region we have found it necessary to surround our spectrometer by an air-tight box from which most of the atmospheric CO_2 could be removed. Under these conditions it was found, by the use of a grating ruled with 3600 lines per inch, that the absorption band due to the remaining atmospheric carbon dioxide resolved itself much more completely than has been reported by earlier investigators. We wish here to report on a set of measurements we have made on the absorption band due to CO_2 in this region after narrowing the spectrometer slits down to about 0.5 cm^{-1}, galvanometer deflections being taken at settings on the spectrometer circle separated from each other by intervals equivalent to 0.5 cm^{-1}. The data are shown graphically in Fig. 1 with galvanometer deflections plotted as ordinates and with scales of frequencies and wave-lengths as abscissae and it will be seen that almost complete resolution has been effected. The number of settings made on any one line may be determined by referring to the above figure where for convenience the experimental points have been indicated by small circles.

The frequency positions of the lines in the band may be found by referring to Table I and it is found that these positions are well represented by the formula

$$\nu = 2350.1 + 0.780N - 0.0031N^2, \qquad (1)$$

where N is the ordinal number of the line measured from the center of the band. It is easily shown that for the P branch N takes numerically the value of J in the initial state while for the R branch it takes numerically the values of J in the final state. Since the nuclear spin of the identical oxygen atoms is zero, half of the rotational levels are absent; in the initial state only those where J is even occur and in the final state only those are present where J takes odd values. It is clear, therefore, that half of the rotational lines will also be missing, N being permitted to take only the values $+1, +3, +5, \cdots$ etc. in the R branch and the values, $-2, -4, -6, -8$, etc. only in the P branch. Eq. (1) is the same as that given by Martin and Barker for the lines in this band except that a convergence factor -0.0031 appears to fit our data definitely better than the value -0.0035 given by them. The value -0.0031 is moreover in agreement with the value predicted by the theory for the CO_2 molecule given by Adel and Dennison.[2]

TABLE I. *Line positions in the 4.3μ CO_2 fundamental.*

N	OBSERVED ν	COMPUTED ν	DIFFERENCE
+55	2383.7	2383.6	+0.1
+53	2382.4	2382.7	− .3
+51	2381.7	2381.8	− .1
+49	2380.9	2380.8	+ .1
+47	2380.2	2379.9	+ .3
+45	2379.0	2378.9	+ .1
+43	2377.8	2377.9	− .1
+41	2376.9	2376.9	0
+39	2375.9	2375.8	+ .1
+37	2375.0	2374.7	+ .3
+35	2373.6	2373.6	0
+33	2372.5	2372.5	0
+31	2371.4	2371.3	+ .1
+29	2369.9	2370.1	− .2
+27	2368.8	2368.9	− .1
+25	2367.3	2367.7	− .4
+23	2366.3	2366.4	− .1
+21	2364.8	2365.1	− .3
+19	2363.7	2363.8	− .1
+17	2362.3	2362.4	− .1
+15	2361.2	2361.1	+ .1
+13	2359.4	2359.7	− .3
+11	2357.9	2358.3	− .4
+ 9	2356.5	2356.9	− .4
+ 7	2355.0	2355.4	− .4
+ 5	2353.6	2353.9	− .3
+ 3	2352.5	2352.4	+ .1
+ 1	2350.9	2350.9	0
− 2	2348.5	2348.5	0
− 4	2347.1	2346.9	+ .2
− 6	2345.9	2345.3	+ .6
− 8	2343.9	2343.7	+ .2
−10	2342.1	2342.0	+ .1
−12	2340.3	2340.3	0
−14	2338.6	2338.6	0
−16	2336.8	2336.8	0
−18	2335.0	2335.1	− .1
−20	2333.2	2333.3	− .1
−22	2331.5	2331.4	+ .1
−24	2329.7	2329.6	+ .1
−26	2327.9	2327.7	+ .2
−28	2325.8	2325.8	0
−30	2324.1	2323.9	+ .2
−32	2322.0	2322.0	0
−34	2320.2	2320.0	+ .2
−36	2318.1	2318.0	+ .1
−38	2316.4	2316.0	+ .4
−40	2314.3	2313.9	+ .4
−42	2312.6	2311.9	+ .7

[2] A. Adel and D. M. Dennison, Phys. Rev. **44**, 99 (1933).

The Seventh Spectrum of Chlorine (Cl VII)

L. W. PHILLIPS
Department of Physics, University of Illinois, Urbana, Illinois
(Received December 10, 1937)

Twenty-two lines have been identified in Cl VII, locating eighteen energy levels. From the series $3d-nf$, it is possible to obtain absolute term values for all levels involved. The ionization potential of Cl VII is found to be 113.73 volts.

THE spectrum of Cl VII has been photographed in the vacuum region, with a spectrograph whose twenty-one-foot grating is set at a grazing angle of three degrees. The instrument and power supply have been described in previous reports.[1] One minor change has been made. In the initial installation, the high potential electrode was water cooled. In spite of the fact that the cooling lines were of rubber tubing about thirty feet in length, there was considerable leakage to ground. Recently the water-cooling system has been replaced by an oil-cooling system, so that leakage to ground has been nearly eliminated.

For the excitation of Cl VII, the positive electrode was prepared by packing copper chloride and boron oxide in an aluminum shell. Boron oxide was added for the purpose of obtaining oxygen lines to serve as standards for the wave-length measurements. The negative electrode was made from spectroscopically pure carbon rod. A bank of condensers, 0.45 mf. capacity, was charged to a potential of 50 kv, and discharged across the vacuum gap, which was spaced at about 6 mm. The spark liberates a considerable amount of chlorine and as a result, after the first spark, the condensers do not build up to ful potential, the charge being continuously drained off because of arc formation. To eliminate the possibility of an arc discharge, an air gap was installed in series with the vacuum gap, allowing the condensers to be charged to full potential before the spark occurs, and hence giving the pumps an opportunity to keep the spark chamber free of excess gas.

TABLE I. *Classified lines of Cl VII.*

INT.	λ (vac.)	ν (cm⁻¹)	CLASSIFICATION
	813.002	123,001	$3s\ ^2S_{1/2} - 3p\ ^2P_{1/2}$
	800.698	124,891	$^2S_{1/2} - {}^2P_{3/2}$
1	605.052	165,275	$3p\ ^2P_{3/2} - 3d\ ^2D_{3/2}$
20	604.785	165,348	$^2P_{3/2} - {}^2D_{5/2}$
12	598.211	167,165	$^2P_{1/2} - {}^2D_{3/2}$
1	456.556	219,031	$3d\ ^2D_{3/2} - 4p\ ^2P_{1/2}$
2	455.273	219,648	$^2D_{5/2} - {}^2P_{3/2}$
18	340.298	293,860	$3d\ ^2D_{5/2} - 4f\ ^2F_{7/2}$
15	340.229	293,920	$^2D_{3/2} - {}^2F_{5/2}$
10	294.889	339,111	$3p\ ^2P_{3/2} - 4s\ ^2S_{1/2}$
8	293.253	341,002	$^2P_{1/2} - {}^2S_{1/2}$
4	240.865	415,170	$3d\ ^2D_{5/2} - 5f\ ^2F_{7/2}$
6	240.829	415,232	$^2D_{3/2} - {}^2F_{5/2}$
10	225.078	444,291	$3p\ ^2P_{3/2} - 4d\ ^2D_{5/2}$
6	224.144	446,141	$^2P_{1/2} - {}^2D_{3/2}$
4d	207.757	481,332	$3d\ ^2D - 6f\ ^2F$
8	196.388	509,197	$3s\ ^2S_{1/2} - 4p\ ^2P_{1/2}$
10	196.123	509,885	$^2S_{1/2} - {}^2P_{3/2}$
4	191.283	522,786	$3p\ ^2P_{3/2} - 5s\ ^2S_{1/2}$
2	190.594	524,675	$^2P_{1/2} - {}^2S_{1/2}$
4	174.603	572,728	$3p\ ^2P_{3/2} - 5d\ ^2D_{3/2}$
3	174.035	574,597	$^2P_{1/2} - {}^2D_{3/2}$

The spectrum of Cl VII is sodium-like. Data on the first four members (Na I-Si IV) of this isoelectronic sequence are given in Bacher and Goudsmit.[2] The classification given by Bowen and Millikan[3] for P V and S VI has recently been extended and the energy level values recomputed by Robinson.[4] In addition, Edlén[5] has located several terms in the ions for K IX to Cu XIX. Previous to this investigation, the only lines known in the Cl VII spectrum were the resonance lines $3s\ ^2S-3p\ ^2P$, reported by Bowen and Millikan.[3]

A complete list of classified lines in Cl VII is given in Table I. The lines $3s\ ^2S-3p\ ^2P$ lie above the range of the instrument used in this investigation, and hence the wave-lengths of these two lines are taken from Bowen and Millikan.[3]

The approximate position of newly classified lines was predicted by means of displaced frequency diagrams, such as Fig. 1, and the doublet

[1] P. G. Kruger, Rev. Sci. Inst. **4**, 128 (1933); Kruger and Shoupp, Phys. Rev. **46**, 124 (1934).

[2] Bacher and Goudsmit, *Atomic Energy States*.

[3] Bowen and Millikan, Phys. Rev. **25**, 295 (1925).

[4] Robinson, Phys. Rev. **51**, 726 (1937); Phys. Rev. **52**, 724 (1937).

[5] Edlén, Zeits. f. Physik **100**, 621 (1936).

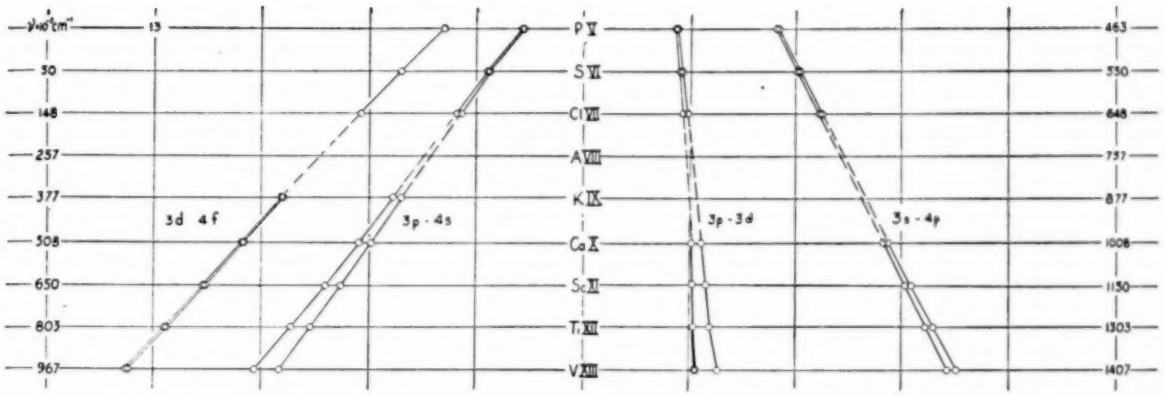

FIG. 1. Displaced frequency diagram. Horizontal scale, 1 div. = 50,000 cm^{-1}. Vertical scale, constant second difference is 11,000 cm^{-1}. The transitions $3p\,^2P-3d\,^2D$ and $3s\,^2S-4p\,^2P$ in Ca X, which have recently been identified in this laboratory, are included in the displaced frequency diagram. Approximate wave numbers are:

$3p\,^2P_{3/2}-3d\,^2D_{5/2}$	808,190
$^2P_{1/2}\quad\;\; ^2D_{3/2}$	813,045
$3s\,^2S_{1/2}-4p\,^2P_{1/2}$	899,305
$^2S_{1/2}\quad\;\; ^2P_{3/2}$	901,210

separations predicted with the $(\Delta\nu)^{\frac{1}{2}}$ law. In almost every case, the multiplets found on the plates were within 200 cm^{-1} of the predicted positions and had the predicted separations to less than 5 cm^{-1}. Moreover, in nearly every case the multiplets are so isolated that no other lines occur near enough to them to cause any difficulty in making the correct assignments.

At 481,332 cm^{-1} one finds a rather diffuse line of intensity 4. This is the predicted position for the $3d-6f$ transition, and the line observed is the only line in the neighborhood. The separation of the $3d\,^2D$ level is known from the $3p-3d$ transition to be 73 cm^{-1}. The $6f\,^2F$ level has not been resolved in any of the ions in the sequence, and hence this separation is assumed to be zero —at least, it will be less than the estimated error (5 cm^{-1}) in the present measurements. If one assumes that the line observed is in reality the three lines $3d\,^2D_{3/2}-6f\,^2F_{5/2}$, $3d\,^2D_{5/2}-6f\,^2F_{5/2,7/2}$, and makes use of the theoretical intensities of these three lines, it is a simple matter to calculate the wave numbers of the two main components. Such a calculation gives 481,303 cm^{-1} for the transition $3d\,^2D_{5/2}-6f\,^2F_{5/2,\,7/2}$ and 481,383 for $3d\,^2D_{3/2}-6f\,^2F_{5/2}$. The series limit with respect to the $3d\,^2D_{5/2}$ level has been calculated with the value 481,303 obtained above, together with the transitions $3d\,^2D_{5/2}-4f\,^2F_{7/2}$ and $3d\,^2D_{5/2}-5f\,^2F_{7/2}$. The form of the function used to calculate the limit and the values obtained for the constants are given below:

TABLE II. *Cl VII terms and effective quantum numbers.*

	TERM VALUES	n^*
$3s\,^2S_{1/2}$	921,902	2.4151
$3p\,^2P_{1/2}$	798,901	2.5943
$^2P_{3/2}$	797,011	2.5974
$3d\,^2D_{3/2}$	631,736	2.9175
$^2D_{5/2}$	631,663	2.9176
$4s\,^2S_{1/2}$	457,899	3.4268
$4p\,^2P_{1/2}$	412,705	3.6095
$^2P_{3/2}$	412,017	3.6126
$4d\,^2D_{3/2}$	352,760	3.9042
$^2D_{5/2}$	352,720	3.9044
$4f\,^2F_{5/2}$	337,816	3.9896
$^2F_{7/2}$	337,803	3.9897
$5s\,^2S_{1/2}$	274,225	4.4281
$5d\,^2D_{3/2}$	224,304	4.8961
$^2D_{5/2}$	224,283	4.8964
$5f\,^2F_{5/2}$	216,504	4.9836
$^2F_{7/2}$	216,493	4.9837
$6f\,^2F$	150,353	5.9802

$$T=A-RZ^2/(n+\mu+\alpha/n)^2,$$

R = Rydberg constant for chlorine,

$A=631{,}663$ cm^{-1},

$\mu=0.96555$,

$\alpha=0.07243$.

From this one obtains 921,902 cm^{-1} as the series limit with respect to the ground state $3s\,^2S$, giving a value of 113.73 volts for the ionization potential of Cl VII. Term values and effective quantum numbers are given in Table II.

In conclusion, the author wishes to express his appreciation to Professor P. Gerald Kruger for many helpful suggestions, and to Mr. W. L. Parker for his assistance in obtaining the spectrograms.

The Electrical Behavior of Thin Metallic Films Condensed at Low Temperatures

H. REES MITCHELL
Johns Hopkins University, Baltimore, Maryland
(Received November 19, 1937)

The change of resistance of thin films of zinc and cadmium condensed at low temperature has been studied. The resistance of a zinc film decreases irreversibly with rising temperature, but it also decreases slowly at a constant temperature above the temperature of deposition. If the surface upon which the film is deposited is of a metal similar to zinc, it influences the temperature resistance relation, but if of a metal not similar to zinc, it does not. The experiments favor the assumption that agglomeration and crystallization are responsible for the changes in resistance.

INTRODUCTION

THE electrical conduction of thin metallic films condensed at low temperature has been often studied in the past, and while this work was in progress many new observations were published which to a great extent agree with ours. Therefore we shall confine ourselves in this paper to the description of results which seem to be new.

The main facts concerning the behavior of these films known hitherto are as follows: Thin films of metals deposited upon a nonconducting surface at the temperature of liquid air show a high resistance, which decreases with rising temperatures, until finally the resistance is of the order of magnitude of that of the normal metal. If such a temperature is reached that the resistance is comparable to that of the normal metal, the cooling of the layer will not again result in a rise of the resistance, but there will be a small decay of the resistance corresponding to the normal positive temperature coefficient of resistance of the bulk metal. According to Zahn and Kramer,[1,2] and Kramer[3–5] and Çelebi[6] the shape of the temperature-resistance curve for all metals is such that the resistance does not change much until a well-defined transition temperature is reached, at which the resistance drops suddenly to normal values. According to other papers, for instance by Suhrmann and his co-workers,[7–10] there is with most metals no such transition temperature, but a continuous decay of the resistance with rising temperature. The change of

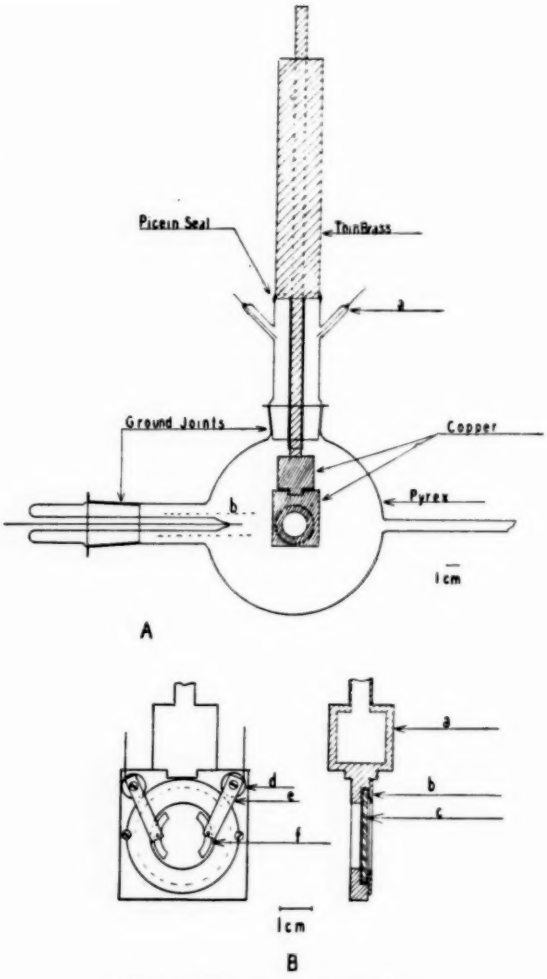

FIG. 1. Diagram of apparatus.

[1] J. Kramer and H. Zahn, Naturwiss. **20**, 792 (1932).
[2] H. Zahn and J. Kramer, Zeits. f. Physik **86**, 413 (1933).
[3] J. Kramer, Ann. d. Physik **19**, 37 (1934).
[4] J. Kramer, Zeits. f. Physik **106**, 675 (1937).
[5] J. Kramer, Zeits. f. Physik **106**, 692 (1937).
[6] Çelebi, Zeits. f. Physik **106**, 702 (1937).
[7] R. Suhrmann and G. Barth, Physik. Zeits. **35**, 971 (1934).
[8] R. Suhrmann and W. Berndt, Physik. Zeits. **37**, 146 (1936).
[9] R. Suhrmann and G. Barth, Zeits. f. Physik **103**, 133 (1936).
[10] Tadao Fukuroi, Nature **139**, 884 (1937).

resistance of the films from low temperature to the temperature at which the resistance is normal is about 50-fold. On the other hand, there are cases of metals showing Zahn and Kramer's sudden transition. A very well-known example of this is the case of antimony, where for instance, electrolysis produces layers which go over explosively with rising temperature. Kramer got analogous results with sputtered films of antimony, and Suhrmann and his co-workers, and we also, studied antimony deposited by evaporation in high vacuum. At the transition point the resistance changes by a factor of a thousand or more. For such transitions one has to accept Zahn and Kramer's explanation of the transition from a nonmetallic state in which each valence electron belongs to one atom or molecule, to the metallic state. We expect such behavior only with metals which like antimony form saturated molecules by exchange forces, which repel other molecules approaching them. These repulsive forces can form a potential barrier against the transition to the metallic state, if the heat of dissociation of the molecules, and correspondingly the repulsive forces, are large enough. In metals forming monatomic vapors, or molecules only by the van der Waals and Coulomb forces, as for instance mercury and cadmium, the formation of a potential barrier seems unlikely.[11] The much smaller irreversible changes of resistance occurring in the latter cases are, as many authors agree, produced by an agglomeration and crystallization process.[12, 13] The following experiments are in accordance with this hypothesis.

Experimental

The thin metallic films were evaporated in high vacuum ($\sim 10^{-6}$ mm of Hg) and condensed on a

[11] But in papers which have recently appeared Kramer and Kramer and Çelebi, references 4, 5, 6, repeat the statement that all metals show sharply defined transition points if deposited under the right conditions. Compare on the other hand, the discussion at the Conference on the Conduction of Electricity in Solids, at Bristol, Proc. Phys. Soc. **49**, 151 (1937), in which most of the authors seem to come to results comparable to ours.

[12] Georg Hass, Naturwiss. **15**, 232 (1937).

[13] E. N. daC. Andrade and J. G. Martindale, Phil. Trans. Roy. Soc. **235**, 69 (1935).

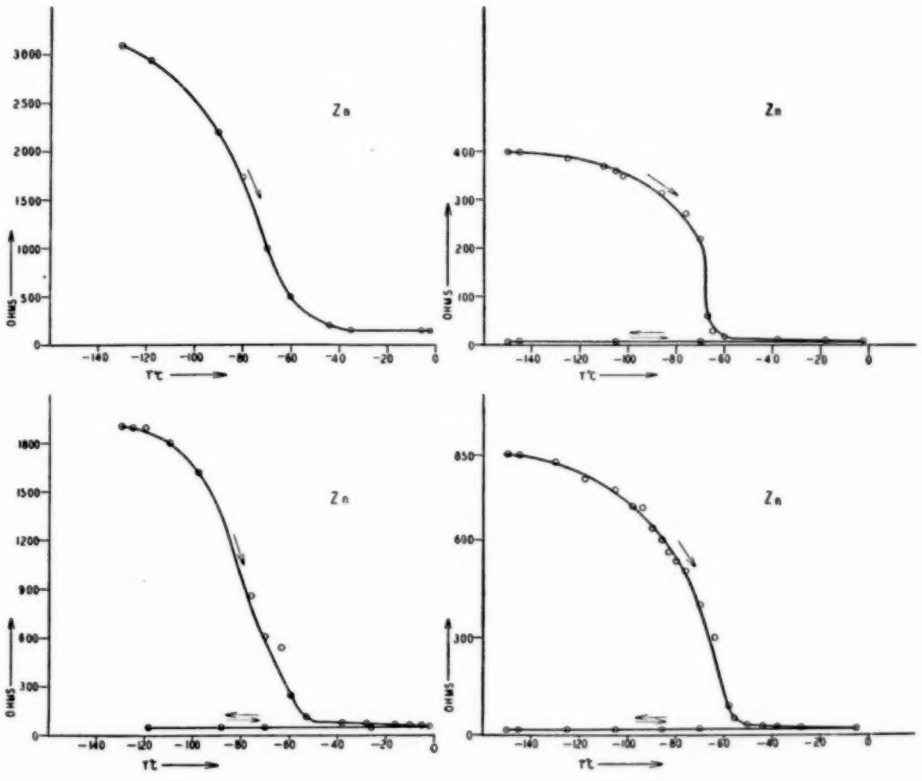

Fig. 2. Resistance of Zn film.

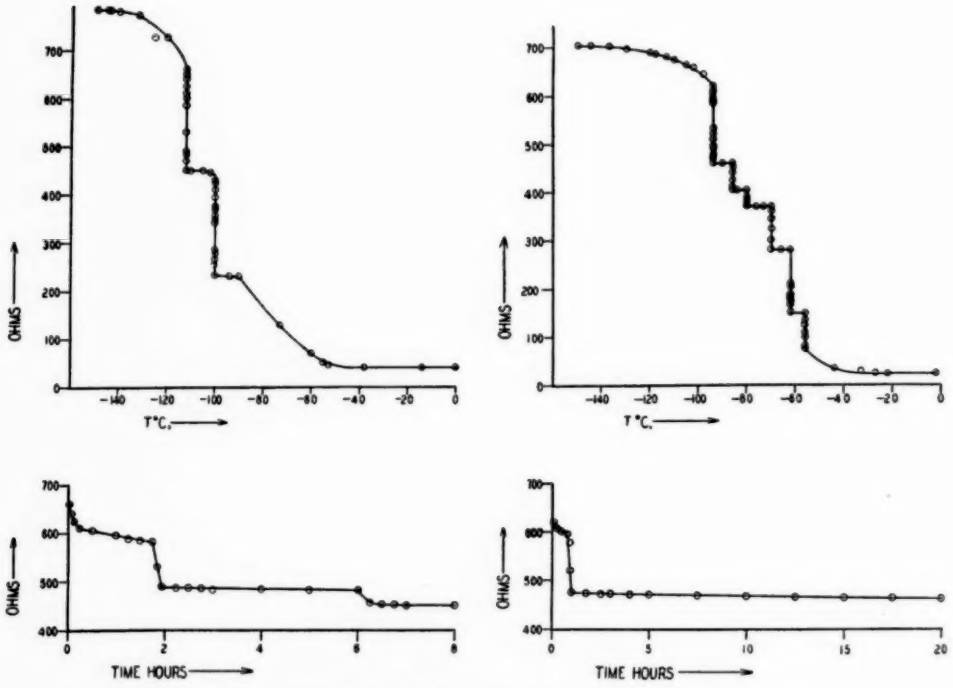

FIG. 3. Resistance of Zn film. Lower curves show change with time.

polished quartz plate cooled with liquid nitrogen. The time of deposition was about 5 minutes. The conductivity was measured in the same vacuum. The apparatus used is shown in Fig. 1. The quartz plate was held in a copper block at the center of the flask (Fig. 1(A)) and leads for the measurement of resistance and temperature were provided. The holder for the quartz plate is shown in detail in Fig. 1(B).

Contact with the films was made by two zones of silver evaporated on the plate in a separate chamber with a clear rectangular strip on the quartz for the metals to be studied. Contact with the silver films was made through spring pressure plates. The temperatures were measured with a thermocouple in contact with the back of the plate. Resistances were measured with a wall galvanometer and source of steady potential for high resistance, and with a Wheatstone bridge for the lower resistances.

RESULTS

The resistance of thin films of zinc has been found, as by other workers[10] to decrease irreversibly with rising temperature (Fig. 2) without a sharp transition point.

However, the resistance also changes with time when the film is held at a constant temperature for a long time. To study this fact, films were condensed at low temperature and the temperature was allowed to rise until the resistance showed a definite decrease, the temperature was then held constant by introducing small amounts of liquid nitrogen or cold gas into the reservoir at frequent intervals. The resistance at first falls rapidly at constant temperature with the time; the fall gradually becoming less rapid until it is nearly zero; after a few hours suddenly another rapid decrease in resistance takes place, followed again by a very slow rate of decrease. The first curve (Fig. 3) shows the result of measurements on one of these films. The curve directly below it shows the change of resistance as a function of time for the first constant temperature part of the curve at −115°C. The upper right-hand curve is the result of another run, in which the temperature was held at −95°C for twenty-five hours; the change in resistance for the first twenty hours is shown below this curve. The total time for the second curve was thirty-eight hours. At the end of the first part of the curve the resistance was still decreasing, at a rate that

indicated that it would take about two weeks for the resistance to fall to its final value. As it was not feasible to keep the temperature of the film constant for so long a time, the temperature was raised with the hope that at a slightly higher temperature the resistance would change at a more rapid rate. This it did with each rise in temperature, but the change always became very slow after a few hours at a constant temperature, and it became impractical to hold the film at that temperature for a more extended time. The resistance at no time ceased to decrease in value at a given temperature, however, indicating that if it could be kept at that temperature for a long enough time it would eventually reach its final value at a temperature much below that at which it would usually do so. It would appear then that the change in resistance is not a function of a given temperature, but that the film will change to a condition such that its resistance is normal in behavior at any temperature above that at which it is condensed. A rise in temperature will increase the speed with which this change will take place, and the change will take place with extreme rapidity as the temperature rises, until the condition of normal behavior is reached when no further change occurs. In other words, the resistance can fall below the usual curve, as of Fig. 2; but will not lie above it with rising temperature. It was found that no matter how rapidly the temperature was raised, the resistance would decrease with rising temperature until it reached a value at which it behaved in the normal manner. The resistance temperature curves taken in a comparatively short time, are then only the envelopes of a large number of step-wise curves taken at many temperatures for various lengths of time.

To study the influence of the material on which the layer is deposited, first one layer of zinc was condensed at a low temperature as usual and the temperature raised to about 0°C, the film now behaving in a normal manner, the temperature was again lowered to about −150°C while the resistance was measured at frequent intervals during the cooling. Then a second film was condensed upon the first and the change of resistance of the two films together was measured as the temperature was raised. The resistance of the upper film could be calculated by considering the two films to be resistances in parallel. The change of the resistance thus calculated is shown for two of these films in Fig. 4. The resistance of these films condensed upon normal films drops with lower temperatures and more rapidly with changing temperature than that of the films condensed upon the quartz. In the film whose curve is shown at the right (Fig. 4), the resistance has already fallen nearly to the final value at the temperature at which it was condensed, and the curve flattens out in approaching the normal behavior at much lower temperatures than that of the films deposited upon the quartz. This film was very thin, as shown by the high final resistance.

From this it is seen that the structure of the surface upon which the film is condensed will

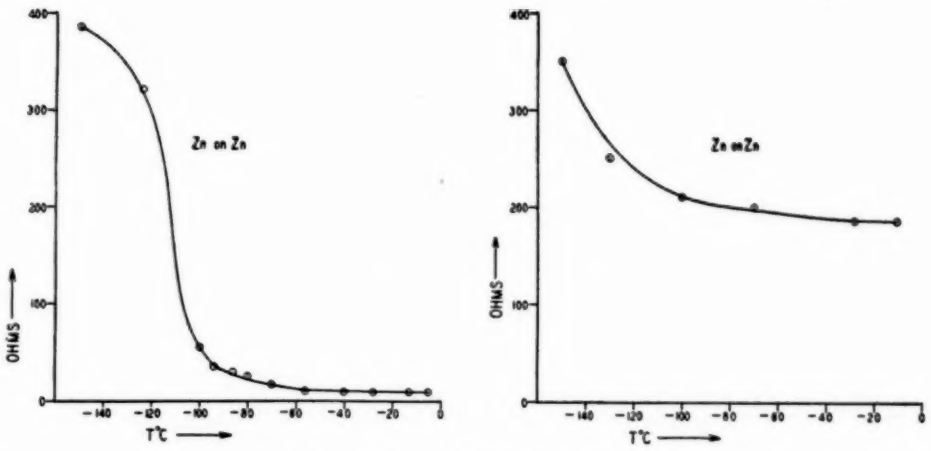

FIG. 4. Resistance of Zn film on a Zn film.

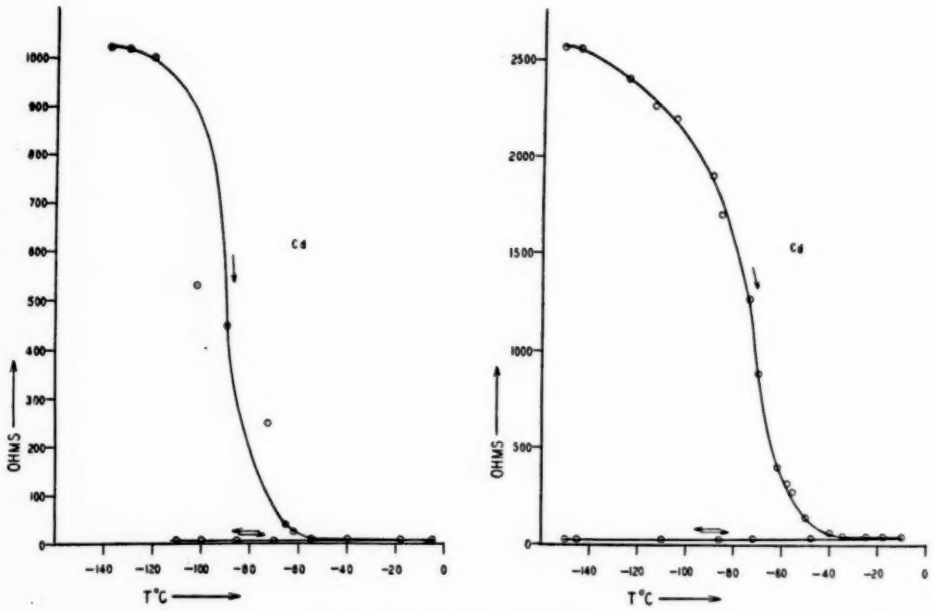

FIG. 5. Resistance of Cd film.

change the temperature at which the film becomes normal in behavior.

Next the influence on the curves of the replacement of the first layer of zinc by another metal was studied. Cadmium was chosen since it has a similar structure to zinc and a low melting point, so that the formation of an alloy at the borderline between the two metals could be expected to a given extent in spite of the low temperatures.

The films of cadmium were condensed at low temperature and their resistance studied at different temperatures. The resistance of cadmium decreases with rising temperature very similarly to that of zinc, except that the effect of different thicknesses is more apparent and the resistance changes by a larger factor than in the case of zinc. The resistance of cadmium changed more rapidly than zinc at low temperatures for thicker films (Fig. 5).

Then the films of cadmium were cooled again to about $-150°C$ and the zinc condensed upon them. The resistance of the two films was measured with rising temperature as with the double films of zinc, and the change in resistance of the upper film of zinc calculated as before. The curve of resistance against temperature for the zinc film upon the cadmium was shifted as in the case of the zinc upon zinc, but to an amount less than in the case of zinc on zinc (Fig. 6). From this it is seen that the structure of the underlying layer influences the temperature at which the zinc film becomes normal in behavior, even though the underlying film is of a metal different from zinc.

It was then desired to find out what effect an underlying film of a metal of different properties would have upon the change in resistance of these zinc films. Since silver has a different crystal form from zinc, a much higher melting point, and different electrical and chemical properties from zinc, it was chosen as an underlying layer. The silver film was prepared in the usual manner and the temperature raised to bring the silver into a normal condition. The silver film was then cooled again, the zinc condensed upon it and the temperature raised. The resistance of the zinc decreased in the usual manner, but there was no shift to lower temperatures as observed with an underlying film of zinc or cadmium. With silver under the zinc films, they behaved in the same way as upon the quartz, (Fig. 7). Apparently a metal of quite different properties has no effect upon the change in resistance of these thin zinc films.

CONCLUSION

From the foregoing results it seems that the following conclusions may be drawn. The change

in these films from a condition of high resistance to one of low resistance with rising temperature is not a transition taking place at a temperature characteristic of the metal. This change occurs more rapidly as the temperature is raised, but will also occur at a constant low temperature, if one waits a long enough time. The curves of Fig. 3 we explain in the following way. There are at first a few small centers of crystallization formed which result in an initial rapid fall of the resistance. This is followed by a gradual growth of crystals about these centers which results in the slow decay of resistance, followed again by a rapid fall of resistance as new centers of crystallization are formed. When the temperature is raised, these centers form more rapidly, and the subsequent growth about them is also more rapid. This behavior would account fully for the results found with the films held at a constant temperature below that at which they usually become normal in behavior.

If the surface under the film is of the same

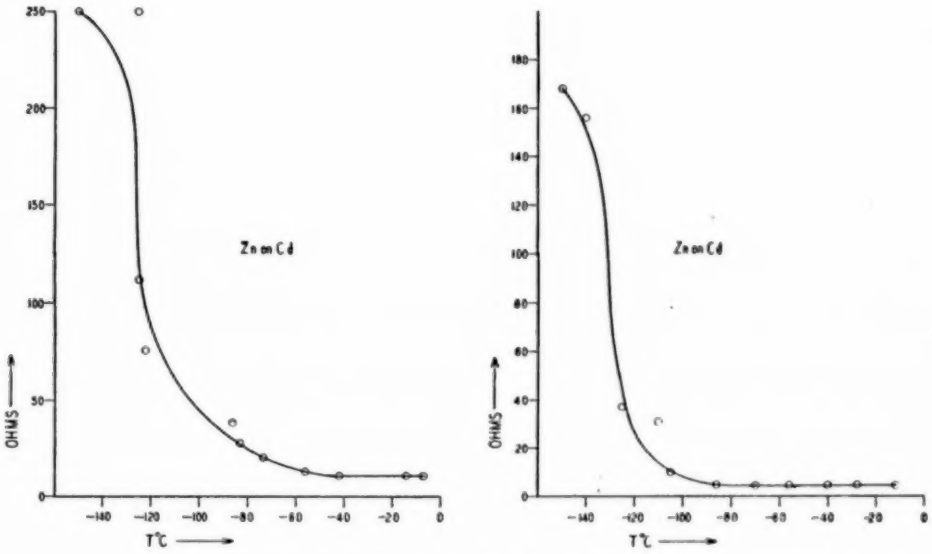

FIG. 6. Resistance of Zn film on Cd film.

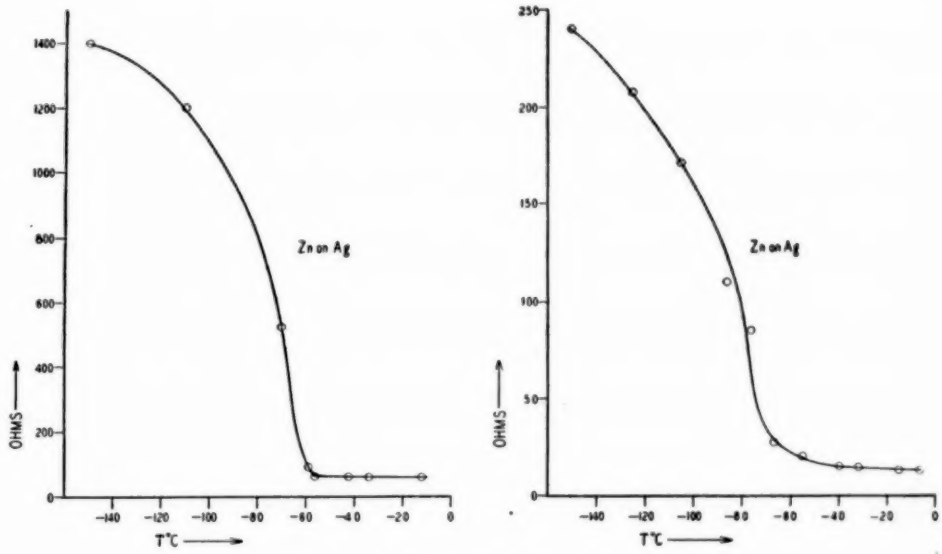

FIG. 7. Resistance of Zn film on Ag film.

metal in a normal condition, or a metal with which the upper film will easily form an alloy at a fairly low temperature, the underlying metal will induce the crystallization and accompanying change to a normal resistance at a lower temperature than when the film is condensed on a quartz surface. If the surface underlying the film is of a metal of quite different properties, the film deposited on it will not form a close association with it and the resistance will change in the same manner as on a nonconductor. This would account for the results as found with the double layer films, represented by Figs. 4, 6, and 7.

I wish to thank Professor Franck for his helpful advice, and Professor Wood, on whose proposal the study of thin films was undertaken, for this suggestion and his cooperation in making special facilities of the laboratory available. I also wish to thank other members of the physics department for their timely help.

FEBRUARY 1, 1938 PHYSICAL REVIEW VOLUME 53

Static Universe and Nebular Red Shift. II

S. SAMBURSKY AND M. SCHIFFER
The Hebrew University, Jerusalem, Palestine
(Received September 22, 1937)

The geometric foundation and the mathematical consequences of the model of a static universe proposed in a previous paper are discussed. The formula for the gravitational constant is proved and some cosmological applications are pointed out.

1. INTRODUCTION AND BASIC ASSUMPTIONS

IN a previous paper,[1] one of the authors has suggested a model of a static universe with shrinking atomic lengths in order to explain the red shift and nebular distribution observed. Such a model is essentially equivalent to that of a nonstatic universe with constant atomic lengths, but has the added advantage of relating cosmic phenomena such as gravitation, with certain atomic properties. It was suggested that, if the world radius R is considered a constant, Hubble's red shift distance law involves the very gradual shrinking with time of Planck's constant h, as well as of the electron charge. Assuming that the differences between the atomic energy levels remain constant while h diminishes, we deduce that light must have been emitted at a lower frequency the further back in time the emission occurred. It must be emphasized here once more that in describing the propagation of light in space, the wave concept must be used, as pointed out by Laue,[2] since this fits satisfactorily with the general theory of relativity and therefore with any relativistic cosmology. According to the wave theory light traveling on a geodesic zero line reaches us with its frequency unchanged, and therefore permits us to observe a red shift. In this way, the energy principle, which is assumed throughout this theory, remains valid for the propagation of light in space. The consistent application of the concept of light quanta would inevitably lead to difficulties in respect of the energy balance in view of the incompatibility of a rigid adherence to the light quanta concept with the general theory of relativity. The dualism involved in the use of the quantum equation $\Delta E = h\nu$ for the process of emission and the description of the propagation of light in terms of waves is therefore inevitable at the present stage of our knowledge.

In this paper the mathematical foundations of this theory will be considered at greater detail, more particularly with regard to the consequences of the shrinkage of the hydrogen atom. We will begin by considering the behavior of a hydrogen atom in a universe with Weylian metric, the geometry of whose space is given by a quadratic to be more closely defined later, and by a linear differential which introduces the necessary gauge. If this universe is a static one, its constant radius of curvature will provide a standard measure of length for any of its points.

[1] S. Samburšky, Phys. Rev. 52, 335 (1937).
[2] M. v. Laue, Zeits. f. Astrophys. 12, 208 (1936).

In this case the existence of a singularity causes the diminution of the electric charge and, because of the constancy with time of the fine structure constant, also the diminution of h.

The important assumption must now be made that the Dirac equation is valid for the behavior of the hydrogen atom in this system whose curvature is constant by the definition of its gauge. Because of the change with time of e and h, a new system of reference must be introduced before the Dirac equation can be integrated; this system will be such that e and h are constant, i.e., that the coordinates of length and time shrink in comparison with those of the first system. In order, now, to obtain the quadratic fundamental for the universe in this system, we must calculate the g_{ik} from the generalized Dirac matrices after the necessary transformation of the Dirac equation has been effected. One particularly interesting aspect of this theory is the fact that the variation of h produces an additional energy term for the hydrogen atom which can be identified with its energy of gravitation. In this way an element open to experimental proof by means of astronomical observation is introduced, since the gravitational constant expressed by means of atomic quantities is found to vary with time.

To resume briefly the physical meaning of the calculations mentioned above, we may say that two systems of reference can be used to describe cosmological processes; their mathematical equivalence was pointed out in the previous contribution. The first of these two systems is one with "cosmical" coordinates, i.e., one whose standard measure of length is the world radius, a system therefore in which relativity mechanics are valid. This system is used to describe the orbits and positions of the celestial bodies: Referred to it, the distances between the spiral nebulae are constant and the universe remains static. The atomic dimensions of length and time, on the other hand, must necessarily be found to shrink if referred to the cosmical coordinates.

The second system of reference, equivalent to the first, and equally suitable for describing cosmological processes, is the "atomic" system. Its standard scales are provided by atomic times and lengths, such as the radius of the electron and all lengths and times proportional to Planck's constant h. To an observer working from this system, the universe will appear to expand, and the nebulae, at least at the first approximation, will appear to recede from him at speeds proportional to their distances. In fact this atomic system of reference is that which is applied in all cosmologies of the expanding universe. The standard measure of length used in these cosmologies has been, though not actually the atomic standard, at least one directly related to it, i.e., the standard meter or the "practical" measure of length. If this practical standard meter is used to describe the world radius, then indeed the latter will be found to be expanding. A meter rod is an aggregate of atoms and molecules essentially bound together by electromagnetic interaction, and must be expected to behave exactly as do its constituents; it will be found to be shrinking if referred to the coordinates of the cosmical system. Similarly, when measured by the atomic system, all distances between celestial bodies, and indeed all lengths not depending on atomic processes, i.e., not only the distances between the spiral nebulae, but also those between binary stars, sun and planets and all other bodies whose interactions are purely gravitational, are found to increase.

In addition to the nebular red shift, therefore, it is also an experimentally interesting consequence of our theory that the distances between celestial bodies as measured by any standard coupled with the atomic units of length, e.g., the meter rod, should increase. If the distances of the spiral nebulae could be determined by measuring their respective parallaxes, measuring, that is, with the aid of a cosmical standard such as the diameter of the earth orbit, then every nebula would show a constant parallax at all times—provided suitable corrections for the real movement of the nebula, and for variation in the diameter of the earth orbit are introduced. Even so, in comparing two "atomic" standards such as h and the meter rod, a constant ratio must necessarily be found.

2. Weylian Metric in a Static World

Let us consider a world in which the generalized Weyl geometry holds.[3] We further lay down

[3] H. Weyl, *Raum, Zeit, Materie*; fifth edition, §40.

that this world is static, and therefore obtain for it the fundamental equations in the form:

$$ds^2=d\sigma^2+\gamma^2dx^{4^2}, \quad x^4=ict \tag{2.1}$$

$$dl/l=\varphi_4 dx^4. \tag{2.2}$$

Here $d\sigma^2$ is the fundamental quadratic form of the three-dimensional space (x^1, x^2, x^3) and γ as well as φ_4 depend only upon the space coordinates x^1, x^2, x^3. We naturally admit that γ and φ can show singularities which are indicated physically as concentration points of mass or charge.

Equations (2.1) and (2.2) in themselves determine the entire geometry of the universe. From them, knowing the gauge factor λ, the curvature of the universe at any point may be calculated. This latter, in general, is not constant, but can be made constant by the use of a suitable gauge. It suffices, according to Weyl, so to regauge the universe as to give the new gauge factor λ' a constant value, e.g., $\lambda'=1$. Then the radius of curvature is also constant in space and time. The transformation equations show that

$$g_{ik}'=\lambda g_{ik}, \quad \varphi_i'=\varphi_i-\frac{1}{\lambda}\frac{\partial\lambda}{\partial x^i}=\varphi_i-\frac{\lambda_i}{\lambda}, \tag{2.3}$$

where the prime indicates the new quantities and $\partial\lambda/\partial x^i=\lambda_i$. Since by (2.2) $\varphi_{1,2,3}=0$, the following potentials occur in a universe gauged to a constant radius of curvature

$$\varphi_i'=-\lambda_i/\lambda \qquad (i=1, 2, 3). \tag{2.4}$$

The Lorentz equation for the potentials

$$\partial/\partial x^i\{(g')^{\frac{1}{2}}\phi'^i\}=0 \tag{2.5}$$

which is also valid in the Weyl theory, leads by an easy transformation to the following differential equation in λ

$$\sum_{i=1}^{3}\frac{\partial}{\partial x^i}\{g^{\frac{1}{2}}\lambda^i\}=0. \tag{2.6}$$

This is the potential equation which must be satisfied by the gauge factor λ of a static universe. The only solution which is regular throughout the entire closed universe is $\lambda=$const. Assuming λ to show singularities, then in the vicinity of the latter λ has the following form

$$\lambda=a+b/r \tag{2.7}$$

and it must be deduced that in a universe of constant radius, the potentials must necessarily assume the form

$$\varphi_i'=-\frac{\lambda_i}{\lambda}=\frac{x^i}{r^3}\frac{\beta}{1+\beta/r} \quad (i=1, 2, 3), \tag{2.8}$$

where $\beta=b/a$. It must be assumed that the absolute length β approximates the radius of that physical entity which we identify with the mathematical singularity. Then the singularity must be become appreciable only for lengths which lie within the order of size of β. Supposing a proton to be the physical cause of the singularity, then β must be of the order of size of the proton radius.

The differential equation (2.6), as well as its solutions (2.7) and (2.8), were already known to Weyl. He, however, declared that the only physically significant solution was the special case $b=0$. He finds support in the following important argument: According to the Weyl theory, a potential φ_1, φ_2, φ_3 which is produced by a charged particle, causes a flow of charge through any surface enclosing it, so that the vector flow is proportional to the vector

$$(\varphi^1 g^{\frac{1}{2}}, \varphi^2 g^{\frac{1}{2}}, \varphi^3 g^{\frac{1}{2}}). \tag{2.9}$$

Assuming the solution (2.7) where $b\neq 0$ for any physically significant singularity, such as an electron or a proton, it follows that a constant loss of charge in time by this elementary particle must occur. Weyl rejects this general solution, however, as he postulates the conservation of the charge by "self-adjustment" (Einstellung).

At this point, our theory intervenes. It constitutes the systematic realization of this very universe model which Weyl rejected. We assume that in the course of time, the charge of elementary particles decreases. The charge of electrons and protons, e, which has hitherto been held to be a natural constant, is held by us to be a uniformly decreasing function of time. This circumstance naturally has far reaching consequences in respect to the quantum theory of the universe. These are discussed in §3. At this point, the following only may be noted: Let us assume what seems plausible.—that the

fine structure constant $\alpha=2\pi e^2/hc$ which is of primary importance in the formation and stability of the atom does not vary in time, and let us retain the fundamental postulate that $c=$const. It follows that the Planck constant h must decrease in time, and at a rate proportional to e^2. The value $dh/dt=\dot{h}$ for the present time was calculated from the distance red shift law by one of us in the paper which has been mentioned above. Assuming a Hubble factor of $1.57\cdot10^{-17}$ sec.$^{-1}$, it follows that

$$\dot{h}=-1.03\cdot10^{-43}\ \text{ergs}. \tag{2.10}$$

Since h constitutes the proportionality constant of all atomic times and lengths, a general shrinkage of all these quantities in relation to the constant radius of the universe was concluded to occur. The following section provides a mathematical basis for this assumption.

3. The Dirac Equation for an Electron in the Field of a Proton

Let us consider an electron which is moving in the field of a proton. This field is centrally symmetric, and is determined by a potential $A_{1,\,2,\,3,\,4}$ of the components

$$A_{1,\,2,\,3}=0,\quad A_4=-ie/r. \tag{3.1}$$

According to §2, this field possesses a gauge factor $\lambda=1+\beta/r$, where β is a constant of the order of size of the proton radius. Gauging to $\lambda=1$, we have the additional potential functions

$$\varphi_k=-\frac{1}{\lambda}\frac{\partial\lambda}{\partial x^k}=\frac{\beta x^k}{r^3}\cdot\frac{1}{1+\beta/r}, \tag{3.2}$$

which, to a factor $\chi\cdot hc/2\pi e$ of the dimension of a charge, indicate the additional electromagnetic potentials. Consequently, we have in the new system the potential field

$$A_k=\chi\frac{hc}{2\pi e}\cdot\frac{\beta x^k}{r^3}\frac{1}{1+\beta/r}\qquad(k=1,\,2,\,3),$$

$$A_4=-ie/r. \tag{3.3}$$

Now, the fundamental assumption of our theory is, that for the electron in this system the Dirac equation

$$\left[\sum_{k=1}^{4}\gamma^k\left\{\frac{\partial}{\partial x^k}-\frac{2\pi ie}{hc}A_k\right\}+\frac{2\pi mc}{h}\right]\psi=0 \tag{3.4}$$

holds. Here γ^k are the usual Dirac matrices obeying the multiplication rules

$$\tfrac{1}{2}(\gamma^i\gamma^k+\gamma^k\gamma^i)=\delta^{ik}. \tag{3.5}$$

In contradistinction to the usual Dirac equation, e and h are here functions of time, a circumstance which naturally works a considerable change in the type of (3.4).

To make possible the utilization of the results obtained with the usual Dirac equation (where e and h are independent of time), the following method is applied:

It follows from the considerations presented in §1 that the orbit radii of electrons must shrink with the same speed as the Planck constant h. (3.4) is therefore transferred to a coordinate system in which all intervals of length and time decrease in the course of time. It may then be expected that Eq. (3.4) will correspond with the usual Dirac equation more closely. Thus let

$$\xi^{1,\,2,\,3}=x^{1,\,2,\,3}f(x^4),\quad \xi^4=\int f(x^4)dx^4, \tag{3.6}$$

or in general

$$\xi^k=\int f(x^4)dx^k,$$

where $f(x^4)$ is a uniformly increasing function, which by

$$h=h_0/f(x^4),\quad e^2=e_0^2/f(x^4),\quad \beta=\beta_0/f(x^4) \tag{3.7}$$

determines the behavior of the natural constants. We make

$$f(0)=1, \tag{3.7a}$$

so that h_0 equals the value of h for the time $t=0$. In the following, the present moment is always identified with $t=0$. Then between length and time intervals in both coordinate systems the relation

$$d\xi^k=f(x^4)dx^k \tag{3.8}$$

must hold, so that for any fixed interval in the ξ system (atomic system) there corresponds an interval which shrinks with h in the x system (cosmic system). If $\psi(x^1,x^2,x^3,x^4)=\varphi(\xi^1,\xi^2,\xi^3,\xi^4)$, then φ satisfies a modified Dirac equation which

may be obtained from (3.4), with the aid of the transformation formulae

$$\partial\psi/\partial x^k=(\partial\varphi/\partial\xi^k)\cdot f \quad (k=1,2,3),$$
$$\frac{\partial\psi}{\partial x^4}=\left(\frac{\partial\varphi}{\partial\xi^1}x^1+\frac{\partial\varphi}{\partial\xi^2}x^2+\frac{\partial\varphi}{\partial\xi^3}x^3\right)\cdot f'+\frac{\partial\varphi}{\partial\xi^4}\cdot f. \tag{3.9}$$

Here and below the following abbreviations: f for $f(x^4)$ and f' for $df(x^4)/dx^4$ are introduced. We divide the equation obtained by f and make $\xi^{1^2}+\xi^{2^2}+\xi^{3^2}=\rho^2$. Then applying (3.3), and $\alpha=2\pi e^2/hc$ we have

$$\left[\sum_{k=1}^{3}\gamma^k\left\{\frac{\partial}{\partial\xi^k}-\chi\frac{i\beta_0\xi^k}{\rho^3}\cdot\frac{1}{1+\beta_0/\rho}\right\}+\gamma^4\left\{\frac{\partial}{\partial\xi^4}+\frac{f'}{f^2}\left(\xi^1\frac{\partial}{\partial\xi^1}+\cdots\right)-\frac{\alpha}{\rho}\right\}+\frac{2\pi mc}{h_0}\right]\varphi=0. \tag{3.10}$$

The only term of this equation which still contains time explicitly is f'/f^2. Now according to (3.7),

$$f'/f^2=i\dot{h}/h_0c=1/\mathrm{P} \tag{3.11}$$

is a number of the order of 10^{-27}, and this very small term may be assumed to be approximately constant. From a mathematical viewpoint, $h=h_0+\dot{h}_0t+\cdots$ has been extended into a Taylor series of time which is terminated after the second term, and so a Dirac equation independent of time was obtained for this approximation. The results of the ordinary quantum theory can now be applied to (3.10). We may give (3.10) a simpler form in which the operators $\partial/\partial\xi^k$ are rearranged:

$$\left[\sum_{k=1}^{4}\alpha^k\left\{\frac{\partial}{\partial\xi^k}-\mathrm{A}_k\right\}+\frac{2\pi mc}{h_0}\right]\varphi=0, \tag{3.12}$$

where
$$\alpha^k=\gamma^k+\gamma^4\xi^k/\mathrm{P} \quad (k=1,2,3), \tag{3.13}$$
$$\alpha^4=\gamma^4,$$

and
$$\mathrm{A}_k=\chi\frac{i\beta_0\xi^k}{\rho^3}\cdot\frac{1}{1+\beta_0/\rho} \quad (k=1,2,3),$$
$$\mathrm{A}_4=\frac{\alpha}{\rho}-\frac{1}{\mathrm{P}}\sum_{k=1}^{3}\mathrm{A}_k\xi^k. \tag{3.14}$$

Eq. (3.12) has the exact form of a usual Dirac equation. Its matrices, however, no longer satisfy the rules of (3.5). We therefore have here a Dirac equation which applies to a non-Euclidian space.

In a general Riemanian space with the fundamental tensor g_{ik} the matrices α^k obey the multiplication rules

$$\tfrac{1}{2}(\alpha^i\alpha^k+\alpha^k\alpha^i)=g^{ik}.^4 \tag{3.15}$$

Since Eq. (3.13) provides the α^k of the new coordinate system, the geometry of the universe as measured from this system may be deduced. By an easy calculation, we have

$$g^{ik}=\delta^{ik}+\xi^i\xi^k/\mathrm{P}^2 \quad (i,k=1,2,3), \tag{3.16}$$
$$g^{i4}=\xi^i/\mathrm{P} \quad (i=1,2,3), \quad g^{44}=1,$$

and
$$|g_{ik}|=1, \quad g_{ik}=\delta_{ik} \quad (i,k=1,2,3),$$
$$g_{i4}=-\xi^i/\mathrm{P} \quad (i=1,2,3), \tag{3.17}$$
$$g_{44}=1+(1/\mathrm{P}^2)\sum_{i=1}^{3}\xi^{i^2}=1+\rho^2/\mathrm{P}^2.$$

It follows for a line element in ξ-space that

$$ds^2=g_{ik}d\xi^id\xi^k=\sum_{i=1}^{3}d\xi^{i^2}-(2/\mathrm{P})\sum_{i=1}^{3}\xi^id\xi^id\xi^4+(1+\rho^2/\mathrm{P}^2)d\xi^{4^2}. \tag{3.18}$$

We introduce polar coordinates into (ξ^1,ξ^2,ξ^3)-space.

$$\xi^1=\rho\cos\varphi\sin\vartheta, \quad \xi^3=\rho\cos\vartheta,$$
$$\xi^2=\rho\sin\varphi\sin\vartheta, \quad \xi^4=\xi^4. \tag{3.19}$$

Then

$$ds^2=d\rho^2+\rho^2d\vartheta^2+\rho^2\sin^2\vartheta d\varphi^2-(2/\mathrm{P})d\rho d\xi^4+(1+\rho^2/\mathrm{P}^2)d\xi^{4^2} \tag{3.20}$$
$$=\rho^2(d\rho/\rho-\alpha\xi^4/\mathrm{P})^2+\rho^2d\vartheta^2+\rho^2\sin^2\vartheta d\varphi^2+d\xi^{4^2}.$$

We put
$$\rho^*=\rho e^{-\int d\xi^4/\mathrm{P}}. \tag{3.21}$$

Then
$$\frac{d\rho^*}{\rho^*}=\frac{d\rho}{\rho}-\frac{d\xi^4}{\mathrm{P}}. \tag{3.22}$$

Substituting this in (3.20), it follows that

$$ds^2=\frac{\rho^2}{\rho^{*2}}(d\rho^{*2}+\rho^{*2}d\vartheta^2+\rho^{*2}\sin^2\vartheta d\varphi^2)+d\xi^{4^2}, \tag{3.23}$$

[4] H. Tetrode, Zeits. f. Physik **50**, 336 (1928).

or, taking (3.21) into consideration,

$$ds^2 = e^{2\int d\xi^4/\mathrm{P}} \cdot d\sigma^2 + d\xi^{4^2}. \tag{3.24}$$

Here $d\sigma^2$ is the line element in a Euclidian subspace (ξ^{1*}, ξ^{2*}, ξ^{3*}). It is of interest actually to calculate ρ^*. Since by (3.8) $d\xi^4 = f \cdot dx^4$, it follows from (3.11) that

$$\int \frac{d\xi^4}{\mathrm{P}} = \int \frac{f'}{f} dx^4 = \log f + C, \tag{3.25}$$

$$\rho^* = C \cdot \frac{\rho}{f}. \tag{3.26}$$

On the other hand, it follows from (3.6) that $r = \rho/f$. Therefore

$$\rho^* = C \cdot r. \tag{3.27}$$

Consequently the coordinate system which must be introduced in order to effect a separation of space from cosmic time (in the sense of relativistic cosmology), is identical in its spatial part with the cosmic coordinate system from which we started.

The line element (3.24) constitutes a well-known normal form of ds^2.[5] It closely approximates the line element of the de Sitter universe which is of the form

$$ds^2 = e^{2\xi^4/a} d\sigma^2 + d\xi^{4^2}, \tag{3.28}$$

where $-ia$ is the radius of curvature of the universe. We have above emphasized the gradual variation of P. With the same approximation as in (3.11) we may in (3.24) make P = const. We then have

$$ds^2 = e^{2\xi^4/\mathrm{P}} d\sigma^2 + d\xi^{4^2}. \tag{3.29}$$

It may be seen that $-i\mathrm{P}$ equals the radius of curvature of the universe at any moment. For greater time intervals, however, P varies.

As regards the function f, no special assumptions have as yet been made. This function will now be defined, however, by assuming that the variation of P in the ξ system is a consequence of the fact that the standard of comparison $d\xi^4$ as measured from the x system shrinks with a velocity $1/f$. This means that seen from the x system the radius of curvature is constant and its variation in the ξ system is only apparent. This is plausible, once the x system, i.e., the cosmic system is gauged to a constant curvature. Then

$$\mathrm{P}h = \mathrm{P}_0 h_0 = \text{const.} \tag{3.30}$$

must hold, where index 0 indicates the values at $t = 0$ (e.g. the present moment). Then from (3.7) and (3.11) we find

$$f/f' = \mathrm{P}_0 \tag{3.31}$$

and by integration of (3.31), adopting the normalization (3.7a), we have

$$f = e^{x^4/\mathrm{P}_0}. \tag{3.32}$$

$R = -i\mathrm{P}_0$ is the radius of curvature of the static x universe. Introducing h we have, because of (3.7) and (3.31)

$$R = -hc/\dot{h}. \tag{3.33}$$

R is naturally positive, as $\dot{h} < 0$. We find for R the value $1.9 \cdot 10^{27}$ cm, when for $\dot{h}$ the value (2.10) is used.

In view of (3.32) we may write for (3.7) and (3.8)

$$h = h_0 e^{-\eta t}, \quad \text{etc.}, \tag{3.34}$$

$$dx^k = d\xi^k \cdot e^{-\eta t}, \tag{3.35}$$

$$\eta = c/R = -\dot{h}/h. \tag{3.36}$$

η is the well-known Hubble factor.

Comparing (3.35) for the time coordinate ($i = 4$) with (3.34), it is seen that in accordance with the Bohr correspondence principle the red shift may be explained as follows: The time unit is larger the deeper into the past we reach. The then slower revolving electrons must have emitted light waves of a smaller frequency, which is carried along unchanged, since the light waves propagate on geodesic zero lines. By this consideration following the principle of correspondence, we again get an explanation of the red shift within the frame of our theory. It would therefore seem that the difficulties which were encounted above when the attempt was made to follow the light quantum theory to its ultimate consequences, are not inherent in the universe model here set up but may be implicit rather in the light quantum theory itself.

4. Dirac Equation and Gravitation

Having by (3.24) determined the metric of the universe with reference to the atomic system

[5] G. Lemaître, J. Math. and Physics (M. J. T.) **4**, 188 (1925); H. P. Robertson, Phil. Mag. **5**, 835 (1928).

of coordinates, we revert to the Dirac equation (3.12) which the atom in this system obeys. A comparison of (3.12) with (3.4) shows that the Dirac equations for the atom in both systems of reference are analogously constructed. Λ_k in (3.12) corresponds to $(2\pi ie/hc)A_k$ in (3.4); as regards $k=1, 2, 3$ the analogy is complete. It is necessary only to substitute for the shrinking values β, x, r, e, h of the cosmic system of reference the constant values β_0, ξ, ρ, e_0, h_0.

For $k=4$, if the analogy was complete, might be expected:

$$\Lambda_4=\frac{\alpha}{\rho}=\frac{\alpha}{e_0^2}\cdot\frac{e_0^2}{\rho}.$$

In fact, however, an additional term

$$-\frac{1}{\mathrm{P}}\sum_{k=1}^{3}\Lambda_k\xi^k$$

is obtained which in view of the proportionality factor α/e_0^2 relating Λ_4 to the energy, and in view of Eqs. (3.11) and (3.14), must correspond to an additional potential

$$E_g=-\frac{e_0^2}{\alpha}\frac{1}{\mathrm{P}}\sum_{k=1}^{3}\Lambda_k\xi^k=\chi\frac{e_0^2\dot{h}\beta_0}{\alpha h_0 c}\cdot\frac{1}{1+\beta_0/\rho}\cdot\frac{1}{\rho}, \quad (4.1)$$

i.e., an electron in the field of a proton moves as it would move according to the ordinary quantum theory, in the presence of an additional potential (4.1). Our cosmological assumptions thus lead us to postulate a force additional to the Coulomb force and derived from potential (4.1).

Expressing (4.1) in the cosmic system we have

$$E_g=\chi\frac{e^2\dot{h}\beta}{\alpha hc}\cdot\frac{1}{1+\beta/r}\cdot\frac{1}{r}=\chi\frac{\dot{h}\beta}{2\pi}\cdot\frac{1}{1+\beta/r}\cdot\frac{1}{r}. \quad (4.1a)$$

The sign of E_g is positive, since $\dot{h}<0$ and $\chi\beta<0$. The latter is easily obtained, if in (2.9) the values φ^i of (2.8) are substituted, and it is laid down that the charge of the proton undergoes a decrease and not an increase. The energy (4.1) therefore corresponds to an attracting force.

Putting the proportionality factor $\chi=1$, as is plausible, and $1/(1+\beta/r)\sim 1$, where β/r for a distance r of the order of size of the hydrogen atom's radius is approximately equal to 10^{-7} and may be neglected, then (4.1a) becomes

$$E_g=\frac{\dot{h}\beta}{2\pi}\cdot\frac{1}{r}. \quad (4.2)$$

The length β must, as was shown in §2, be of the order of size of the proton radius:

$$\beta=\text{const.}\dot{e^2}/Mc^2, \quad (4.3)$$

where the numerical factor const. is still undetermined. Trying $\beta=e^2/Mc^2=1.5\cdot 10^{-16}$ cm, the relation of the energy (4.2) to the Coulomb energy E_c is approximately $=10^{-41}$. But the atom is known to manifest only one type of energy which decreases with r as does the Coulomb energy, and is smaller in this tremendous order of size than the latter. This is the energy of gravitation. We have

$$\frac{E_g}{E_c}=\frac{GMm}{e^2}=4.35\cdot 10^{-40}, \quad (4.4)$$

where G is Newton's gravitational constant. We therefore have no choice but to identify (4.2) with the gravitational energy of the hydrogen atom, and so to put the hitherto undetermined numerical factor in (4.3) equal to $4\pi^2$:

$$\beta=4\pi^2e^2/Mc^2. \quad (4.5)$$

Then by (4.2) and (4.5), we have exactly

$$E_g=\frac{2\pi e^2\dot{h}}{Mc^2}\cdot\frac{1}{r}=\frac{GMm}{r}, \quad (4.6)$$

wherein the gravitational constant is coupled in a simple relation with atomic quantities.

From (3.33) and (4.6), it may be seen how the gravitation of the hydrogen atom as well as the metric of the universe are determined by the decrease of h. Gravitation essentially appears here as a consequence of the existence of the electromagnetic field and the decrease of the charges. If h were constant, the gravitational energy of the hydrogen atom would disappear, and the metric of space as seen from the atomic system would become Euclidian. The same universal conditions, therefore, which produce the gravitation of the proton on the electron also determine the boundaries of the universe, since it is they which essentially govern its metric.

From (4.6) it follows that

$$G=2\pi e^2\dot{h}/M^2mc^2, \quad (4.7)$$

where, since by (3.34) $\dot{h}$ and e^2 decrease at the rate of h, G is no constant but decreases with h^2. This decrease in time of the gravitational "constant" involves several astronomic conclusions which may be compared with the observational results and theories of astrophysics. The following discussions deal only with the decrease of the mass of the stars.

During the formation of stars, certain equilibrium conditions between the forces of gravitation and inertia must prevail. The latter does not vary in time, as it is dependent only upon the mass and the velocity of the particles concerned. At the time of star formation, therefore, the forces of gravitation must always be the same. These forces are given as a geometric function, dependent upon the distance between the particles concerned, which is multiplied by a factor GM, where M is the total mass of the particles. As our theory assumes the constancy of the cosmic geometry, this geometric function may be regarded as independent of time. Hence in the process of the formation of any star, the expression GM should always have the same statistical average value. Since G decreases in time, it follows that the quantity of matter M required for the formation of a star is larger the later the date, since always the same dynamical processes are followed.

These considerations show that the so-called nonrelativistic (radiationless) decrease of mass can be explained within the framework of the universe model here described without resort to any additional hypothesis. As is known, it is necessary to accept this mass decrease when, interpreting the Russell diagram as a purely evolutionary diagram of the development of the stars, one adopts the so-called short time scale of 10^{10} years, for which indeed weighty arguments may be adduced. In applying the statistical data collected by Nernst[6] for sixty binary stars to test our conclusions, the material referring to young stars ($<7\cdot10^7$ years) must be excluded, as undoubtedly in their case the mass decrease due to radiation is still considerable. Similarly, the material referring to the oldest stars ($>2\cdot10^9$ years) must be excluded, as in this case the calculations of the ages are uncertain, and, as Nernst himself admits, probably too high.

For stars whose ages range from $7\cdot10^7$ to approximately 10^9 years, however, the apparent mass decrease shows a quite good correspondence with the decrease of G within this time interval. The average masses of the stars at both points of time are to each other, according to Nernst (reference 4, Table II) as 1.6 : 1, whereas G within this time decreases by a factor 2.1. In view of the uncertainty of the estimated ages of the stars, this discrepancy of 25 percent is still definitely admissible.

As has been pointed out above, the product GM must have the same value at the moment of formation of any star. This process once concluded, since M is constant, GM of any star or stellar system must naturally decrease. This decrease of gravitational force in time leads to further consequences which may be tested experimentally.

It is not impossible, for example, that our theory may provide an explanation of the cosmic radiation. In view of the decrease of gravitation, the existence of particles at any point in space which travel at a speed approaching that of light can be predicted.

Let us imagine a particle which falls towards a spiral nebula and passing it continues its way. Then the acceleration of the particle in approaching the nebula will exceed its retardation when moving away, since gravitation meanwhile has decreased. If this process is repeated a sufficient number of times our particle must thus attain a velocity which approximates more and more closely that of light. Assuming an average distance between nebulae of 10^6 light years and an average mass of 10^{10} suns pro nebula, a particle which started to move about 10^{10} years ago will enter our galaxy at a speed approaching that of light.

A detailed calculation of this problem will be given elsewhere.

[6] W. Nernst, Zeits. f. Physik **97**, 511 (1935).

LETTERS TO THE EDITOR

Prompt publication of brief reports of important discoveries in physics may be secured by addressing them to this department. Closing dates for this department are, for the first issue of the month, the eighteenth of the preceding month, for the second issue, the third of the month. Because of the late closing dates for the section no proof can be shown to authors. The Board of Editors does not hold itself responsible for the opinions expressed by the correspondents.

Communications should not in general exceed 600 words in length.

The Vectorial Photoelectric Effect in Barrier-Layer Cells

It is a well-known fact that polarized light falling on the surface of a photoelectric cell has a greater effect if its electric vector lies in the plane of incidence than if it is perpendicular to the plane of incidence. H. E. Ives[1] has developed an explanation of the effect which checks the experimental results very well.

Although barrier-layer photovoltaic cells are different in construction from photoelectric cells in several respects, the action in both cases consists of the movement of electrons across a boundary. Hence it seems probable that there should be an effect in the case of barrier-layer cells similar to that in photoelectric cells although perhaps not so marked. L. Bergmann[2] carried out an experiment with a selenium barrier-layer cell to test this possibility and came to the conclusion that no such effect was present. However his calculations of the light absorbed were, as he stated, not rigorous and his results are therefore somewhat doubtful.

The author, realizing that calculations for this type of cell are not reliable, designed an experiment to obviate this difficulty. The light absorbed was measured instead of calculated so that the results are more valid.

A Weston photronic cell was chosen as the cell for the experiment. Its sensitive disk was removed from the Bakelite case to get rid of the shadows cast by the rim and also to cut out absorption by the glass. For the purpose of measuring the absorbed light a small spherical integrator was used. The sensitive disk was placed inside and the light reflected at various angles of incidence was measured. The light absorbed was assumed to be the difference between the reflected light and the incident light. The total amount of light falling on the surface was measured by replacing the cell by a piece of magnesium carbonate such as is commonly used in photometric measurements. The piece used had a reflection factor of 99.5 percent so that only a very small error was introduced by this procedure.

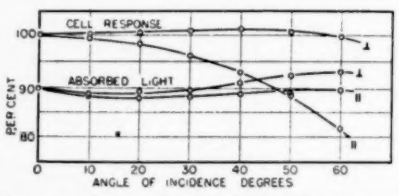

FIG. 1. The comparison of observed light and cell response referred to values for zero angle of incidence. The symbols ⊥ and || refer to the orientation of the plane of polarization to the plane of incidence.

The integrator was a sphere twelve inches in diameter, coated on the inside with precipated magnesium carbonate. The light source used was one electrode of an S-1 sunlamp. The light from the electrode passed through a large Nicol prism and then through a collimating tube so that it was parallel within 15′. The angle of incidence of the beam could be measured within about 15′.

The response of the cell to polarized light at the different angles of incidence was measured at the same time as the amount of light reflected. The two values were compared. The result shows definitely an effect of the kind expected. The two sets of curves in Fig. 1 show the data obtained.

The difference between the effects of light polarized in and perpendicular to the plane of incidence is not as marked as in the case of most photoelectric cells. The fact that the light has to pass through a thin layer of silver undoubtedly affects the results to some extent. It is practically impossible to analyze the effect of the silver layer and of the irregularities of the surfaces involved and no attempt was made to do so. The results then are purely qualitative as far as any conclusions which may be drawn from them go.

ROBERT G. WILSON

University of Dubuque,
Dubuque, Iowa,
January 12, 1938.

[1] H. E. Ives, Phys. Rev. **38**, 1209–1218 (1931).
[2] L. Bergmann, Physik. Zeits. **33**, 17–19 (1932).

Evidence Against the Existence of Heavy Beta-Particles

Jauncey[1] has suggested that all the beta-particles from a given species of nucleus have the same total energy, the slower ones being endowed with a rest mass greater than that of a planetary electron. Earlier, Zahn and Spees considered a similar hypothesis, and concluded that their deflection experiments[2] definitely contradict it. At the December, 1937, meeting of the American Physical Society Jauncey reported deflection experiments and interpreted them as supporting his hypothesis.

We have made an independent test of the hypothesis. Champion[3] obtained 35,000 magnetically curved cloud chamber tracks of Ra E beta-particles in nitrogen and oxygen. Thus he observed 15 close collisions between beta-particles and electrons, of quality suitable for an accurate test of the conservation of energy and momentum. Fourteen of these satisfied the conservation relations closely, and are suitable for the present study. Let βc be the velocity of a beta-particle whose rest mass is R times greater than that of an ordinary electron, and let

$\gamma=(1-\beta^2)^{-\frac{1}{2}}$. On Jauncey's theory,

$$R\gamma=\gamma_m,$$

where γ_m corresponds to the upper limit of the spectrum; its value is 3.44 ± 0.06 for Ra E.[4] Assuming strict conservation of energy and momentum, and also that the incident particle has a mass Rm_0, we have calculated values of $R\gamma$ from Champion's data. $R\gamma$ represents the energy of the incident beta-particle, in units m_0c^2. $R\gamma$ ranges from 1.65 to 2.74, most of the values being below 2. Their mean is less than 2, while Jauncey's theory predicts the constant value of 3.44 for this product. These results constitute a definite disproof of the hypothesis of heavy beta-particles, supplementing the evidence given by Zahn and Spees.

Our conclusion has no bearing on the possibility that the heavy particles reported in cosmic-ray experiments are electrons of exceptional rest mass. Results which are valid in the region of one million electron volts should be extrapolated to the domain of one billion electron volts.

University of North Carolina,
Chapel Hill, North Carolina,
January 12, 1938.

ARTHUR RUARK
CREIGHTON C. JONES

[1] Jauncey, Phys. Rev. **53**, 106 (1938).
[2] Zahn and Spees, Phys. Rev. **52**, 524 (1937).
[3] Champion, Proc. Roy. Soc. **136**, 630 (1932).
[4] O'Conor, Phys. Rev. **52**, 303 (1937).

Heavy Beta-Rays—More Theory and Experimental Evidence

Positives of the fifth and eighth films taken with the apparatus described in my third letter[1] are shown in Fig. 1. The line A is due to alpha-rays and the line C to ordinary beta-rays. According to my view the band B is due at least partly to heavy beta-rays. The data for the photographs are:

Film	H	V	β	s	p
5B	318	3372	0.338	1.02	3.37
8B	125	1296	0.328	.47	2.80
8C	125	1296	0.328	1.40	1.07

By reversing both fields I found that the alpha-line was shifted by an amount $H\times1.0\times10^{-4}$. Correction has been made for this in determining s. The value of $p=1.07$ for the C line of film 8 shows that the apparatus records ordinary electrons and removes all doubt as to the electric field in the selector. The theoretical value of p for the heavy electrons from Ra E for $\beta=0.328$ is 2.89 in excellent agreement with the experimental value. Film 8 was not covered with aluminum, while film 5 and films 1, 2, 3 of my third letter[1] were covered with $\frac{1}{2}$ mil of aluminum. The absorption in aluminum varies very rapidly with p and the center of the B band is shifted. This is possibly the explanation of the high values of p found from films 3 and 5.

The expression on the right side of (1) is the force on the particle in the velocity selector and $1/\rho'$ is the curvature of the path in the selector:

$$pm_0\beta^2c^2/\rho'e(1-\beta^2)^{\frac{1}{2}}=e(H\beta c-E). \qquad (1)$$

There are two solutions for $\rho'=\infty$: (a) $\beta=E/Hc$ and (b)

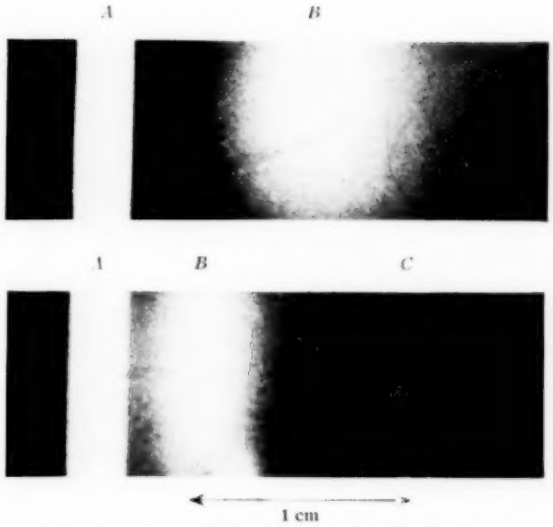

FIG. 1. Mass spectra of electrons. Film 5, top; film 8, bottom.

$\beta=1$. For each solution there is a maximum tolerance given by $\rho'=l^2/8w$, where l is the length and w the distance apart of the selector plates. For film 5 the tolerance for (b) is $\beta=0.964$ to $\beta=1$, when $p=1$. This should give a band from $s=0$ to 0.32 cm. No such band appears. Moreover the maximum β for Ra E is 0.945. The conclusion that the B band is due to heavy electrons seems inescapable.

Comparing B and C of film 8, we find a width in the band due to the heavies over and above the width of the line due to the ordinaries. I suggest that part of this extra width may be due to the heavies changing back to the ordinaries. Following the theory outlined in my first two letters,[2] the conservation principles yield

$$\alpha'=(p^2-1)/2p_{\max}(1-\beta\cos\phi), \qquad (2)$$

where $\alpha'm_0c^2$ is the energy of a photon emitted in a direction ϕ with the direction of the velocity βc of a heavy electron of mass pm_0 when it returns to mass m_0 and recoils with a velocity $\beta'c$ in a direction θ. The change from pm_0 to m_0 may occur at any point along the arc either in the selector or in the magnetic field. That ordinary electrons of the selector velocity are produced in the selector has been shown by placing $\frac{1}{2}$ mil of aluminum first in front of the film when the line for the ordinaries of $\beta=0.44$ was missing on the film and then transferring the aluminum foil to a position between the Ra E and the selector when the line for the ordinaries appeared again on the film. These ordinaries are produced as secondaries at the plates of the selector or are produced from the heavies. Ordinaries would always be found in Doctor Zahn's arrangement. In closing, I repeat my statement at Indianapolis that evidence for heavy beta-rays is shown in Bucherer's papers.[3]

G. E. M. JAUNCEY

Wayman Crow Hall of Physics,
Washington University,
St. Louis, Missouri,
January 14, 1938.

[1] Jauncey, Phys. Rev. **53**, 197 (1938).
[2] Jauncey, Phys. Rev. **52**, 1256(L) (1937); **53**, 106(L) (1938).
[3] Bucherer, Ann. d. Physik **30**, 974 (1909).

Evidence for a Particle of Intermediate Mass

While making observations on the stopping power of lead for recoil electrons produced by the 17 Mev gamma-rays from Li+H[1], the track shown in Fig. 1 appeared in our cloud chamber. Although the continuous, dense ionization is suggestive of a proton or an alpha-particle, its radius of curvature is only 9 cm in a 2850 gauss field. The radius of curvature for a proton of range equal to the visible length of this track is about 65 cm, and for an alpha-particle about 130 cm. The fact that its curvature is continuous makes it seem improbable that its curvature is due to scattering in the gas. Judging from the width and photographic density of the track we believe that the particle arrived after the chamber had expanded and after the camera had opened. This eliminates any possibility that its curvature is due to turbulence of the gas in the chamber.

The radius of curvature of the track decreases in going in a direction away from the lead plate (horizontal line across center of chamber). If this change of curvature is due to loss of energy by ionization along the path, the direction of motion can be assumed to be away from the plate, which means that it is a positively charged particle. A measurement of the rate of change of radius of curvature gives 0.6 ± 0.2 cm/cm. This value, together with the radius of curvature, gives a unique solution for the mass of the particle, provided it is singly charged. It is 120 ± 15 times the electron mass. If we use more liberal limits of error for the rate of change of radius of curvature, namely 0.6 ± 0.4, the mass is found to be $120\pm30m_0$. This is nearly the same as the mass of a negative particle found by Street and Stevenson,[1] but is much smaller than those found by Corson and Brode[2] and by Nishina, Takeuchi and Ichimiya.[3]

We suppose that this track is associated with cosmic radiation for two reasons: 1. The energy of the lithium gamma-ray is insufficient to create such a particle. 2. Another track, similar in density and curvature, but much shorter, can be seen in the same picture, and it is more probable that two would appear simultaneously in a cosmic-ray shower, than that they would be produced simultaneously by the gamma-radiation.

ARTHUR J. RUHLIG
H. R. CRANE

University of Michigan,
Ann Arbor, Michigan,
January 13, 1937.

[1] Street and Stevenson, Phys. Rev. **52**, 1003 (1937).
[2] Corson and Brode, Abstract, Stanford Meeting, Dec. 18, 1937.
[3] Nishina, Takeuchi and Ichimiya, Phys. Rev. **52**, 1198 (1937).

FIG. 1. Photograph showing a heavily ionizing, curved track in the lower half of the chamber. The path of the particle seems to make about a 15° angle with the plane of the chamber, because it passes out of the light beam near the edge of the chamber. The lead plate, 0.4 mm thick appears as a horizontal line across the center of the chamber. Several electron tracks are visible, which are produced by the 17 Mev gamma-radiation from Li+H[1]. The small blobs scattered throughout the chamber are due to low energy electrons produced by x-rays.

Analysis of Neutron Absorption in Boron

It is the purpose of this note to suggest a method for the determination of slow neutron energy distributions and of the energy shapes of capture cross sections in certain elements. Consider a beam of slow neutrons, filtered through a thickness x of boron and detected by the activity $A(x)$ produced in a thin layer of an element which has a capture cross section $\sigma(E)$ depending on the energy E. Supposing the number of neutrons incident on the boron per sq. cm per sec. in the energy range dE to be $p(E)dE$ and assuming that boron captures as $1/E^{\frac{1}{2}}$ we have

$$A(x)/A(0)=c\int_0^{\infty}\sigma(E)p(E)\exp\,(-kx/E)^{\frac{1}{2}}dE,$$

where c normalizes the expression on the right to unity when $x=0$ and k is known from the absorption in boron at thermal energies. The change of variable $y=1/E^{\frac{1}{2}}$ gives

$$A(x)/A(0)=\int_0^{\infty}\varphi(y)\exp\,(-kxy)dy,$$

where $$\varphi(y)=2c\sigma(1/y^2)p(1/y^2)/y^3.$$

This can be considered as an integral equation in the unknown function $\varphi(y)$. A numerical solution for this equation has been devised by Eckart,[1] who has performed necessary preliminary calculations. It has the advantages of simplicity and validity over a wide range in the variable y. Supposing that boron is first used as detector, we have $\sigma(E)\propto 1/E^{\frac{1}{2}}$, so that $\varphi(y)\propto p(1/y^2)/y^2$. Eckart's solution then serves to determine $p(E)$. A second experiment with some other element as detector will determine $\sigma(E)$ for that element.

The method, unfortunately, is valid only when $\varphi(y)$ has no sharp peaks or breaks, and so it is of little use when $\sigma(E)$ contains very sharp resonances, as is generally the

case. It should, however, be extremely useful in the important case of cadmium and should serve to remove present uncertainties in regard to the shape of the low energy resonance.[2] Furthermore, if one can be reasonably certain that a single resonance is responsible for the cross section in a given case, a preferable alternative method would be as follows. First find the background $p(E)$ as suggested above and then determine the resonance energy and width by a least square fit to the observed absorption curve. The latter mode of attack should be valid even for fairly sharp resonance.

Numerous other applications, such as the investigation of "thermal" distributions and of possible negative levels suggest themselves. Finally, it should be possible to obtain an experimental check on the validity of the $1/v$ law in boron at energies higher than one volt by analyzing in this fashion and with boron detection the distribution in a cadmium filtered beam. The result for $p(E)$ should be comparable to the Fermi distribution $p(E) \propto 1/E$. The assumption is made that cadmium does not absorb appreciably above one volt. It is perhaps safer to assume the $1/v$ law in boron and use the method to test the truth of the latter statement. In any case, success is more or less dependent on the care taken in making proper geometrical corrections.

HENRY C. TORREY

Pennsylvania State College,
State College, Pennsylvania,
January 10, 1938.

[1] C. Eckart, Phys. Rev. **45**, 851 (1934).
[2] J. G. Hoffman and M. S. Livingston, Phys. Rev. **52**, 1228 (1937).